NASA Technical Memorandum 105351
ICOMP–91–25; CMOTT–91–10

A Critical Comparison of Second Order Closures With Direct Numerical Simulation of Homogeneous Turbulence

Tsan-Hsing Shih
Institute for Computational Mechanics in Propulsion
and Center for Modeling of Turbulence and Transition
Lewis Research Center
Cleveland, Ohio

and

John L. Lumley
Cornell University
Ithaca, New York

November 1991

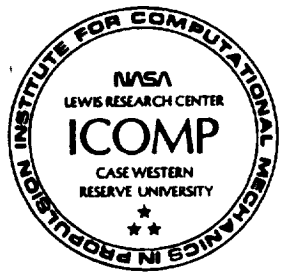

NASA

A Critical Comparison of Second Order Closures with Direct Numerical Simulations of Homogeneous Turbulence

Tsan-Hsing Shih
Institute for Computational Mechanics in Propulsion and
Center for Modeling of Turbulence and Transition
Lewis Research Center
Cleveland, Ohio 44135

John L. Lumley
Cornell University
Ithaca, New York 14853

ABSTRACT

Recently several second order closure models have been proposed for closing the second moment equations, in which the velocity-pressure gradient (and scalar-pressure gradient) tensor and the dissipation rate tensor are the two of the most important terms. In the literature, these correlation tensors are usually decomposed into a so called rapid term and a return-to-isotropy term. Models of these terms have been used in global flow calculations together with other modeled terms. However, their individual behavior in different flows have not been fully examined because they are un-measurable in the laboratory. Recently, the development of direct numerical simulation (DNS) of turbulence has given us the opportunity to do this kind of study. With the direct numerical simulation, we may use the solution to exactly calculate the values of these correlation terms and then directly compare them with the values from their modeled formulations (models). In this paper, we make direct comparisons of five representative rapid models and eight return-to-isotropy models using the DNS data of forty five homogeneous flows which were done by Rogers et al. (1986) and Lee et al. (1985). The purpose of these direct comparisons is to explore the performance of these models in different flows and identify the ones which give the best performance. The paper also describes the modeling procedure, model constraints, and the various evaluated models. The detailed results of the direct comparisons are discussed, and a few concluding remarks on turbulence models are given.

1. Introduction

Homogeneous turbulent flows have been used for studying many important phenomena of turbulence. In these flows, the mean flow field is decoupled from the dynamical equations of turbulence and, therefore, the detailed turbulence structure and related turbulent transfer have no influence on the mean flow field. On the other hand, however, the mean flow field directly affects the evolution of turbulence through the turbulence dynamical equations. This unique feature of the homogeneous turbulence enables us to selectively and efficiently study the effect of the mean flow field on the turbulence.

From turbulence modeling point of view, the homogenous turbulence has been also considered as a base for developing advanced closure models, especially the second order closure and the spectrum closure (or two-point closure). For the second order closure (or second moment closure), the homogeneous turbulence greatly simplifies the turbulence equations by excluding the turbulent diffusion term, and thus enables us to concentrate on the velocity-pressure gradient correlation tensor and the dissipation rate tensor, which are two of the most important terms in the Reynolds-stress equations. In addition, the homogeneous turbulence provides us with some nice symmetry properties for turbulence correlations which are very helpful in the model development.

In this paper, we describe several representative second order closure models for the homogeneous turbulence, which are also used or extended to the inhomogeneous turbulence. Thirteen models[1]–[12] are included in this study. To explore the behavior of these models in a wide range of flows and to identify the ones which represent the state of the art, we have made direct comparisons of these models with the data of direct numerical simulations. That is, we use the solution of the DNS to calculate the exact values of the terms which need to be modeled and then compare them with the values from the respective model formulations. This kind of comparison removes the ambiguity and confusion present in a global indirect comparison, which compares the solutions of the modeled second moment equations. In this indirect comparison, the models of the other terms in addition to the model we want to evaluate are also involved. In practice, we often encounter the situations in which two wrong things (models) compensate each other to make the solution of the specific flow correct, and therefore, we cannot draw a definite conclusion about the certain models from this kind of indirect comparisons.

The DNSs used in this paper are homogeneous shear flows (Rogers et al.[13]) and homogeneous irrotational strain and relaxation flows (Lee et al.[14]). The DNS data of forty five different turbulent flows are used for the direct comparisons of turbulence models.

Section 2 lists the basic equations and model terms, and then briefly describes the model

constraints and the modeling procedure. Section 3 describes various second order closure models proposed by different researchers. A brief comment on each model is also given. Section 4 shows the detailed direct comparisons between models and DNS data. Finally, a few concluding remarks are made in section 5.

2. Turbulence equations and model terms

For incompressible turbulent flows with constant density ρ, the mean equations can be written as:

$$U_{i,i} = 0 \tag{1}$$

$$\frac{D}{Dt}U_i = -\frac{1}{\rho}P_{,i} - (\overline{u_i u_j})_{,j} + \beta_i \Theta + \nu U_{i,jj} \tag{2}$$

$$\frac{D}{Dt}\Theta = -(\overline{\theta u_j})_{,j} + \gamma \Theta_{,jj} \tag{3}$$

where $(\ \ )_{,i}$ represents the spacial derivative, and $\frac{D}{Dt} = \frac{\partial}{\partial t} + U_k \frac{\partial}{\partial x_k}$. U_i, Θ and P are the mean of the velocity, the scalar and the pressure. u_i, θ and p are the corresponding fluctuating quantities. $\beta_i (= g_i/\rho)$, ν and γ are the buoyancy vector, the kinematic viscosity and the thermal diffusivity respectively. To close above equations we need models for the second order moments: $\overline{u_i u_j}$, $\overline{\theta u_i}$, which represent the Reynolds stress and the turbulent scalar flux (e.g., heat flux). At the second order closure level, these second moments are provided with a set of modeled transport equations.

The exact equation for the Reynolds-stress tensor $\overline{u_i u_j}$ can be written as:

$$\frac{D}{Dt}\overline{u_i u_j} = D_{ij} + P_{ij} + F_{ij} + T_{ij} + \Pi_{ij} - \varepsilon_{ij} \tag{4}$$

where,

$$D_{ij} = \nu(\overline{u_i u_j})_{,kk}$$

$$P_{ij} = -\overline{u_i u_k}U_{j,k} - \overline{u_j u_k}U_{i,k}$$

$$F_{ij} = \beta_i \overline{\theta u_j} + \beta_j \overline{\theta u_i}$$

$$T_{ij} = -[\overline{u_i u_j u_k} + \frac{1}{\rho}(\overline{u_i p}\delta_{jk} + \overline{u_j p}\delta_{ik})]_{,k}$$

$$\Pi_{ij} = \frac{1}{\rho}\overline{p(u_{i,j} + u_{j,i})}$$

$$\varepsilon_{ij} = 2\nu \overline{u_{i,k} u_{j,k}}$$

D_{ij} and T_{ij} are the viscous diffusion and the turbulent diffusion; P_{ij} and F_{ij} are the shear and buoyancy production terms; and finally Π_{ij} and ε_{ij} represent the pressure-strain rate tensor and the dissipation rate tensor respectively. δ_{ij} is the Kronecker's delta. Obviously,

to close above Reynolds-stress equation, we must model the new unknowns T_{ij}, Π_{ij} and ε_{ij}. At the level of the second order closure, these new unknowns are usually modeled with algebraic equations in terms of the second moments and the mean quantities (with the exception of the trace $\varepsilon_{kk} = 2\varepsilon$, which is modeled with a transport equation).

The exact heat flux $\overline{\theta u_i}$ equation is:

$$\frac{D}{Dt}\overline{\theta u_i} = D_{i\theta} + P_{i\theta} + F_{i\theta} + T_{i\theta} + \Pi_{i\theta} - \varepsilon_{i\theta} \tag{5}$$

where,

$$\begin{aligned}
D_{i\theta} &= \gamma(\overline{u_i\theta_{,k}})_{,k} + \nu(\overline{u_{i,k}\theta})_{,k} \\
P_{i\theta} &= -\overline{\theta u_k}U_{i,k} - \overline{u_i u_k}\Theta_{,k} \\
F_{i\theta} &= \beta_i\overline{\theta^2} \\
T_{i\theta} &= -[\overline{\theta u_i u_k} + \frac{1}{\rho}\overline{p\theta}\delta_{ik}]_{,k} \\
\Pi_{i\theta} &= \frac{1}{\rho}\overline{p\theta_{,i}} \\
\varepsilon_{i\theta} &= (\nu+\gamma)\overline{\theta_{,k}u_{i,k}}
\end{aligned}$$

The physical meaning of above terms is similar to the terms in the Reynolds-stress equation. If $\gamma = \nu$, $D_{i\theta}$ can be written as $\nu(\overline{\theta u_i})_{kk}$. Again, in order to close the heat flux equation, $T_{i\theta}$, $\Pi_{i\theta}$ and $\varepsilon_{i\theta}$ must be modeled and they are usually modeled with algebraic equations in terms of the second moments and the mean quantities.

In general, we also need an equation of the temperature variance $\overline{\theta^2}$:

$$\frac{D}{Dt}\overline{\theta^2} = \gamma(\overline{\theta^2})_{,kk} - 2\overline{\theta u_k}\Theta_{,k} - (\overline{\theta^2 u_k})_{,k} - 2\gamma\overline{\theta_{,k}\theta_{,k}} \tag{6}$$

Again, the last two terms in the above equation must be modeled.

In a general turbulent shear flow with moderate inhomogeneity, the turbulent diffusion terms in the second moment equations are usually smaller than the other terms. However, the pressure-strain rate and dissipation rate tensors are always among the leading terms. Therefore, the performance of modeled equations largely depends on the models of pressure-strain rate tensor and dissipation rate tensor.

For the homogeneous turbulence with constant gradients of the mean velocity and the mean temperature, the equations (1-3) will be decoupled from the equations of second moments (4), (5) and (6), and hence the mean flow field of the homogeneous turbulence will not be affected by the turbulence. However, the converse is not ture. The mean flow field (U_i

and Θ) will directly affect the evolution of turbulence through the terms on the right hand side of the second moment equations. In addition, the turbulent diffusion terms will not be present in the homogeneous turbulence, which enables us to isolate the pressure-strain rate tensor and the dissipation rate tensor from the complicated triple correlation tensor (turbulent diffusion term).

In this paper, we will only concentrate on the models of the pressure-strain rate tensor and the dissipation rate tensor for the velocity field. However, for the purpose of describing the modeling procedure, we will also include the scalar field.

Realizability:

For constructing turbulence models, various model constraints have been proposed by different authors in an attempt to make the model equations as general (or universal) as possible. Besides the conventional model constraints (e.g. invariance principle), the most recent ones are the realizability principle (Schumann[15], Lumley[7]), the linearity principle (Pope[16]), the rapid distortion theory (Reynolds[17]), and the material indifference principle (Speziale[18]). However, some of the above mentioned principles are not universal. For example, the material indifference is not valid for general turbulence in which the fluctuating velocities are three dimensional. The principle of linearity is also not universal, as it holds only for passive scalars. On the other hand, realizability (defined as the requirement of the non-negativity of turbulence energy components and Schwarz' inequality between any fluctuating quantities) is the basic physical and mathematical principle that the solutions of any governing equations should obey. Hence, among all the above mentioned model constraints, realizability is the most universal, important principle and is also the minimal requirement to prevent the turbulence model equations from producing unphysical results. Realizability can be applied to various turbulence quantities, for example, the Reynolds stresses $\overline{u_i u_j}$, the scalar fluxes $\overline{\theta u_i}$ and the triple correlations. For one-point second moment equations, realizability for $\overline{u_i u_j}$ and $\overline{\theta u_i}$ is most important (for more details, see Shih et al.[19], Lumley[23]).

Modeling procedure:

A traditional way to treat pressure-strain rate tensor was first proposed by Chou[20]. It starts with the following equation of the fluctuating pressure:

$$-\frac{1}{\rho}p_{,jj} = 2U_{i,j}u_{j,i} + u_{i,j}u_{j,i} - \beta_i\theta_{,i} - \overline{u_{i,j}u_{j,i}} \tag{7}$$

Based on the linearity of p, this equation can be split into three parts:

$$-\frac{1}{\rho}p^{(1)}_{,jj} = 2U_{i,j}u_{j,i} \tag{8}$$

$$-\frac{1}{\rho}p^{(2)}_{,jj} = u_{i,j}u_{j,i} \tag{9}$$

$$-\frac{1}{\rho}p^{(3)}_{,jj} = -\beta_i\theta_{,i} \tag{10}$$

Then the pressure related correlation terms in the second moment equations can be written as:

$$\Pi_{ij} = \Pi^{(1)}_{ij} + \pi^{(2)}_{ij} + \Pi^{(3)}_{ij} \tag{11}$$

$$\Pi_{i\theta} = \Pi^{(1)}_{i\theta} + \pi^{(2)}_{i\theta} + \Pi^{(3)}_{i\theta} \tag{12}$$

where, the first term on the right which is explicitly related to the mean velocity gradient is called the rapid term, the second term which is related only to the pure fluctuating quantities is commonly called slow term, and the third term which is directly related to the buoyancy is called buoyancy term. In the literature, the slow term $\pi^{(2)}_{ij}$ is often combined with the deviatoric part of the dissipation rate tensor (the dissipation is also related only to the pure fluctuating quantities). They both drive the turbulence towards isotropic state. Therefore Lumley[7] defined Φ_{ij} and $\Phi_{i\theta}$:

$$-\Phi_{ij}\varepsilon = \pi^{(2)}_{ij} - \varepsilon_{ij} + \frac{2}{3}\varepsilon\delta_{ij} \tag{13}$$

$$-\Phi_{i\theta}\frac{\varepsilon}{\overline{q^2}} = \pi^{(2)}_{i\theta} - \varepsilon_{i\theta} \tag{14}$$

which are called the return-to-isotropy terms in the second moment equations. Here $\overline{q^2} = \overline{u_k u_k}$, $\varepsilon = \frac{1}{2}\varepsilon_{kk}$.

For the rapid and buoyancy terms, one may obtain their exact expressions for homogeneous turbulence using the solution of Eq.(8) and Eq.(10):

$$\begin{aligned}\Pi^{(1)}_{ij} &= -2U_{p,q}\frac{1}{4\pi}\int_V [(\overline{u_q(r)u_i(r')})_{,pj} + (\overline{u_q(r)u_j(r')})_{,pi}]\frac{dv}{|r-r'|} \\ &= 2U_{p,q}(X_{pjqi} + X_{piqj})\end{aligned} \tag{15}$$

$$\begin{aligned}\Pi^{(1)}_{i\theta} &= -2U_{j,k}\frac{1}{4\pi}\int_V [\overline{u_k(r)\theta(r')}]_{,ij}\frac{dv}{|r-r'|} \\ &= 2U_{j,k}X_{ijk}\end{aligned} \tag{16}$$

$$\begin{aligned}\Pi^{(3)}_{ij} &= \beta_k\frac{1}{4\pi}\int_V [(\overline{\theta(r)u_i(r')})_{,kj} + (\overline{\theta(r)u_j(r')})_{,ki}]\frac{dv}{|r-r'|} \\ &= -\beta_k(Y_{kji} + Y_{kij})\end{aligned} \tag{17}$$

$$\Pi_{i\theta}^{(3)} = \beta_k \frac{1}{4\pi} \int_V [\overline{\theta(r)\theta(r')}]_{,ik} \frac{dv}{|r-r'|}$$
$$= -\beta_k Y_{ik} \tag{18}$$

where the tensors X and Y are the integrals of two-point correlations over the entire physical space. To model the rapid and buoyancy terms is now to model these tensors. We notice that the exact expressions of X and Y in Eqs.(15-18) do not provide the models in terms of the second moments. However, they do give us a hint to model them, because these integrals tell us some important properties of X and Y:

$$\begin{aligned} X_{pjqi} &= X_{jpqi}, \quad X_{pjqi} = X_{pjiq} \\ X_{ijk} &= X_{jik} \\ Y_{kji} &= Y_{jki} \\ Y_{ik} &= Y_{ki} \end{aligned} \tag{19}$$

$$\begin{aligned} X_{pjpi} &= 0, \quad X_{ikk} = 0 \\ Y_{kjj} &= 0 \end{aligned} \tag{20}$$

$$\begin{aligned} X_{ppqi} &= \overline{u_q u_i}, \quad X_{iik} = \overline{\theta u_k} \\ Y_{kki} &= \overline{\theta u_i}, \quad Y_{kk} = \overline{\theta^2} \end{aligned} \tag{21}$$

Eq.(19) is the symmetry condition, Eq.(20) is the incompressibility condition, and Eq.(21) is called the normalization condition (Rotta[6]). Theses equations are very helpful for constructing models of X and Y. In fact, they have been used in all conventional turbulence models. A model which does not satisfy the above conditions has little hope of success in general applications.

In this paper, we only present the models for the velocity field which will be directly compared with the available DNS data. These models are for the rapid term $\Pi_{ij}^{(1)}$ and the return-to-isotropy term $-\varepsilon\Phi_{ij}$ (denoted as $\Pi_{ij}^{(2)}$).

3. Closure models:

In this section, we will describe five models for the rapid term and eight models for the return-to-isotropy term. These models were proposed by different researchers and have been indirectly tested in different selected flows.

3.1 Models for the rapid term $\Pi_{ij}^{(1)}$:

Launder, Reece and Rodi (LRR):[1]

$$\begin{aligned}\frac{\Pi_{ij}^{(1)}}{2\overline{q^2}} &= 0.2S_{ij} + \frac{9C_2+6}{22}(b_{ik}S_{jk} + b_{jk}S_{ik} - \frac{2}{3}\delta_{ij}b_{kl}S_{kl}) \\ &+ \frac{10-7C_2}{22}(b_{ik}\Omega_{jk} + b_{jk}\Omega_{ik})\end{aligned} \tag{22}$$

where $C_2 = 0.4$, and

$$\begin{aligned}b_{ij} &= \frac{\overline{u_iu_j}}{\overline{q^2}} - \frac{1}{3}\delta_{ij}, \\ S_{ij} &= \frac{1}{2}(U_{i,j} + U_{j,i}), \\ \Omega_{ij} &= \frac{1}{2}(U_{i,j} - U_{j,i})\end{aligned}$$

This model is linear in the Reynolds-stress. It contains only one model constant C_2. This model satisfies the conventional model constraints Eqs.(19-21). It is the most general form at the level of linear dependence on the Reynolds-stress. However, as Lumley[7] pointed out that this model may violate realizability as turbulence approaches two component state.

Speziale, Sarkar and Gatski (SSG):[2]

$$\begin{aligned}\frac{\Pi_{ij}^{(1)}}{2\overline{q^2}} &= \frac{0.2 - C_3^{**}}{4}S_{ij} - \frac{C_1^*P}{2\overline{q^2}}b_{ij} \\ &+ \frac{C_4}{4}(b_{ik}S_{jk} + b_{jk}S_{ik} - \frac{2}{3}\delta_{ij}b_{kl}S_{kl}) \\ &+ \frac{C_5}{4}(b_{ik}\Omega_{jk} + b_{jk}\Omega_{ik})\end{aligned} \tag{23}$$

where,

$$\begin{aligned}C_3^{**} &= C_3^*b_{ij}b_{ij}, \quad P = -\overline{u_iu_j}U_{i,j} \\ C_1^* &= 1.8 \quad C_3^* = 1.3, \quad C_4 = 1.25, \quad C_5 = 0.4\end{aligned}$$

This model is quasi-linear in the Reynolds-stress, because the coefficients in the first two terms are not constant, they depend on the invariant of the Reynolds-stress tensor and the production P. This model contains four model constants (C_1^*, C_3^*, C_4, C_5), therefore one may imagine that it will be difficult to correctly calibrate them. In addition, this model does not satisfy the basic model constraint Eq.(21). If we impose this constraint, then the four coefficients will reduce to only one, and this model will reduce to the LRR model. Finally, like the LRR model, the SSG model may also violate realizability.

Fu, Launder and Tselepidakis (FLT):[3]

$$\begin{aligned}\frac{\Pi_{ij}^{(1)}}{2\overline{q^2}} &= 0.2S_{ij} + 0.3(b_{ik}S_{jk} + b_{jk}S_{ik} - \frac{2}{3}\delta_{ij}b_{kl}S_{kl}) \\ &+ \frac{1.3}{3}(b_{ik}\Omega_{jk} + b_{jk}\Omega_{ik}) \\ &+ 0.2(b_{il}^2S_{jl} + b_{jl}^2S_{il} - 2b_{kj}b_{li}S_{kl} - 3b_{ij}b_{kl}S_{kl}) \\ &+ 0.2(b_{il}^2\Omega_{jl} + b_{jl}^2\Omega_{il}) \\ &+ r[4b_{nn}^2(b_{ik}\Omega_{jk} + b_{jk}\Omega_{ik}) \\ &+ 12b_{mi}b_{nj}(b_{mk}\Omega_{nk} + b_{nk}\Omega_{mk})]\end{aligned} \tag{24}$$

where $r = 0.7$, $b_{ij}^2 = b_{ik}b_{kj}$.

This model is cubic in the Reynolds-stress. The final selected form contains one model constant. This model only satisfies a part of realizability condition, that is the two component state of turbulence. However, when scalar field is involved, this model will not be able to satisfy the Schwarz' inequality between velocity and temperature. This part of realizability is sometimes called the joint realizability.

Shih and Lumley (SL):[4]

$$\begin{aligned}\frac{\Pi_{ij}^{(1)}}{2\overline{q^2}} &= 0.2S_{ij} + 3\alpha_5(b_{ik}S_{jk} + b_{jk}S_{ik} - \frac{2}{3}\delta_{ij}b_{kl}S_{kl}) \\ &+ \frac{1}{3}(2 - 7\alpha_5)(b_{ik}\Omega_{jk} + b_{jk}\Omega_{ik}) \\ &+ 0.2(b_{il}^2S_{jl} + b_{jl}^2S_{il} - 2b_{kj}b_{li}S_{kl} - 3b_{ij}b_{kl}S_{kl}) \\ &+ 0.2(b_{il}^2\Omega_{jl} + b_{jl}^2\Omega_{il})\end{aligned} \tag{25}$$

where,

$$\alpha_5 = \frac{1}{10}(1 + 0.8F^{1/2}), \quad F = 1 + 9b_{ij}b_{jk}b_{ki} - \frac{9}{2}b_{ij}b_{ij}$$

This model is quasi-quadratic in the Reynolds-stress, because the model coefficient α_5 is the function of the invariants of Reynolds-stress tensor. We emphasize that this model is obtained from a more general form of the expression than the FLT, and satisfies both the two component condition and the Schwarz' inequality between the velocity and scalar fields. In addition, the final form is simpler than the model of FLT.

Shih and Mansour (SM):[5]

$$\begin{aligned}\frac{\Pi_{ij}^{(1)}}{2\overline{q^2}} &= 0.2S_{ij} + 3\alpha_5(b_{ik}S_{jk} + b_{jk}S_{ik} - \frac{2}{3}\delta_{ij}b_{kl}S_{kl}) \\ &+ \frac{1}{3}(2 - 7\alpha_5)(b_{ik}\Omega_{jk} + b_{jk}\Omega_{ik}) \\ &+ 0.2(b_{il}^2S_{jl} + b_{jl}^2S_{il} - 2b_{kj}b_{li}S_{kl} - 3b_{ij}b_{kl}S_{kl}) \\ &+ 0.2(b_{il}^2\Omega_{jl} + b_{jl}^2\Omega_{il})\end{aligned} \tag{26}$$

where, $\alpha_5 = \frac{1}{10}\{1 + 3.5[1 - (1 - F)^{1/4}])\}$.

This model has the same form as the SL model. It was derived in a different way and contains a different model coefficient α_5 which was calibrated from one of the DNS data (Rogers[13]). This model, like the SL model, fully satisfies realizability conditions.

3.2 Models for the return-to-isotropy term $\Pi_{ij}^{(2)}$:

Rotta:[6]

$$\Pi_{ij}^{(2)} = -\varepsilon C b_{ij} \tag{27}$$

where, $C = 3.0$.

This model is linear in the Reynolds stress, and contains one model constant. It was widely used and adopted in the LRR model. We notice that this model will not allow the turbulence to reach the state of two component, because when any turbulent component reduces to $\overline{q^2}/9$, the model Eq.(27) will force it to grow.

Lumley:[7]

$$\Pi_{ij}^{(2)} = -\varepsilon[\beta b_{ij} + \gamma(b_{ij}^2 + 2II\delta_{ij}/3)] \tag{28}$$

where, $\gamma = 0$ and

$$\beta = 2 + \frac{F}{9}\exp(-7.77/\sqrt{Re})\{72/\sqrt{Re} + 80.1\ln[1 + 62.4(-II + 2.3III)]\}$$

$$Re = \frac{\overline{q^2}^2}{9\varepsilon\nu}$$

This model is quasi-linear in the Reynolds stress, because γ is set to zero, and β is a function of the invariants of Reynolds stress tensor. This model is simple, and satisfies realizability.

Sarkar and Speziale (SS):[8]

$$\Pi_{ij}^{(2)} = -\varepsilon[C_1 b_{ij} - 3(C_1 - 2)(b_{ij}^2 - \frac{1}{3}b_{kk}^2\delta_{ij})] \tag{29}$$

where $C_1 = 3.4$.

This is a quadratic model in the Reynolds-stress tensor. It satisfies what they call the weak realizability condition. Like the Rotta model Eq.(27), this model will not produce unphysical results. However, it will not allow the turbulence to approach the two component state, which could occur in some situations, for example, in the near-wall turbulence.

Haworth and Pope (HP):[9]

$$\Pi_{ij}^{(2)} = -\varepsilon\{C_1 b_{ij} - C_2[\frac{1}{3}b_{ij} + b_{ij}^2 - b_{kk}^2(b_{ij} + \delta_{ij}/3)]\} \tag{30}$$

where $C_1 = 8.3, \quad C_2 = 14.8$.

Eq.(30) is the slow part of the Haworth and Pope's model for the situations with no mean velocity gradient. This model, like the SS model, will not produce unphysical results, however, it will also not allow the turbulence to approach the two component state.

Choi and Lumley (CL):[10]

If $III \geq 0$,

$$\Pi_{ij}^{(2)} = -\varepsilon[\beta b_{ij} + \gamma(b_{ij}^2 + 2II\delta_{ij}/3)] \tag{31.1}$$

where,

$$\beta = 2 + \frac{\rho^* F^{1/2}}{1 + G\,\chi^2}$$

$$\gamma = \frac{\rho^* F^{1/2}}{1 + G\,\chi^2}\frac{G}{\xi}$$

$$\xi = (III/2)^{1/3}, \quad \eta = (-II/3)^{1/2}$$

$$\chi = \frac{\xi}{\eta}, \quad G = -\chi^4 + 0.8\chi^6$$

$$\rho^* = \exp[-9.29/Re^{1/2}]\{(\frac{7.69}{Re^{1/2}} + \frac{73.7}{Re}) - [296 - 16.2(\chi + 1)^4]II\}$$

$$Re = \frac{\overline{q^2}^2}{9\varepsilon\nu}, \quad II = -b_{ij}b_{ij}/2, \quad III = b_{ij}b_{jk}b_{ki}/3$$

If $III < 0$,

$$\Pi_{ij}^{(2)} = Eq.(28) \tag{31.2}$$

The model coefficients in Eq.(31.1) were obtained using their comprehensive measurements of turbulence relaxing from axisymmetric expansion. Both Eq.(30.1) and Eq.(31.2) satisfy realizability, however, Eq.(31.1) is valid only for $III \geq 0$, because ξ is not defined when $III < 0$.

Craft and Launder (C&L):[11]

$$\Pi_{ij}^{(2)} = -C_1\varepsilon[2b_{ij} + 4C_1'(b_{ij}^2 - b_{kk}^2\delta_{ij}/3)] - 2\varepsilon b_{ij} \tag{32}$$

where,

$$C_1 = 3.1(A_2 A)^{1/2}, \quad C_1' = 1.2$$

$$A_2 = 4\ b_{ij}b_{ji}, \quad A_3 = 8\ b_{ij}b_{jk}b_{ki}, \quad A = 1 - \frac{9}{8}(A_2 - A_3)$$

This model is tensorially quadratic in the Reynolds stress, and satisfies realizability.

Yamamoto and Arakawa (YA):[12]

$$\Pi_{ij}^{(2)} = -\varepsilon[\alpha_1 b_{ij} + \alpha_2(b_{ij}^2 - b_{kk}^2\delta_{ij}/3)] \tag{33}$$

where,

$$\alpha_1 = 2 + p\ F\ [q\ (b_{kk}^2)^r + |b_{kk}^3|^s sign(b_{kk}^3)]$$

$$\alpha_2 = 3\ (\alpha_1 - 2)$$

$$p = -12, \quad q = -0.65, \quad r = 0.4, \quad s = 0.45$$

$$F = 1 - \frac{9}{2}b_{kk}^2 + 9\ b_{kk}^3$$

The YA model tried to fit the situations with both positive and negative b_{kk}^3. It also meets the requirement of realizability.

Shih and Mansour (S&M):[5]

$$\Pi_{ij}^{(2)} = -\varepsilon\{(2.0 + C_f F^{\xi})b_{ij} + \gamma[b_{ij}^2 + (1/3 + 2II)b_{ij} + \frac{2}{3}II\delta_{ij}]\} \tag{34}$$

where,

$$C_f = (1/9)\exp(-7.77/\sqrt{Re})\{72/\sqrt{Re} + 80.1\ln[1 + 62.4(-II + 2.3III)]\}$$

$$\gamma = \gamma_0(1 - F^{\eta}), \quad Re = \frac{\overline{q^2}^2}{9\varepsilon\nu}$$

$$F = 1 + 9II + 3III$$

$$II = -\frac{1}{2}b_{ij}b_{ij}, \quad III = \frac{1}{3}b_{ij}b_{jk}b_{ki}$$

$$\xi = 17/20, \quad \eta = 1/20, \quad \gamma_0 = -2$$

This model matches the data of Comte-Bellot and Corrsin[21] and meets the requirement that there will be no return to isotropy in the zero Reynolds number limit. This model also satisfies realizability.

4. Direct comparison between models and DNS data

The direct numerical simulations of the homogeneous turbulence used for the direct comparisons in this paper were done by Rogers et al[13] and Lee et al[14]. The Rogers et al.'s flows are homogeneous shear flows with different shear rate S and different turbulent Reynolds number $\overline{q^2}^2/(\nu\varepsilon)$. Four of them are marked as C128U, C128V, C128W and C128X. They are used for direct comparisons with both rapid and return-to-isotropy models. The Lee et al.'s flows are irrotational strain flows and relaxation flows from various irrotational strains. The irrotational strain flows include axisymmetric contractions (AXK-AXM), axisymmetric expansions (EXO-EXQ) and plane strains (PXA-PXE: the cases of suppression in "22" direction, expansion in "33" direction and no strain in "11" direction). Eleven of them are used for our direct comparisons with rapid models. The relaxation flows are from axisymmetric contractions (K3R-M5R), axisymmetric expansions (O3R-Q6R) and plane strains (A2R-H4R). Thirty of them are used for direct comparisons with return-to-isotropy models.

Figures 1-4 show the direct comparisons of five rapid models with the Rogers et al.'s DNS data (C128U, C128V, C128W and C128X). The two tensorially linear models (LRR[1] and SSG[2]) deviate from the DNS data significantly for the $\Pi_{11}^{(1)}$ and $\Pi_{22}^{(1)}$ components for all the four cases. However they perform reasonably well for the $\Pi_{33}^{(1)}$ and $\Pi_{12}^{(1)}$ components except for the case of C128V in which the models are off for the $\Pi_{33}^{(1)}$ component. For most thin shear layer flows, the component $\overline{u_1u_2}$ is more important than others. Therefore we may expect that the LRR and SSG models would predict thin shear layer flows reasonably well. However for flows where all components are important, the above linear models would not perform well. We also notice that the SSG model is a quasi-linear model with four model coefficients, but according to all test cases, it seems that the SSG model does not show any better performance than the LRR model. Apparently, either the model coefficients in the SSG model are not chosen properly or the deficiency due to the inconsistency with Eq.(21) shows up in these comparisons. On the other hand, three tensorially nonlinear models (FLT[3], SL[4] and SM[5]) perform much better than the linear models, expecially the SL and SM models, they compare very well with the Rogers et al.'s DNS data for all the cases and all the components.

Figures 5-8 compare seven return-to-isotropy models with the Rogers et al.'s DNS data. Two of them (Rotta[6] and Lumley[7]) are tensorially linear in the Reynolds stress, others are nonlinear. We notice that all the return-to-isotropy models can be written in a basic form of Eq.(28) which was proposed by Lumley. In fact, Eq.(28) is the most general form provided that $\Pi_{ij}^{(2)}$ is an isotropic function of b_{ij} and Re, where β and γ are functions of II, III and Re. Therefore, all the return-to-isotropy models are just the variations of Eq.(28), depending on the choice of model coefficients β and γ. It is evident from these

direct comparisons that the linear Rotta[6] model does not perform very well except for the component $\Pi_{33}^{(2)}$, in which the Rotta[6] model does very well. However this component is not very important for most shear flows. The SS model[8] and the YA model[12] are nonlinear models; they behave very much like the Rotta model except in the component $\Pi_{33}^{(2)}$. On the overall, the SS and YA models perform worse than the Rotta model. The C&L model[11] is also a nonlinear model, it behaves better than the Rotta model for all the cases except in the component $\Pi_{33}^{(2)}$ in which the C&L model is the worst one among all the models. Apparently, the model coefficients in the above mentioned models are not appropriate according to the Rogers et al.'s shear flows. However, surprisingly enough, the Lumley's quasi-linear model[7] performs very well for all the cases. It was well known that the Lumley's model works excellent for the flows in which $III < 0$, but it would not work very well for the cases[10] with $III > 0$. Here in the Rogers et al.'s flows, $III > 0$, and it still works quite well. We think this is partly due to the low Reynolds number behavior of the Lumley's model and the Rogers et al.'s DNSs are the low Reynolds number flows. The CL model[10] is particularly designed for the cases with $III > 0$ based on their experiments of flows relaxing from the axisymmetric expansion. It also works reasonably well in all the Rogers et al.'s flows. Finally, the S&M model[5], which is derived from Eq.(28) using realizability and matches the behavior of the low Reynolds number turbulence (final period of decay), performs very much like the Lumley's linear model with just a little improvement over it.

From these direct comparisons, it is clear that the SL[4] and SM[5] nonlinear models perform the best among the five rapid models. For the return-to-isotropy models it is also clear that the Lumley's linear model[7], the S&M[5] model and the CL[10] model are the best among the seven models tested here.

The Lee et al.'s flows are also homogeneous but their characteristics are very different from the Rogers et al.'s homogeneous shear flows. Even though these flows do not often occur in the nature, it is still interesting to see how do the models of rapid and return-to-isotropy terms perform in these critical numerical simulations. We will first look at the comparisons of the rapid models and then the return-to-isotropy models.

Figures 9-11 compare the rapid models with the three axisymmetric contraction flows. These figures show that no rapid models, except the SL[4] and SM[5], can predict the simulation data well. The SSG and LRR models, which are tensorially linear, perform the worst. The SSG is even worse than the LRR. The nonlinear model FLT is much better than the SSG and the LRR, but still significantly deviates from the DNS data, especially in the case AXM, which has high shear rates ($S = 38.2 - 96.5$). We notice that in the axisymmetric contraction flows, only the SL and SM rapid models show very good performance for all the cases and all the components. Figures 12-14 compare the same

rapid models with the three axisymmetric expansion flows. This time, no rapid models can follow the DNS data well. However, the SM model performs a little better than others, and the SSG model is the worst, especially when the shear rate becomes larger. Figures 15-19 compare the rapid models with the five plane strain flows. The linear LRR model does a good job for the $\Pi_{22}^{(1)}$ component, but bad job for the $\Pi_{33}^{(1)}$ component. The SSG model performs worse than the LRR model. The nonlinear models (FLT, SL and SM) do good job for the $\Pi_{33}^{(1)}$ component, but for the $\Pi_{22}^{(1)}$ components, they are even worse than the linear models.

Now let us look at the direct comparisons of eight return-to-isotropy models with the Lee et al.'s relaxation flows. Figures 20-25 compare the models with the six flows relaxing from axisymmetric contractions (K3R-M5R). In these flows, $III < 0$, the Lumley's model works excellent for all the cases and all the components (the CL model in this case is the Lumley's model). The nonlinear model of S&M works as good as the Lumley's model. All other models deviate from the DNS data significantly, especially when the flows relaxing from higher strain rates (e.g. M5R). It is also interesting to note that the simple Rotta model works better than the nonlinear models of SS, YA, C&L and HP[9]. The HP model performs worst among all the models. Figures 26-27 compare the models with the two flows relaxing from axisymmetric expansions (O3R, O6R), for which $III \geq 0$. Figures show that the nonlinear models of S&M[5] and CL have better behavior than the other models. This time, the model of C&L performs the worst. Finally, Figures 28-49 compare the models with the twenty two relaxation flows from plane strains (A2R-H4R). In these flows, the Lumley's linear model and nonlinear models of S&M and CL predict the $\Pi_{33}^{(2)}$ component very well for all the cases. For $\Pi_{22}^{(2)}$, they are also the best among others. However, this time, the SS[8] and HP[9] models appear to be the best in the $\Pi_{11}^{(2)}$ component, and the YA and C&L models are the worst among others.

From the above critical comparisons with the Lee et al.'s irrotational strain flows, we see that the rapid models of SL[4] and SM[5] work very well in all the axisymmetric contraction flows. In the axisymmetric expansion flows and plane strain flows they do not work very well. However, on the overall they still perform better than others. The comparisons of return-to-isotropy models with relaxation flows show that the Lumley's linear model[7] is perfect for all the cases with $III < 0$, so is the model of S&M[5]. For the relaxation flows from the axisymmetric expansions and plane strains, the S&M[5] and CL[10] models show better performance.

5. Concluding remarks

We have made the direct comparisons of five rapid models and eight return-to-isotropy models with the direct numerical simulations of Rogers et al.[13] and Lee et al.[14] Forty

five DNS flows are used for the direct comparisons. We notice that the Reynolds number in all these simulations is low, and therefore, they may not represent the real turbulence in the nature. However, the model terms concerned here are mainly pressure related correlations. Eq.(7) indicates that the fluctuating pressure is not directly related to the viscosity, hence the pressure related correlation terms may not be directly affected by the Reynolds number, especially the rapid term. The return-to-isotropy term which includes the deviatoric part of dissipation rate tensor may have some dependence on the Reynolds number. According to the above consideration, we think that the direct comparisons with the low-Reynolds DNS data are legitimate, although we should keep in mind the possible low-Reynolds number effect of the DNS data.

We have directly compared five rapid models with fifteen DNS flows: four of the Rogers et al.'s shear flows, eleven of the Lee et al.'s irrotational strain flows (axisymmetric contraction, axisymmetric expansion and plane strain). Comparing the performance of the LRR and SSG models, which are tensorially linear in the Reynolds stress, we conclude that the SSG model gives very little improvement over the LRR model. In fact in many cases, it is worse than the LRR model. The reason is not very clear. However, we notice that the SSG model does not satisfy the normalization condition of Eq.(7) which may be a cause for its poor behavior. If we impose the constraint of Eq.(7) on the SSG model, then it will exactly reduce to the LRR model. In fact it can be shown that the most general form of the rapid model, which is tensorially linear in the Reynolds stress, is the LRR model. Therefore, in general, the treatment used in the SSG model would hardly give any improvement over the LRR model. A natural way to improve the model is to use a more general nonlinear form and more general model constraints. A typical example is the SL[4] model. It starts with the most general form, using full realizability constraints together with the other conventional constraints given by Eq.(5)-Eq.(7). The result is a well behaved model. Indeed, from the direct comparisons with the DNS data, the SL[4] model and its variation form of SM[5] model give the best performance in most of the cases. As to the FLT[3] model, it is also a nonlinear model. It starts with a tensorially cubic dependance on the Reynolds stress with *constant* coefficients (in general, these coefficients should not be restricted to constants). In addition, the two component conditions of turbulence have been imposed. However, the FLT model ignores the Schwarz' inequality. Its final form contains two undetermined model constants, but one of them is set to zero. The performance of the FLT model, from the direct comparisons with the DNS data, is on the overall better than the linear models, but does not compare with the performance of the SL and SM models. So from these direct comparisons of the rapid models, we conclude that the SL[4] model and its variation form SM[5] are clearly the best. Having said this we notice that, as Reynolds[22] pointed out, any of the above rapid models will not show any effect of the rotation on the invariants (II, III) of the anisotropy tensor b_{ij}. This is clearly a theoretical deficiency of the current rapid models. A further investigation is needed to find

that how serious this deficiency will be in the practice.

We have directly compared eight return-to-isotropy models with thirty four DNS flows: four shear flows and thirty relaxation flows from axisymmetric contraction, axisymmetric expansion and plane strain. As was discussed earlier, all the return-to-isotropy models are the variation of Eq.(28) derived by Lumley[7]. Therefore the differences in the models are due to the different choices of the model coefficients. Two linear models are the Rotta[6] and Lumley[7] (which is quasi-linear in b_{ij}). The Lumley's model satisfies realizability, matches the data of Comte-Bellot and Corrsin[21] and the limit of the final period of decaying turbulence. It performs perfectly when $III < 0$. It also compares well with the DNS data in which $III \geq 0$. The Rotta's model does not compare with the performance of the Lumley's model. In fact, the nonlinear models of SS, YA, HP and C&L also do not compare with the performance of the Lumley's model. Apparently the model coefficients chosen in these models are not appropriate. The CL[10] model is designed for the flows with $III \geq 0$ and is based on their experiments of the relaxing turbulence. It does work better than the Lumley's model when $III \geq 0$. Finally, the S&M[5] model is a nonlinear model, it works just like the Lumley's model when $III < 0$. When $III \geq 0$, it shows an improvement over the Lumley's model according to the DNS data. So from these direct comparisons of the return-to-isotropy models, we conclude that the combination of the Lumley's model and the Choi's model, that is the CL[10] model, will give the best performance. The S&M[5] model seems as good as the CL model according to these comparisons. Having said this, we notice that the existing return-to-isotropy models do not follow the relaxation flows from expansion and plane strain very well. Therefore there is still a need to further investigate and improve the return-to-isotropy models.

ACKNOWLEDGMENTS

One of the authors, T.-H. Shih, is grateful to Dr. Nagi N. Mansour for his guidance in using the DNS data for direct comparisons of turbulence models. Thanks are also due to Dr. Aamir Shabbir for his useful advice and discussion.

REFERENCES

[1] Launder, B.E., Reece, G.J., & Rodi, W. 1975., " Progress in the development of a Reynolds-stress turbulence closure," *J. Fluid Mech.* (1975), vol. 68, pp.537-566.

[2] Speziale, C.G., Sarkar, S. and Gatski, T.B., "Modeling the pressure-strain correlation of turbulence: an invariant dynamical systems approach," *J. Fluid Mech.* (1991), vol. 227, pp.245-272.

[3] Fu, S., Launder, B.E. and Tselepidakis, D.P., "Accommodating the effects of high strain rates in modeling the pressure-strain correlation. *UMIST Mech. Engng Dept Rep.* TFD/87/5, 1987.

[4] Shih, T.-H. & Lumley, J.L., 1985. Modeling of pressure correlation terms in Reynolds stress and scalar flux equations. Rep. FDA-85-3, *Sibley School of Mech. & Aero. Engrg.*, Cornell University.

[5] Shih, T.-H. and Mansour, N.N., "Reynolds Stress Modeling of Homogeneous Turbulence and Comparison with Numerical Simulations," *Center for Turbulence Research* Proceedings of the Summer Program 1987.

[6] Rotta, J.C., Z. Phys. **129**, 547 (1951).

[7] Lumley, J.L., "Computational modeling of turbulent flows," *Adv. Appl. Mech.* 1978, 18, 123.

[8] Sarkar, S. and Speziale, C.G., "A simple nonlinear model for the return to isotropy in turbulence," *Phys. Fluids*, A2 (1), January, 1990.

[9] Haworth, D.C. and Pope, S.B., "A generalized Langevin model for turbulent flows," *Phys. fluid* **29** (2), February 1986.

[10] Choi, K.S. and Lumley, J.L., *Proceedings of the IUTAM symposium, Kyoto, 1983, Turbulence and Chaotic phenomena in Fluids*, edited by T.Tatsumi (North-Holland, Amsterdam, 1984), p.267.

[11] Craft, T.J. and Launder, B.E., "Computation of Impinging Flows Using Second-Moment Closure," Eighth Symposium on Turbulent Shear Flows, Technical University of Munich, September 9-11,1991.

[12] Yamamoto, M. and Arakawa, c., "Study on the pressure-strain term in Reynolds stress model," *Eighth Symposium on Turbulent Shear Flows*, Technical University of Munich, September, 9-11, 1991.

[13] Rogers, M.M., Moin, P. & Reynolds, W.C., 1986, The structure and modeling of the hydrodynamic and passive scalar fields in homogeneous turbulent shear flow. Dept. Mech. Engng. Rep. TF-24, Stanford University: Stanford California.

[14] Lee, M.J. & Reynolds, W.C. 1985. Numerical experiments on structure of homogeneous turbulence. Dept. Mech. Engng. Rep. TF-24, Stanford University: Stanford California.

[15] Schumann, U. 1977. Realizability of Reynolds Stress Turbulence Models. Phys. Fluids, 20, 721-725.

[16] Pope, S.B. 1983. Consistent Modeling of Scalars in Turbulent Flows, Phys. Fluids, Vol. 26, 404-408.

[17] Reynolds, W.C. (1987) Fundamentals of Turbulence for Turbulence Modeling and Simulation. Lecture Notes for Von Karman, March 16-17, 1987.

[18] Speziale, C.G. 1983.Closure Models for Rotating Two-dimensional Turbulence. Geophys. and Astrophys. Fluid Dynamics, 23,69.

[19] Shih, T.-H., Shabbir, A. and Lumley., "Advances in Modeling the Pressure Correlation terms in the Second Moment Equations," NASA TM 104413, ICOMP-91-09; CMOTT-91-03.

[20] Chou, P.-Y. Quart. App. Math. vol. 3, 38, 1945.

[21] Comte-Bellot, G. and Corrsin, S. 1966. The use of a contraction to improve the isotropy of grid-generated turbulence. J. Fluid Mech. 25, 657-682

[22] Reynolds, W.C. 1989. Effect of Rotation on Homogeneous Turbulence. Tenth Australian Fluid Mechanics Conference, December 11-15.

[23] Lumley, J.L. 1983. Turbulence Modeling. ASME Journal of Applied Mechanics, vol. 50, pp. 1097-1103.

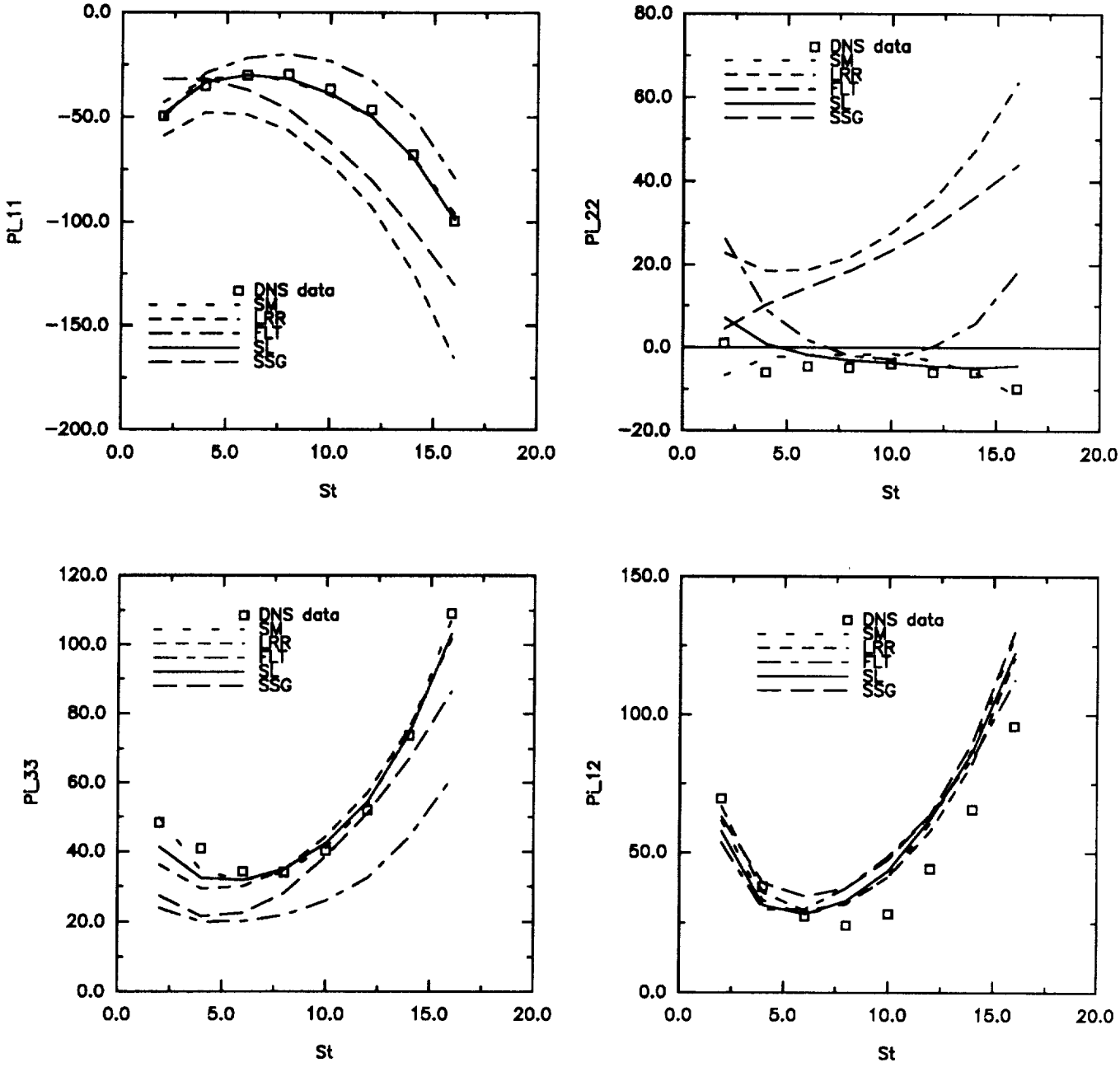

Figure 1. Direct comparison of the rapid models with the DNS data of the homogeneous shear flow C128U (Rogers et al.[13]).

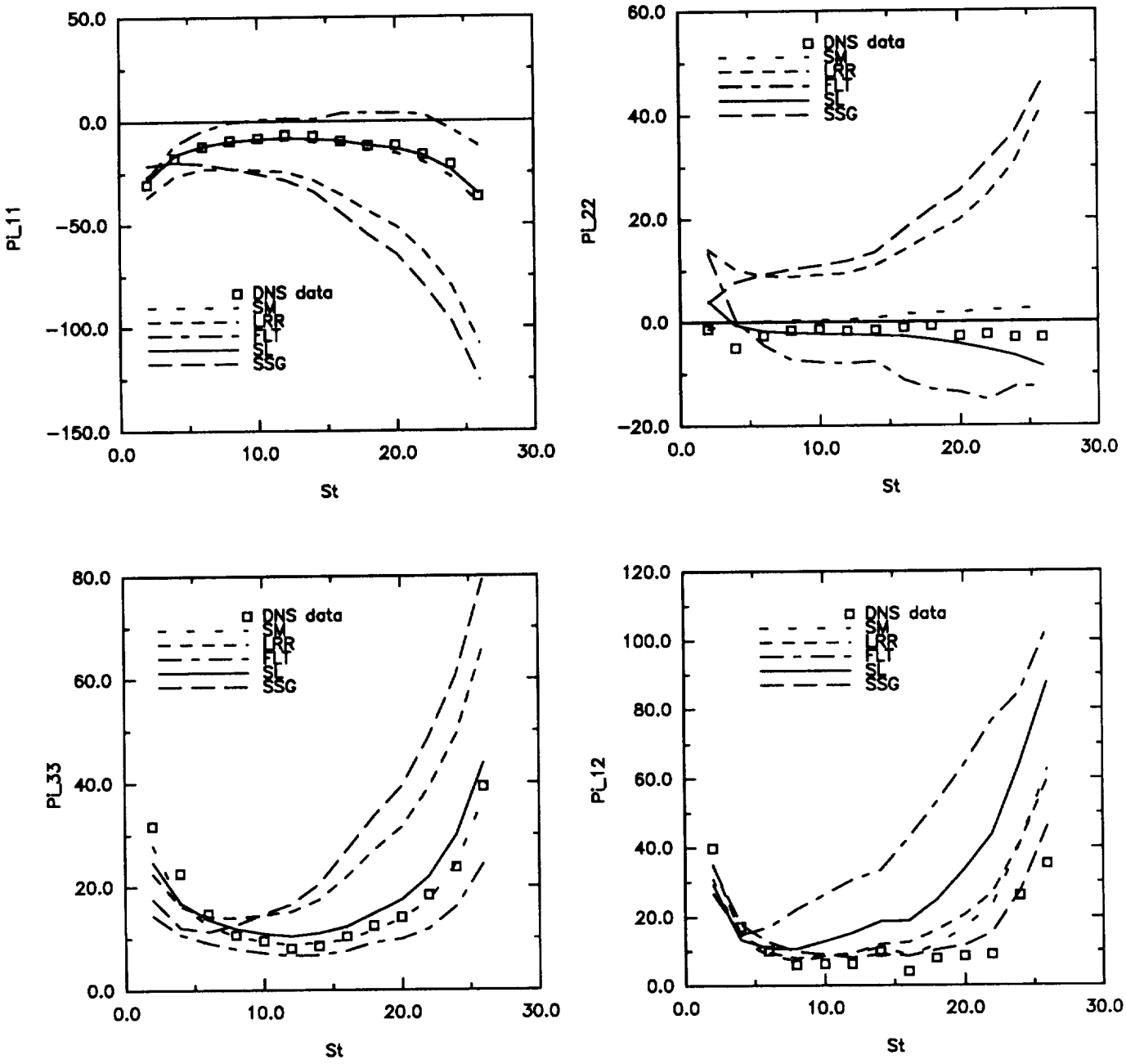

Figure 2. Direct comparison of the rapid models with the DNS data of the homogeneous shear flow C128V (Rogers et al.[13]).

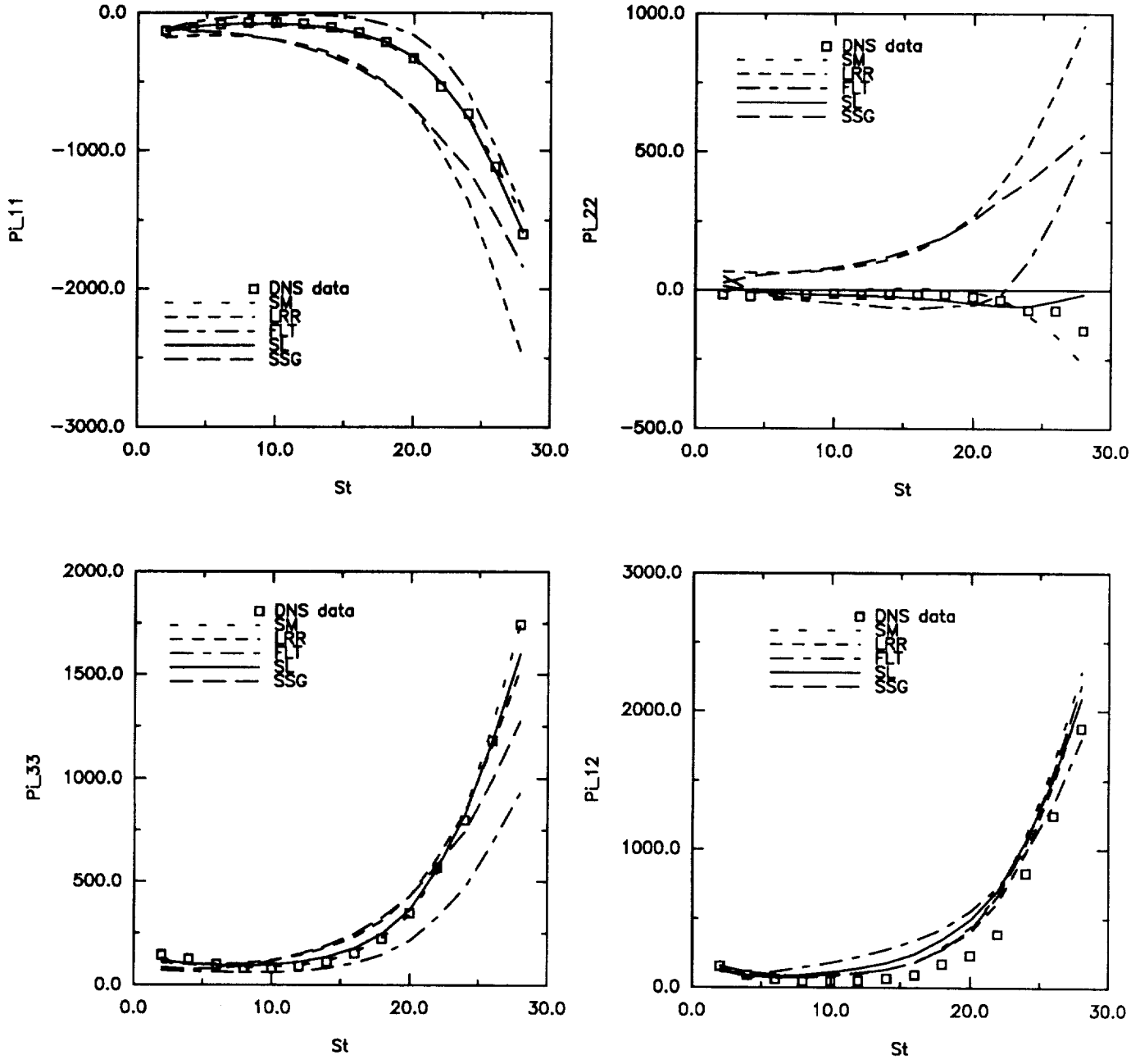

Figure 3. Direct comparison of the rapid models with the DNS data of the homogeneous shear flow C128W (Rogers et al.[13]).

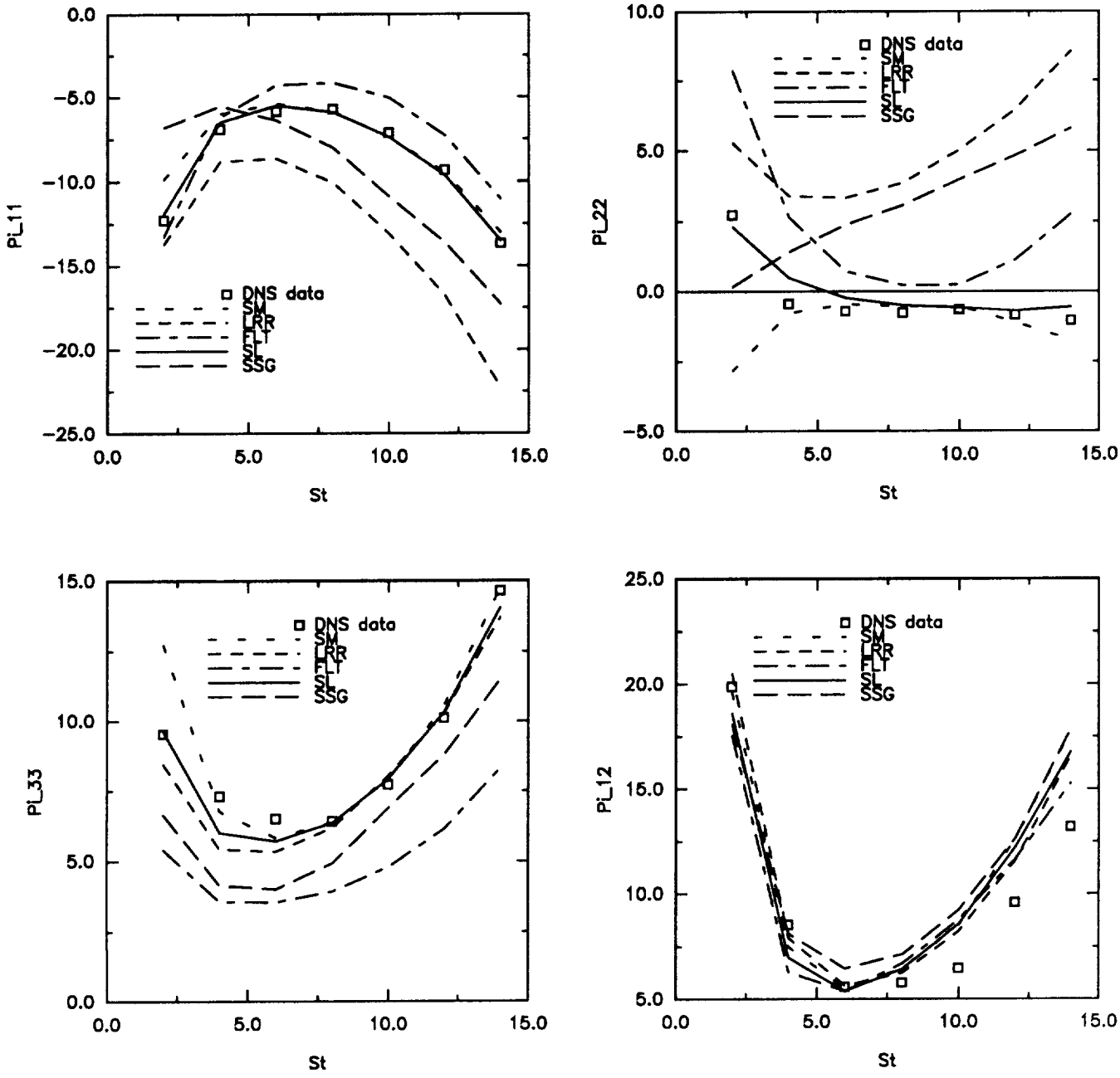

Figure 4. Direct comparison of the rapid models with the DNS data of the homogeneous shear flow C128X (Rogers et at.[13]).

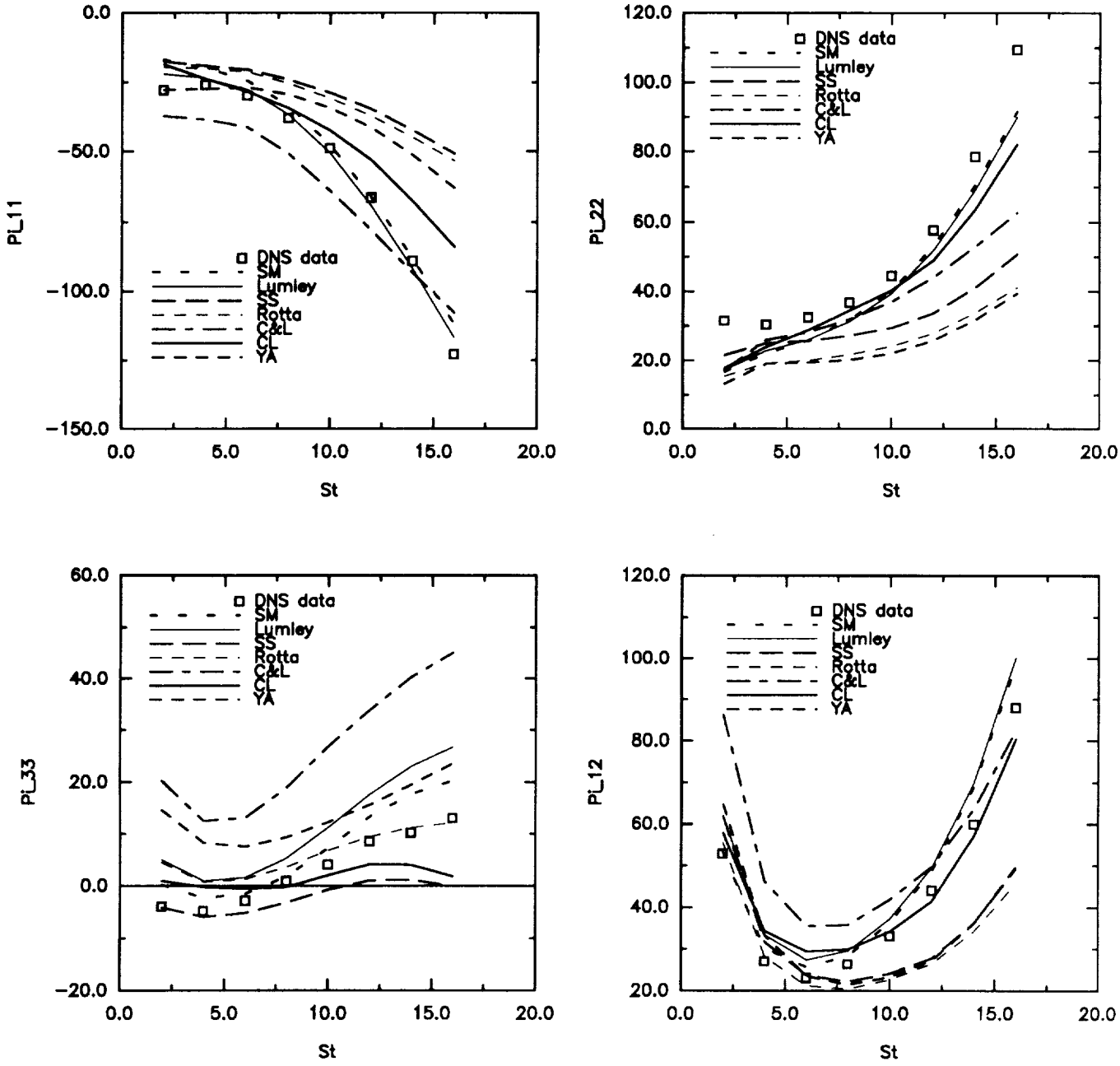

Figure 5. Direct comparison of the return-to-isotropy models with the DNS data of the homogeneous shear flow C128U (Rogers et al.[13]).

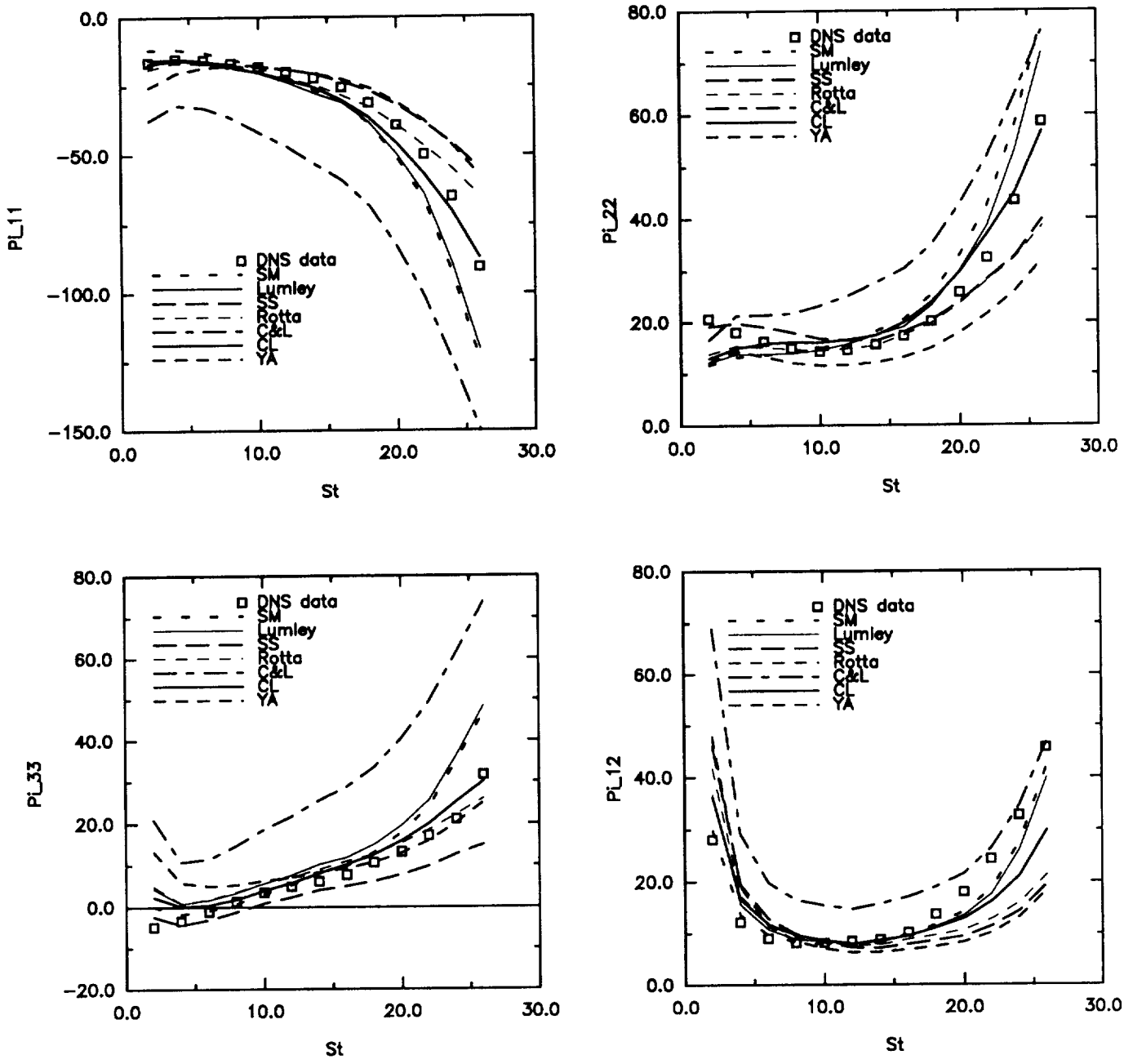

Figure 6. Direct comparison of the return-to-isotropy models with the DNS data of the homogeneous shear flow C128V (Rogers et al.[13]).

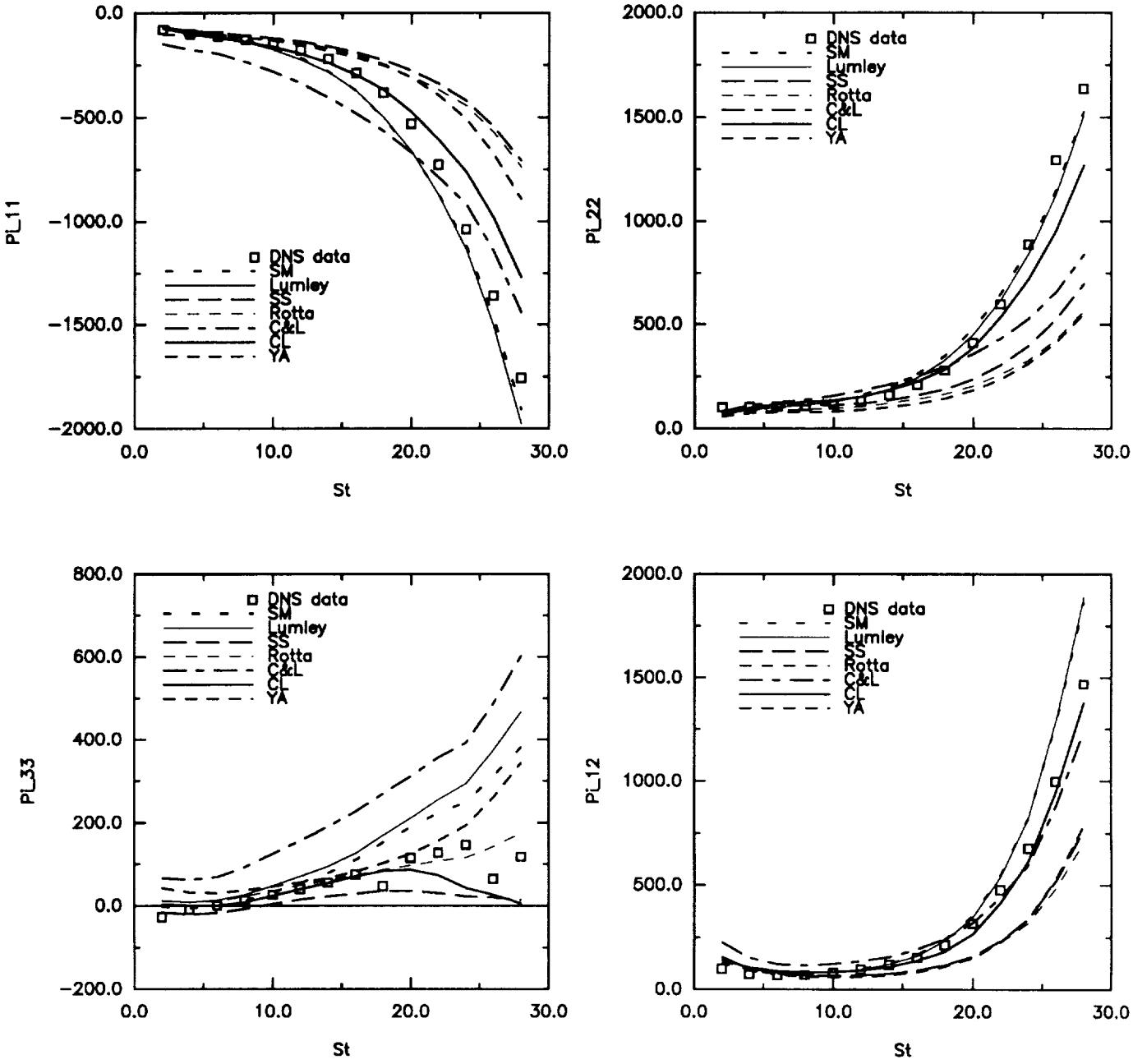

Figure 7. Direct comparison of the return-to-isotropy models with the DNS data of the homogeneous shear flow C128W (Rogers et al.[13]).

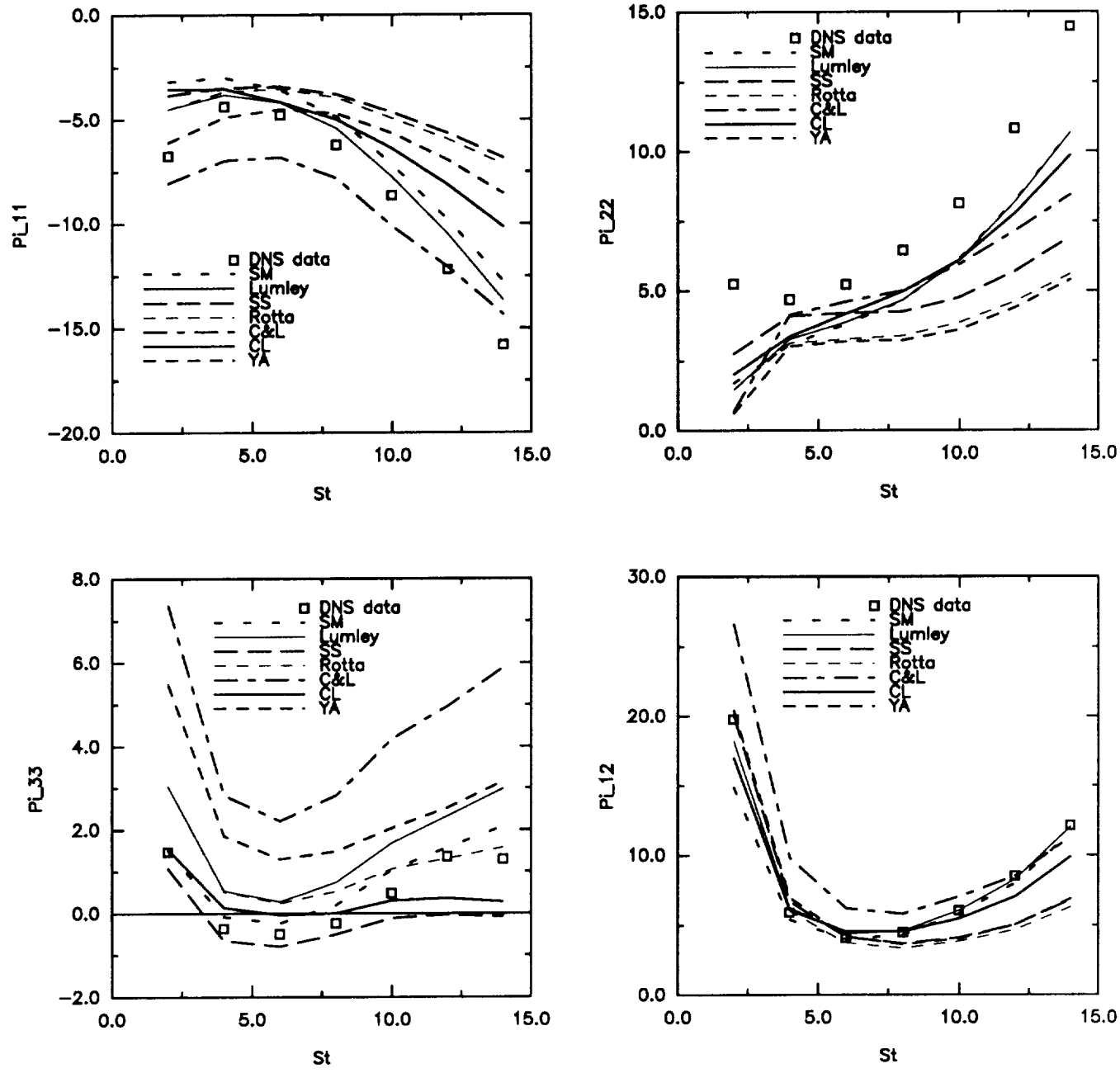

Figure 8. Direct comparison of the return-to-isotropy models with the DNS data of the homogeneous shear flow C128X (Rogers et at.[13]).

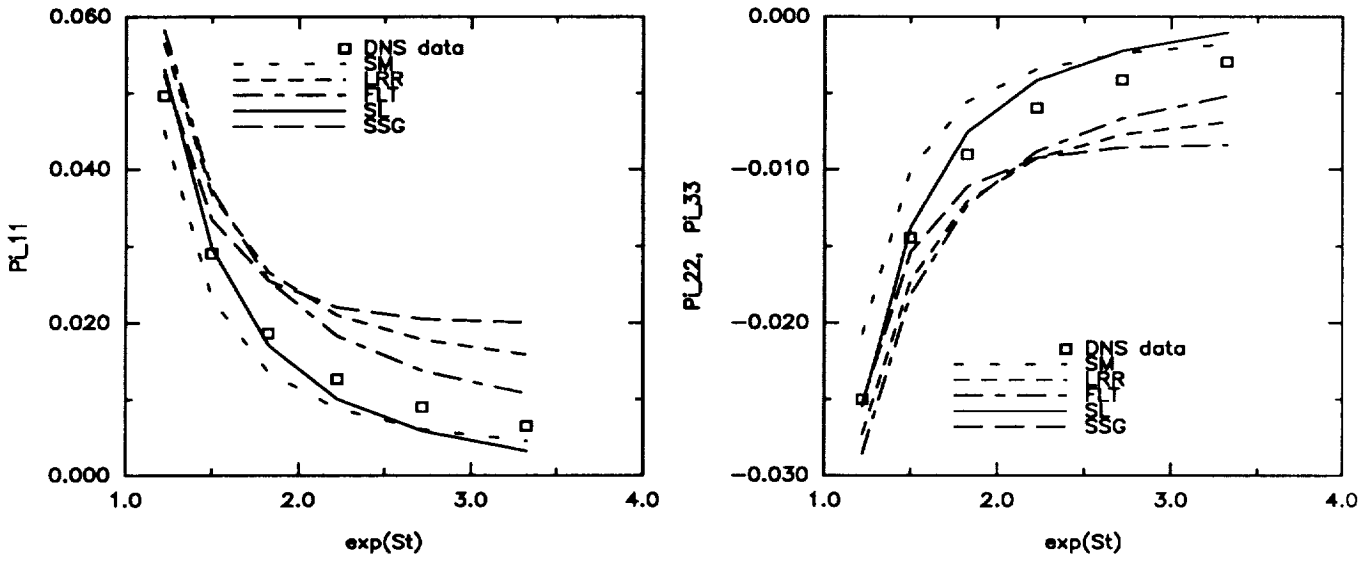

Figure 9. Direct comparison of the rapid models with the DNS data of the axisymmetric contraction AXK (Lee et al.[14]).

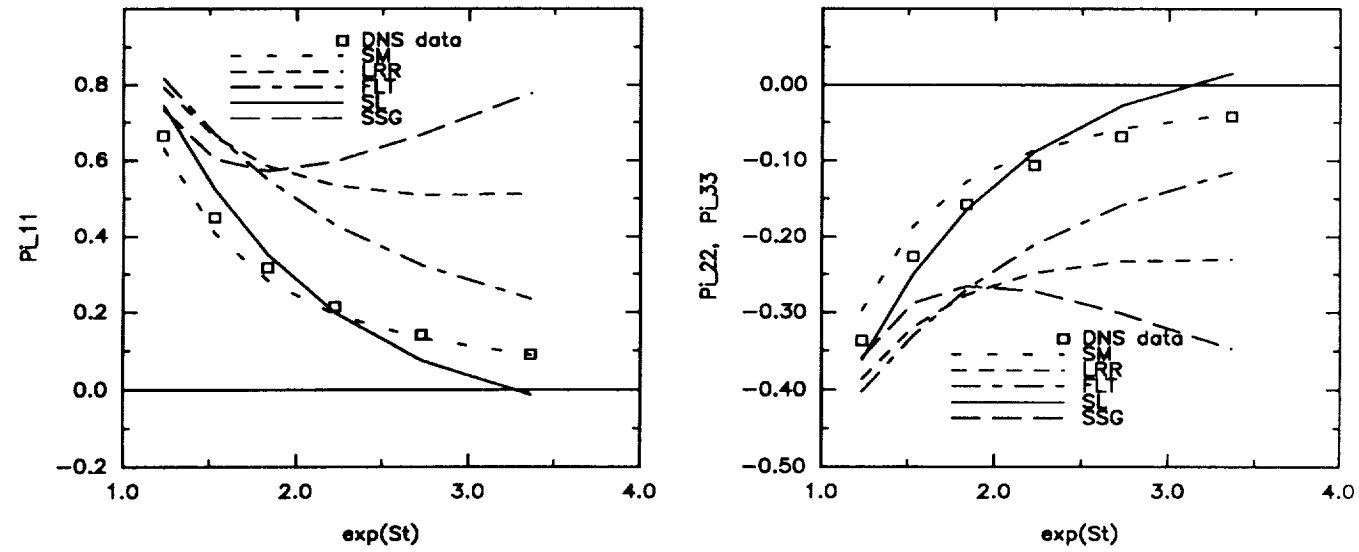

Figure 10. Direct comparison of the rapid models with the DNS data of the axisymmetric contraction AXL (Lee et al.[14]).

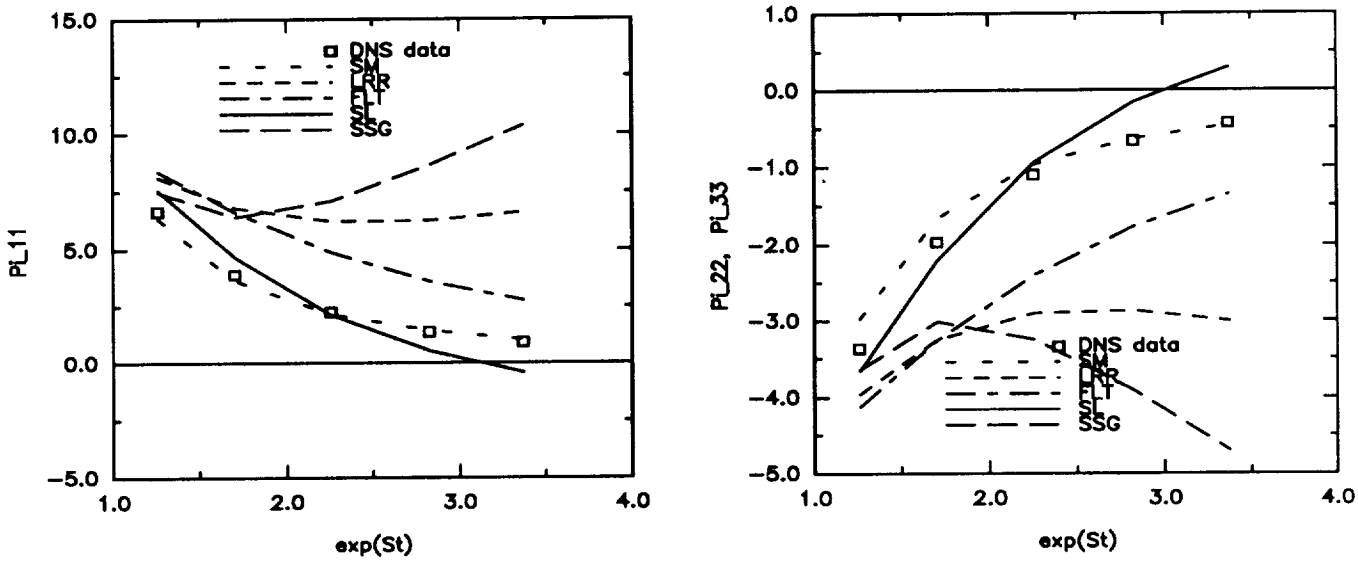

Figure 11. Direct comparison of the rapid models with the DNS data of the axisymmetric contraction AXM (Lee et al.[14]).

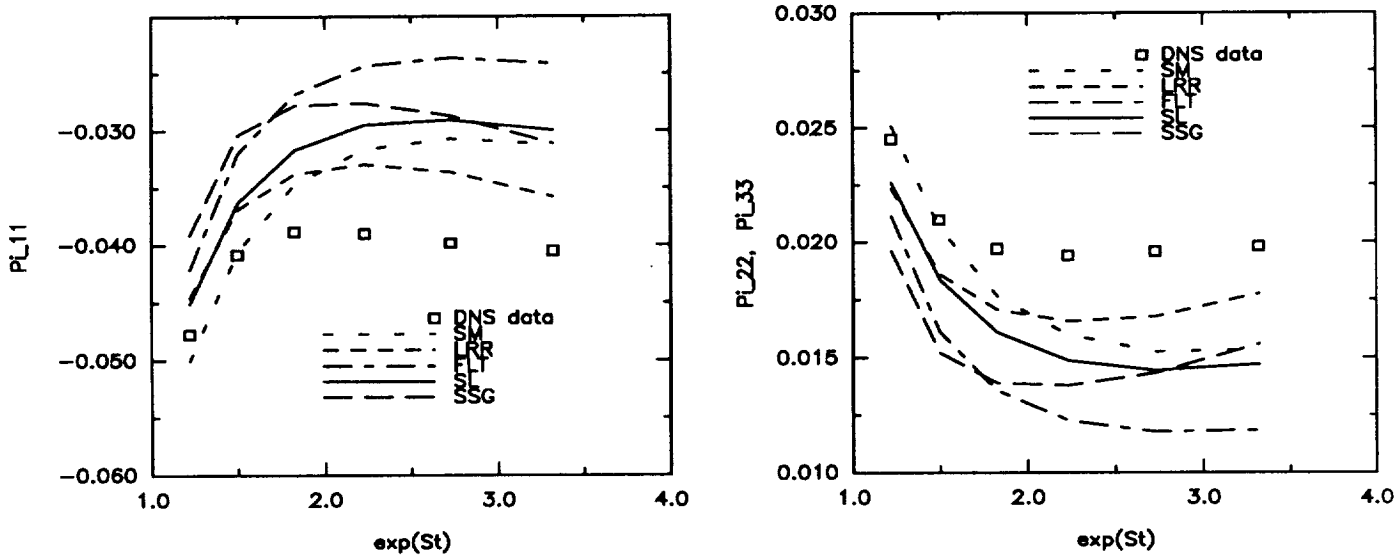

Figure 12. Direct comparison of the rapid models with the DNS data of the axisymmetric expansion EXO (Lee et al.[14]).

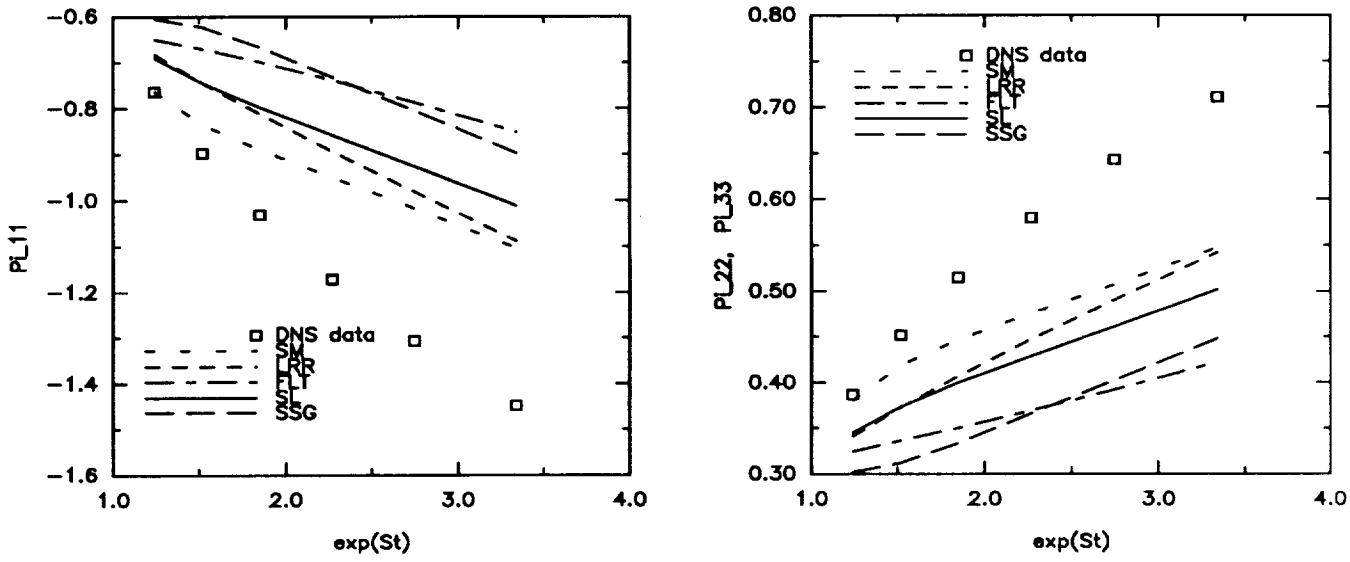

Figure 13. Direct comparison of the rapid models with the DNS data of the axisymmetric expansion EXP (Lee et al.[14]).

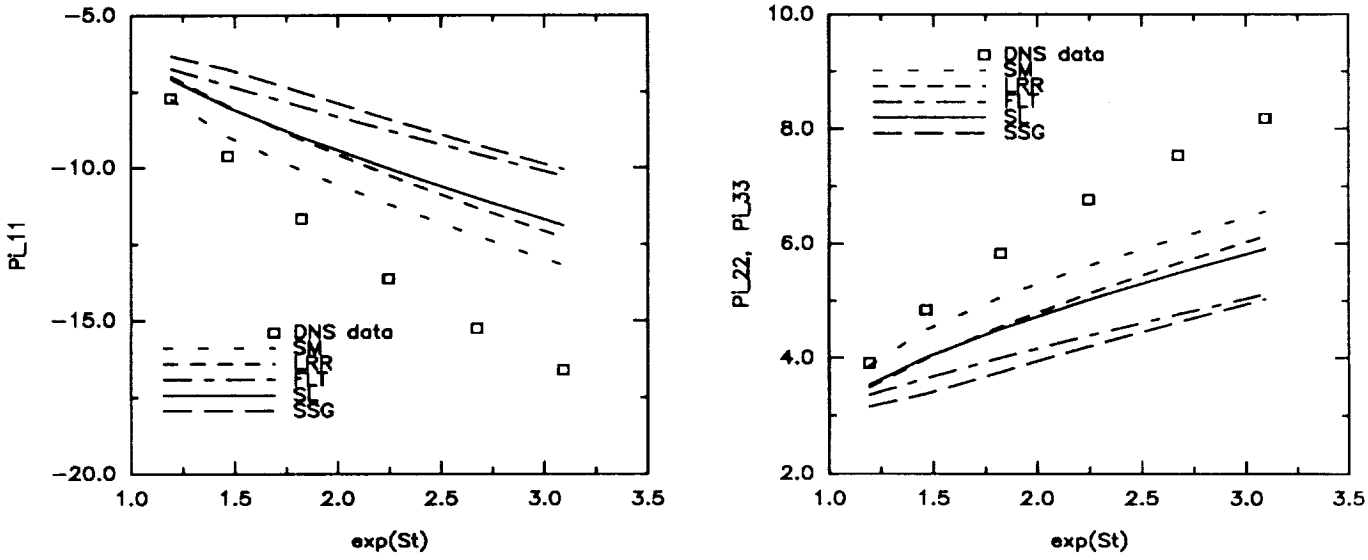

Figure 14. Direct comparison of the rapid models with the DNS data of the axisymmetric expansion EXQ (Lee et al.[14]).

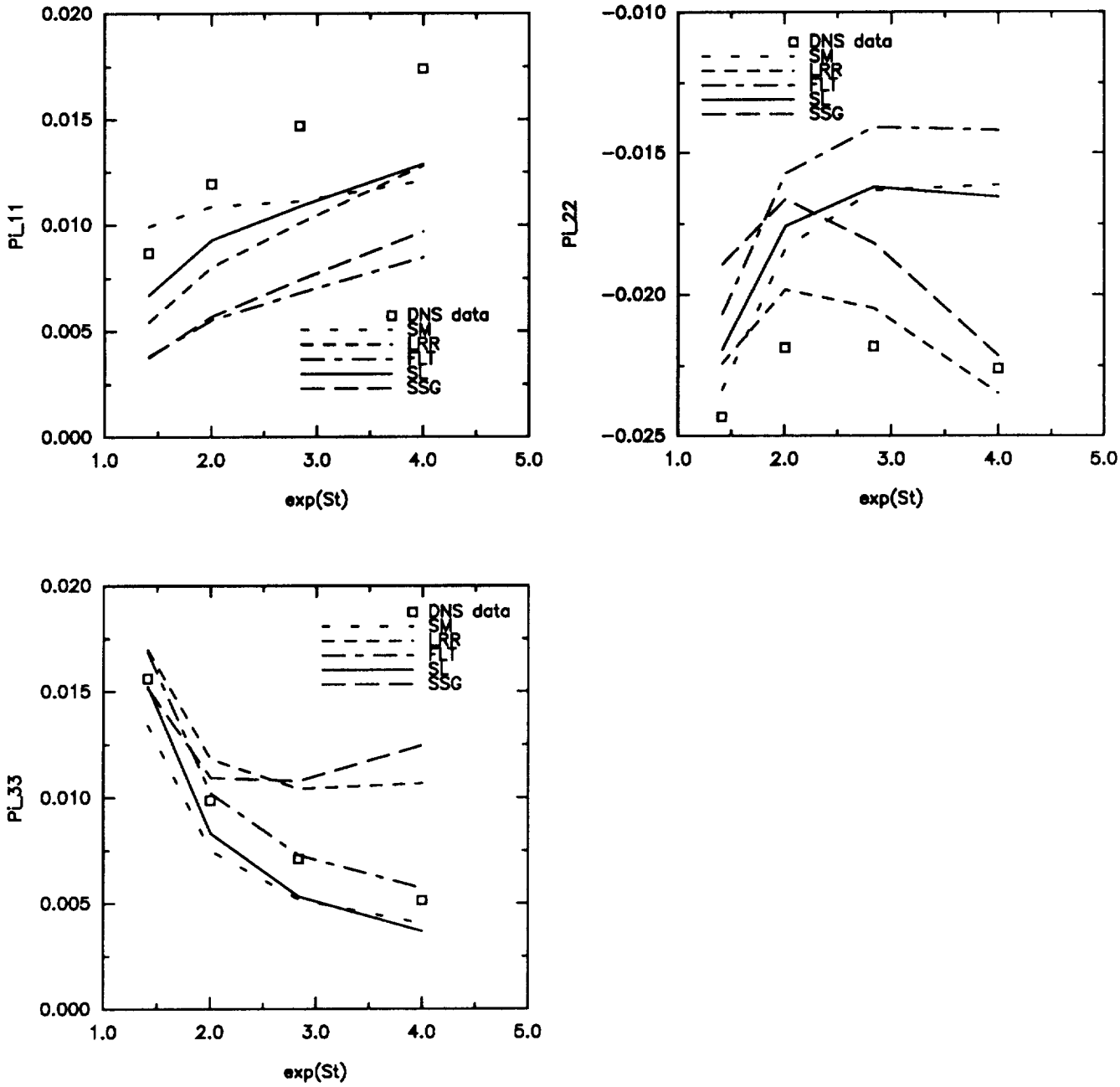

Figure 15. Direct comparison of the rapid models with the DNS data of the plane strain PXA (Lee et al.[14]).

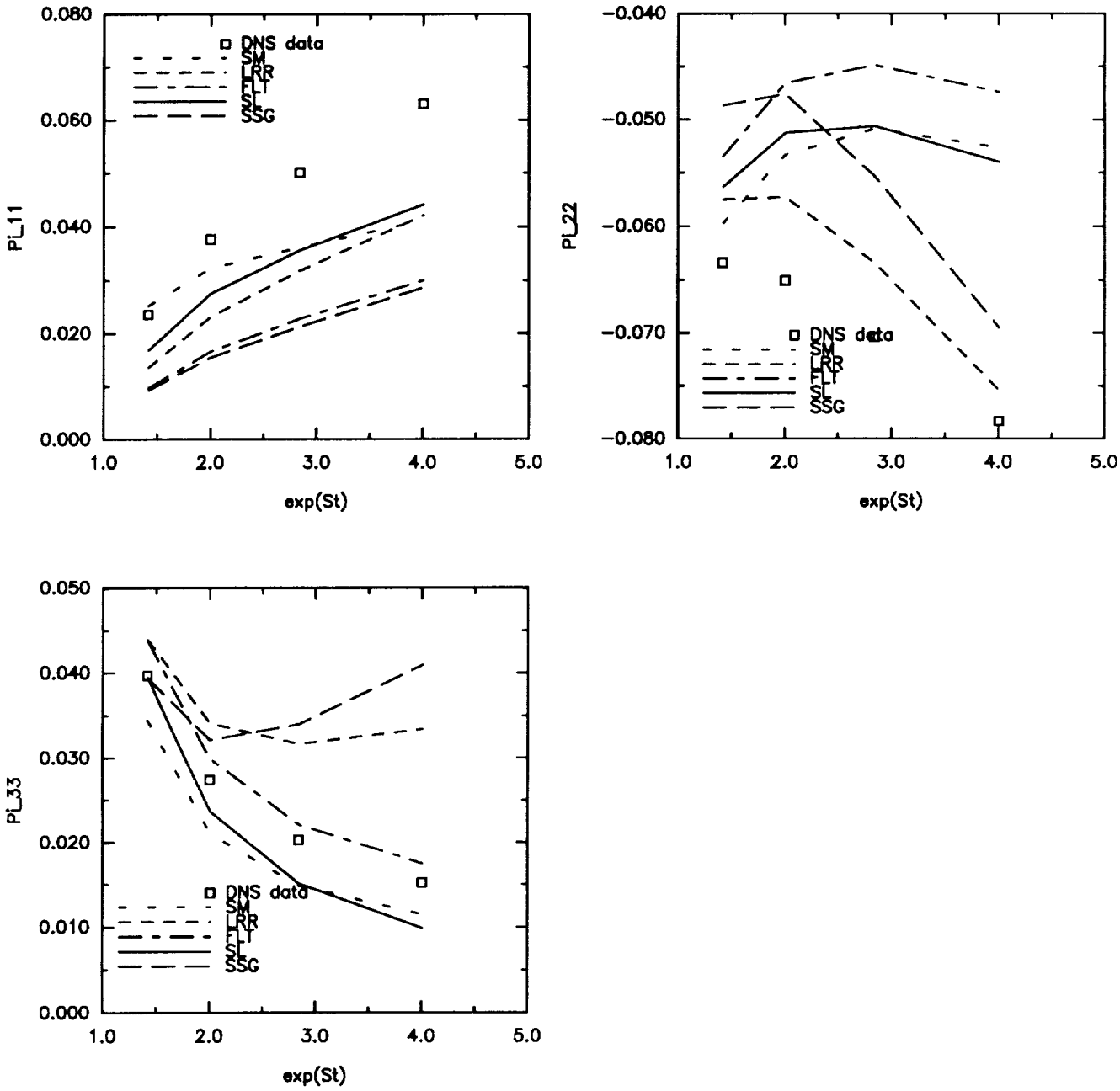

Figure 16. Direct comparison of the rapid models with the DNS data of the plane strain PXB (Lee et al.[14]).

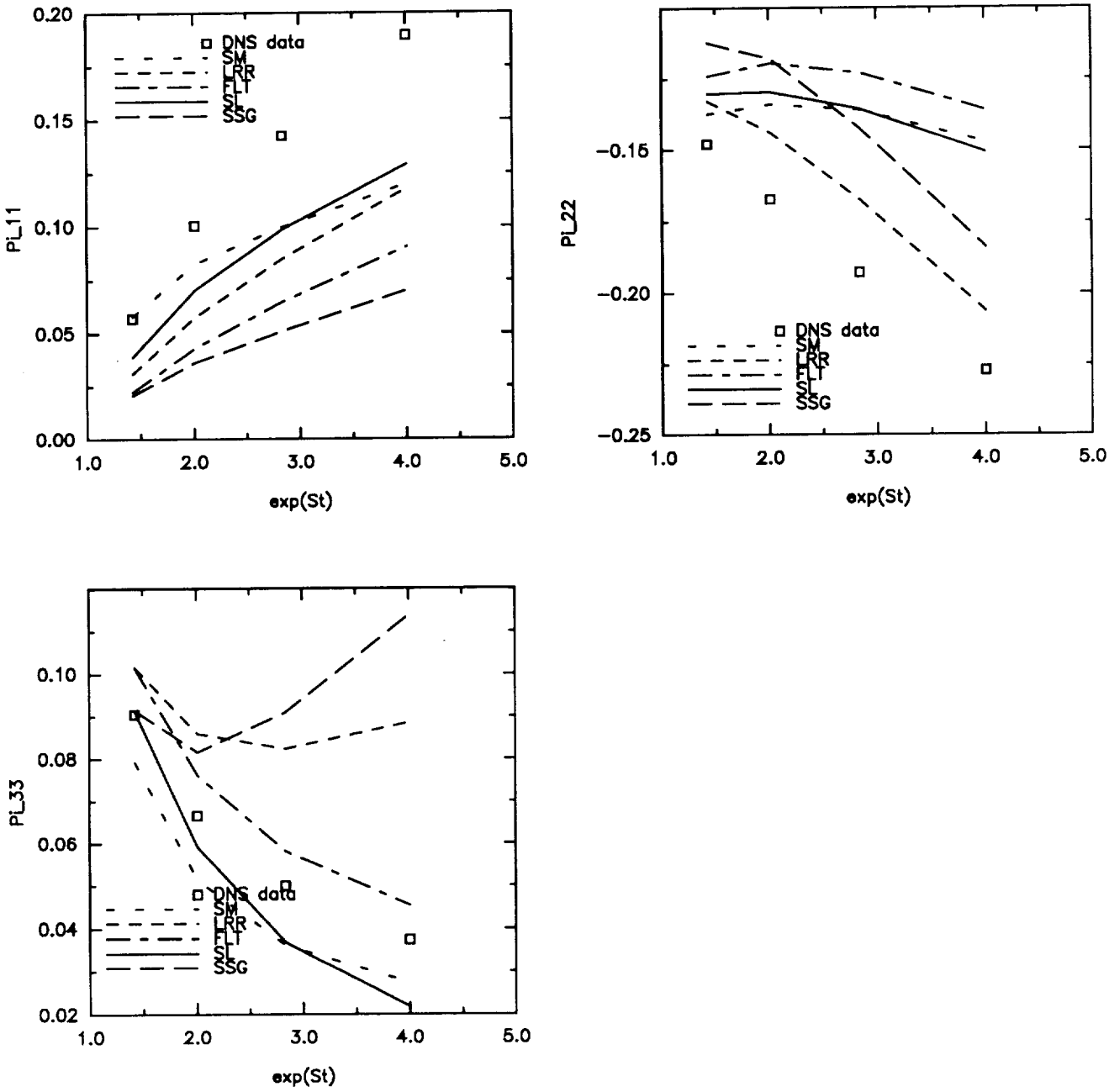

Figure 17. Direct comparison of the rapid models with the DNS data of the plane strain PXC (Lee et al.[14]).

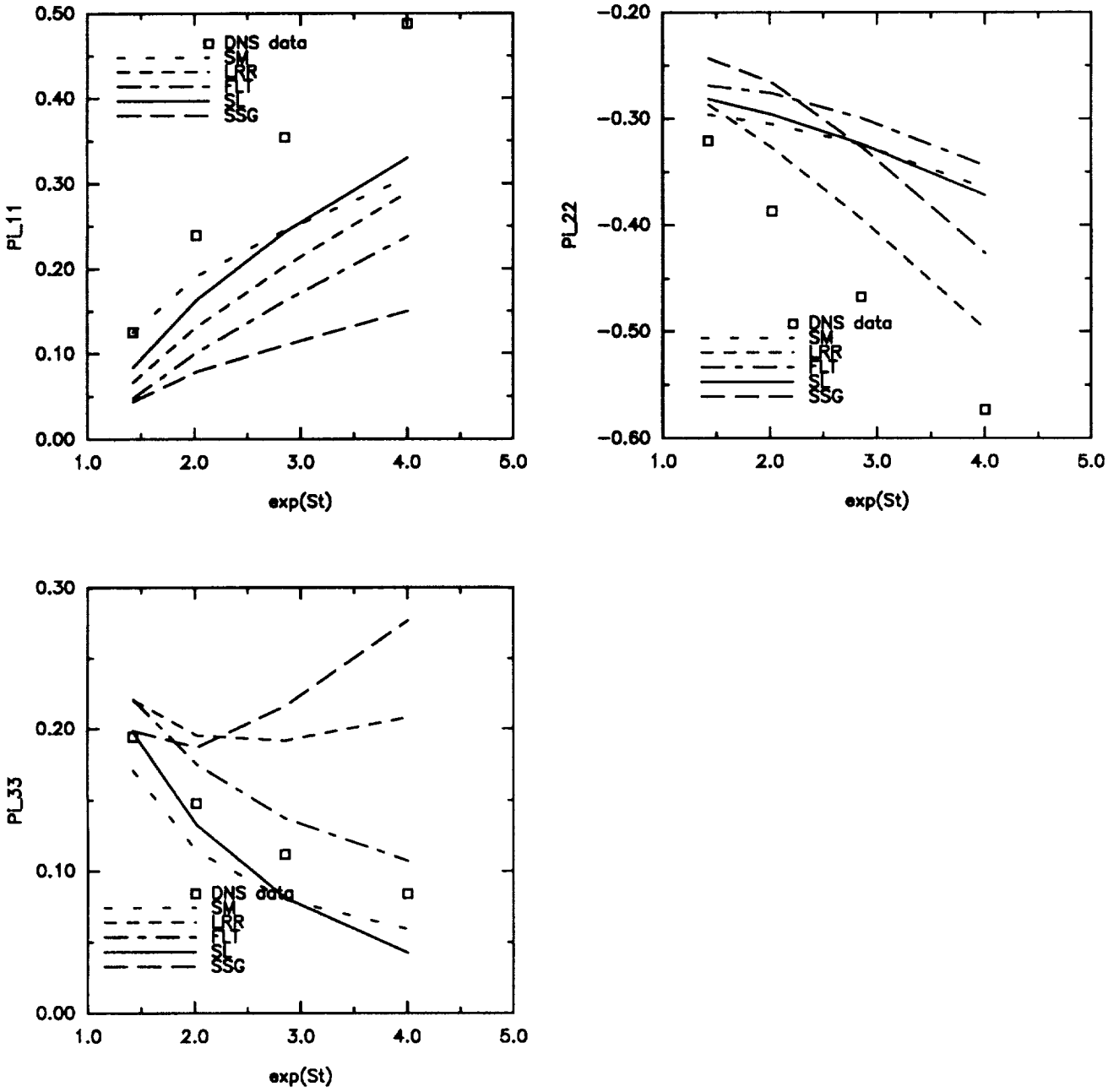

Figure 18. Direct comparison of the rapid models with the DNS data of the plane strain PXD (Lee et al.[14]).

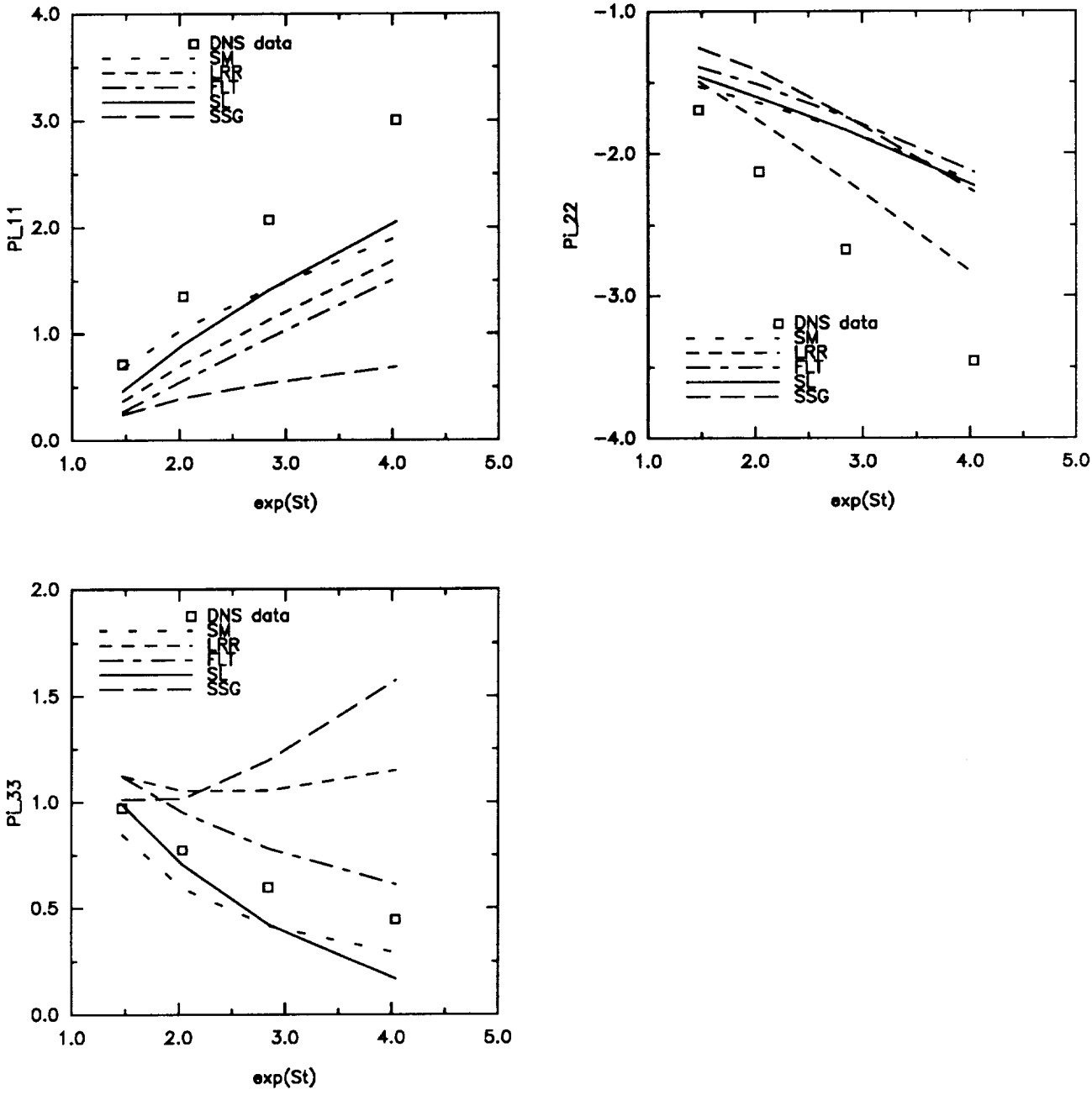

Figure 19. Direct comparison of the rapid models with the DNS data of the plane strain PXE (Lee et al.[14]).

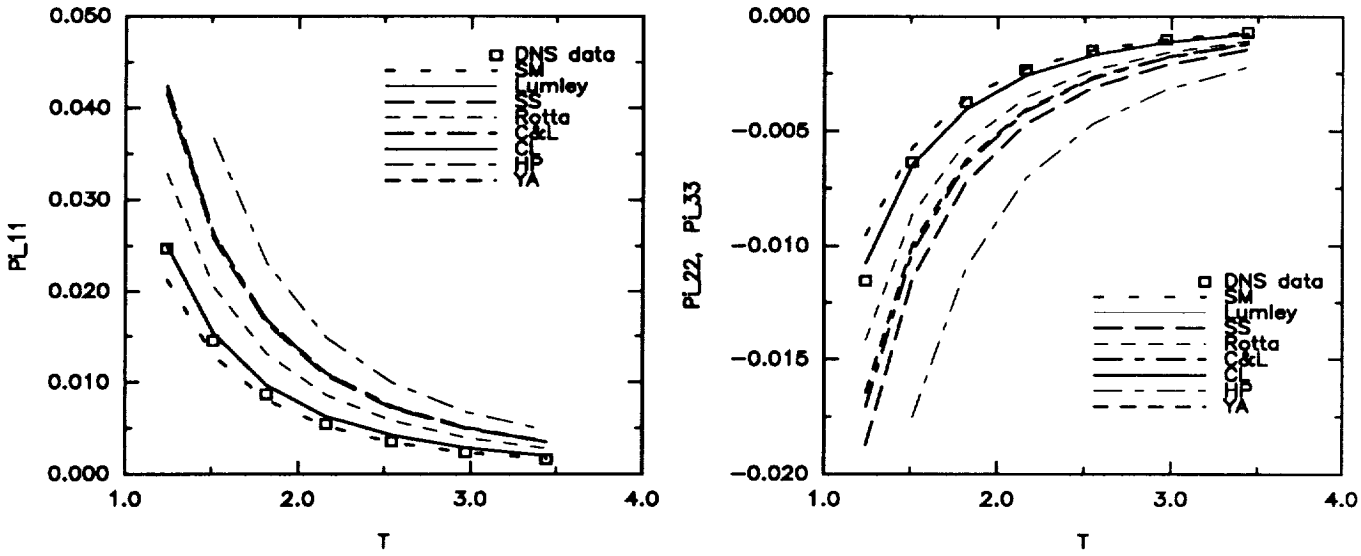

Figure 20. Direct comparison of the return-to-isotropy models with the DNS data of relaxation from axisymm. contraction K3R (Lee et al.[14]).

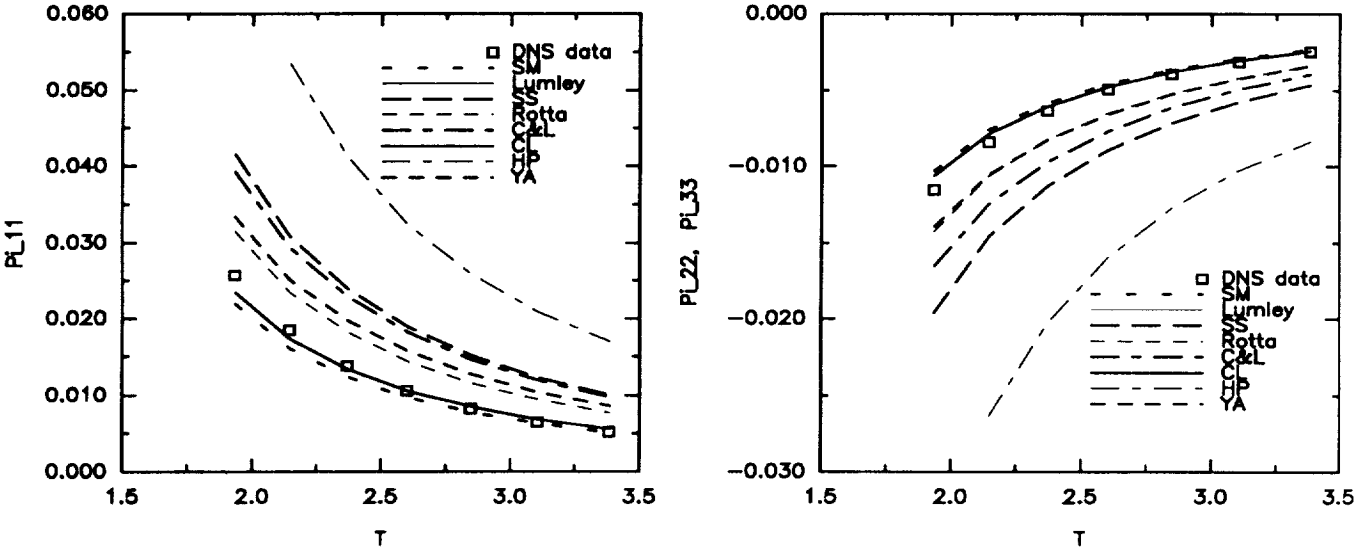

Figure 21. Direct comparison of the return-to-isotropy models with the DNS data of relaxation from axisymm. contraction K6R (Lee et al.[14]).

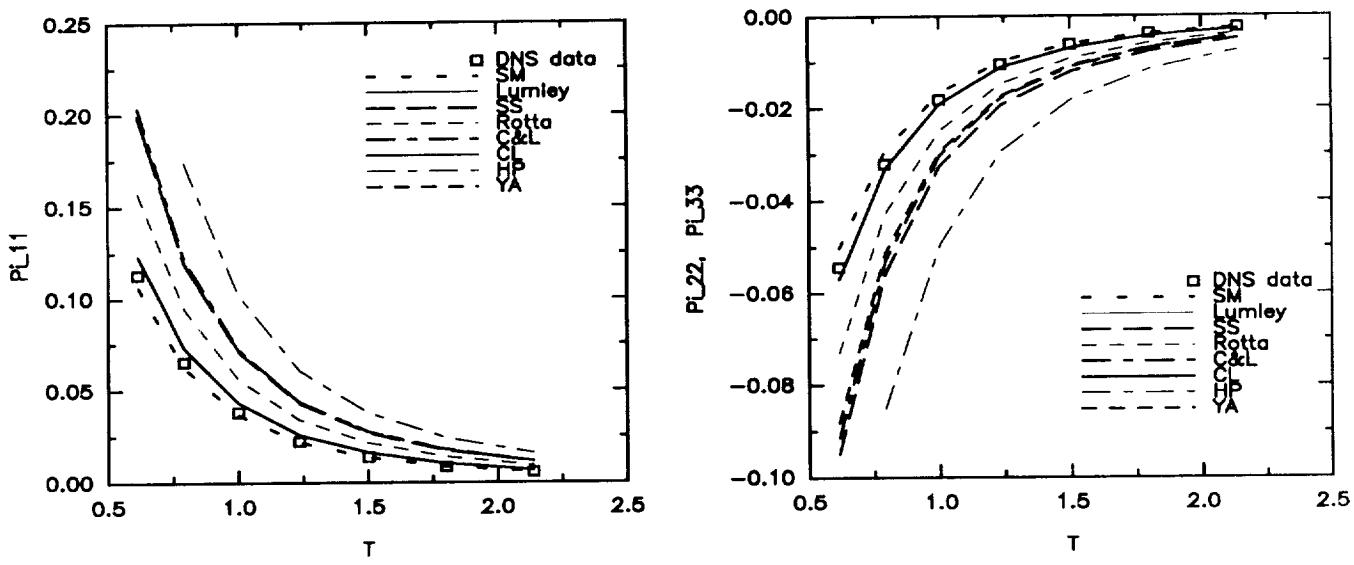

Figure 22. Direct comparison of the return-to-isotropy models with the DNS data of relaxation from axisymm. contraction L3R (Lee et al.[14]).

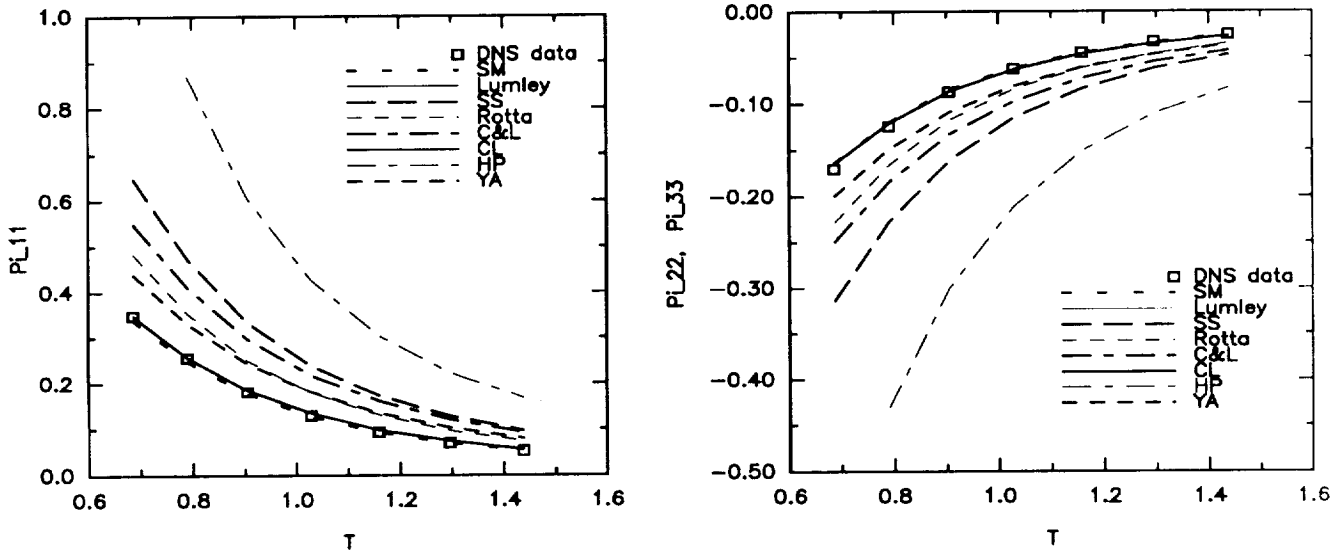

Figure 23. Direct comparison of the return-to-isotropy models with the DNS data of relaxation from axisymm. contraction L6R (Lee et al.[14]).

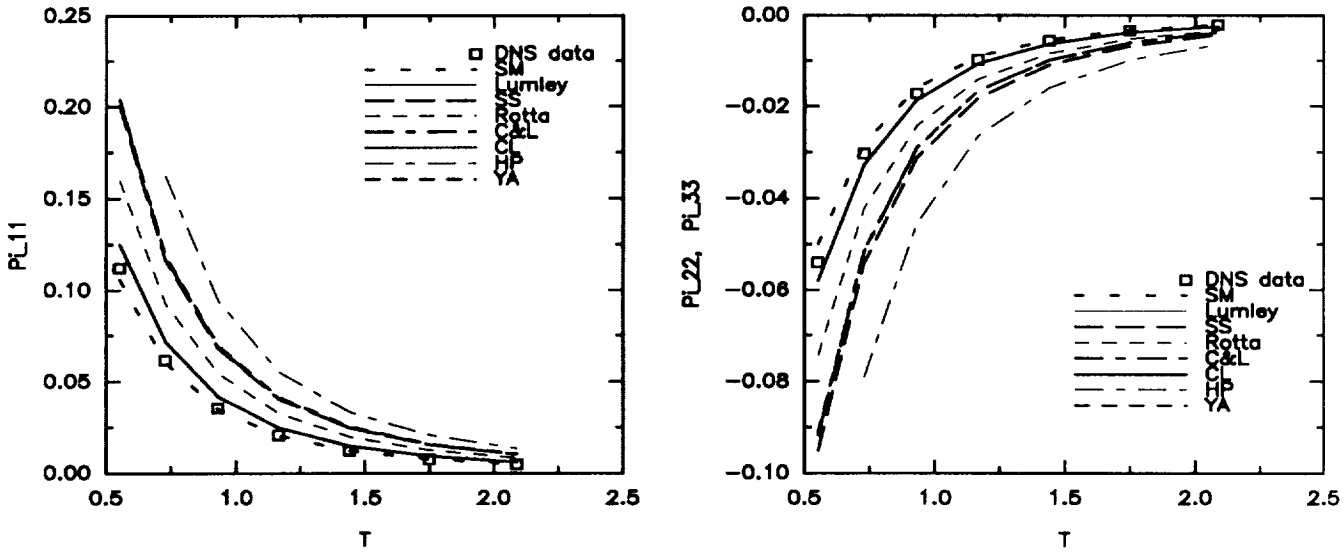

Figure 24. Direct comparison of the return-to-isotropy models with the DNS data of relaxation from axisymm. contraction M2R (Lee et al.[14]).

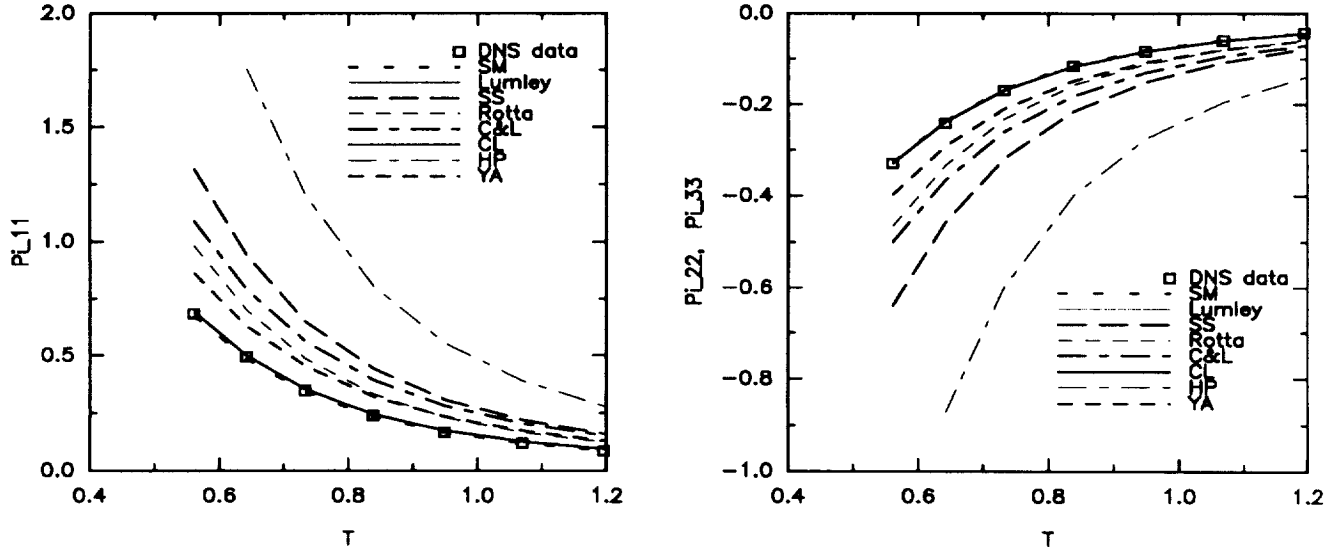

Figure 25. Direct comparison of the return-to-isotropy models with the DNS data of relaxation from axisymm. contraction M5R (Lee et al.[14]).

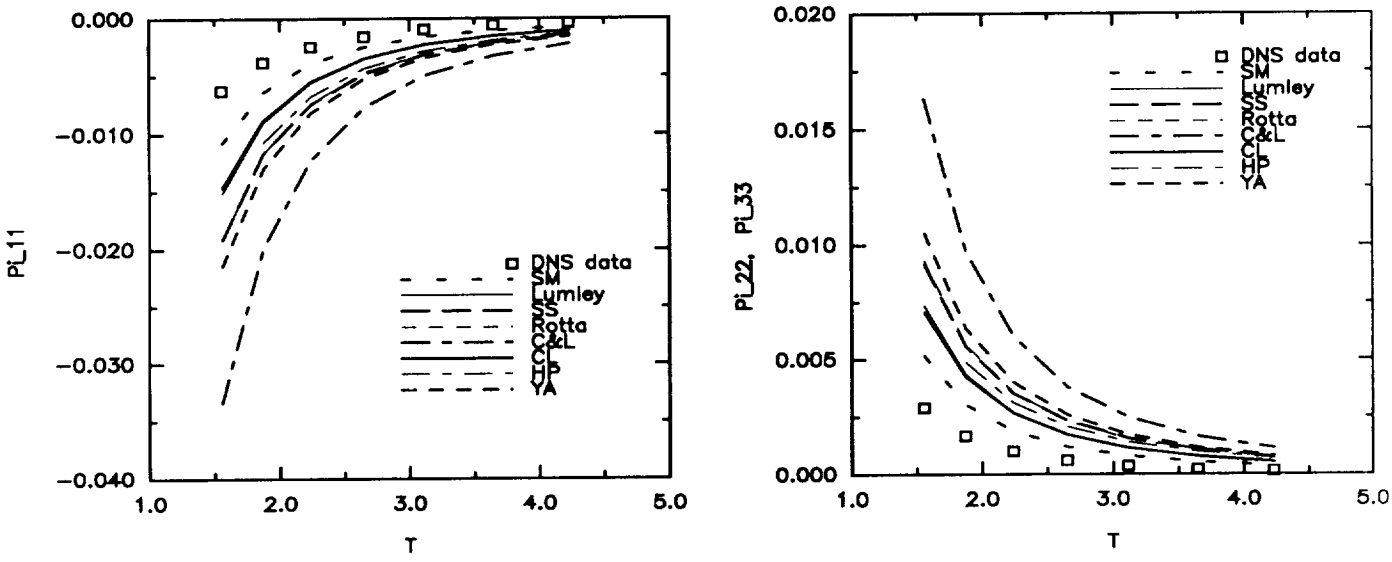

Figure 26. Direct comparison of the return-to-isotropy models with the DNS data of relaxation from axisymm. expansion O3R (Lee et al.[14]).

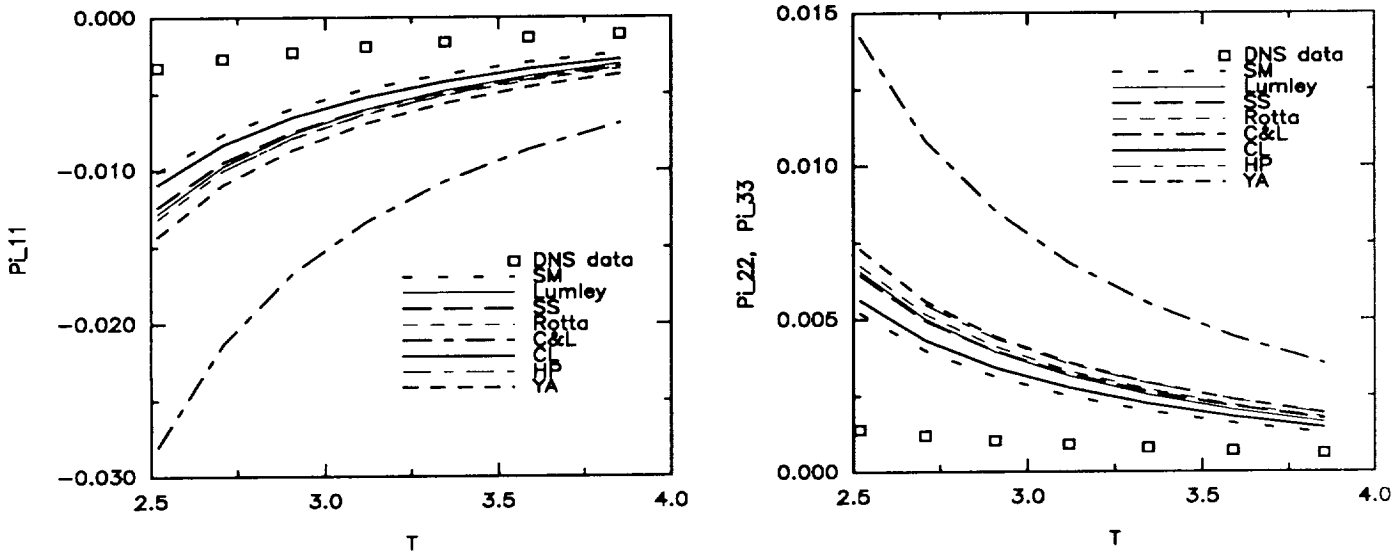

Figure 27. Direct comparison of the return-to-isotropy models with the DNS data of relaxation from axisymm. expansion O6R (Lee et al.[14]).

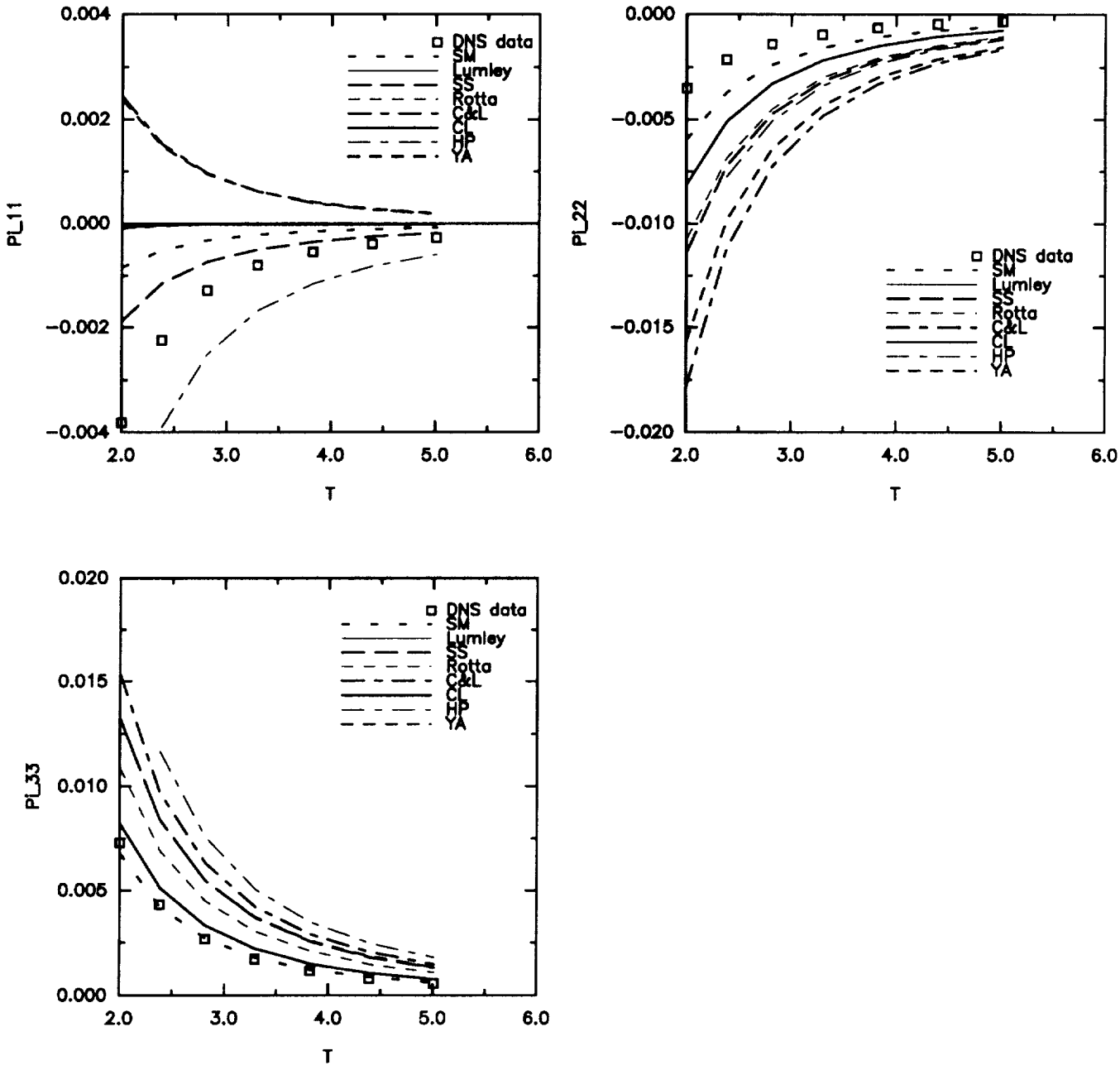

Figure 28. Direct comparison of the return-to-isotropy models with the DNS data of the relaxation from the plane strain A2R (Lee et al.[14]).

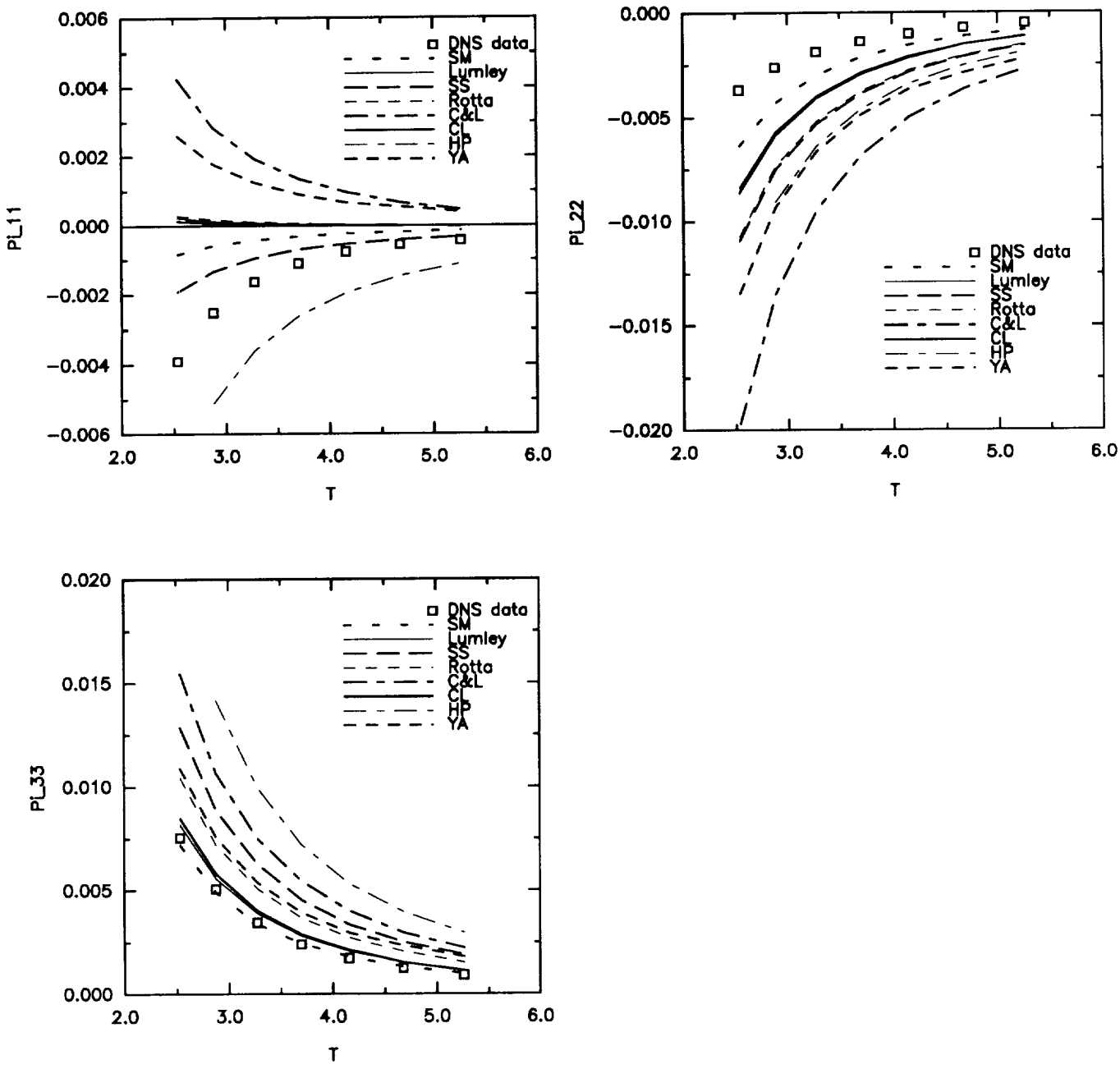

Figure 29. Direct comparison of the return-to-isotropy models with the DNS data of the relaxation from the plane strain A3R (Lee et al.[14]).

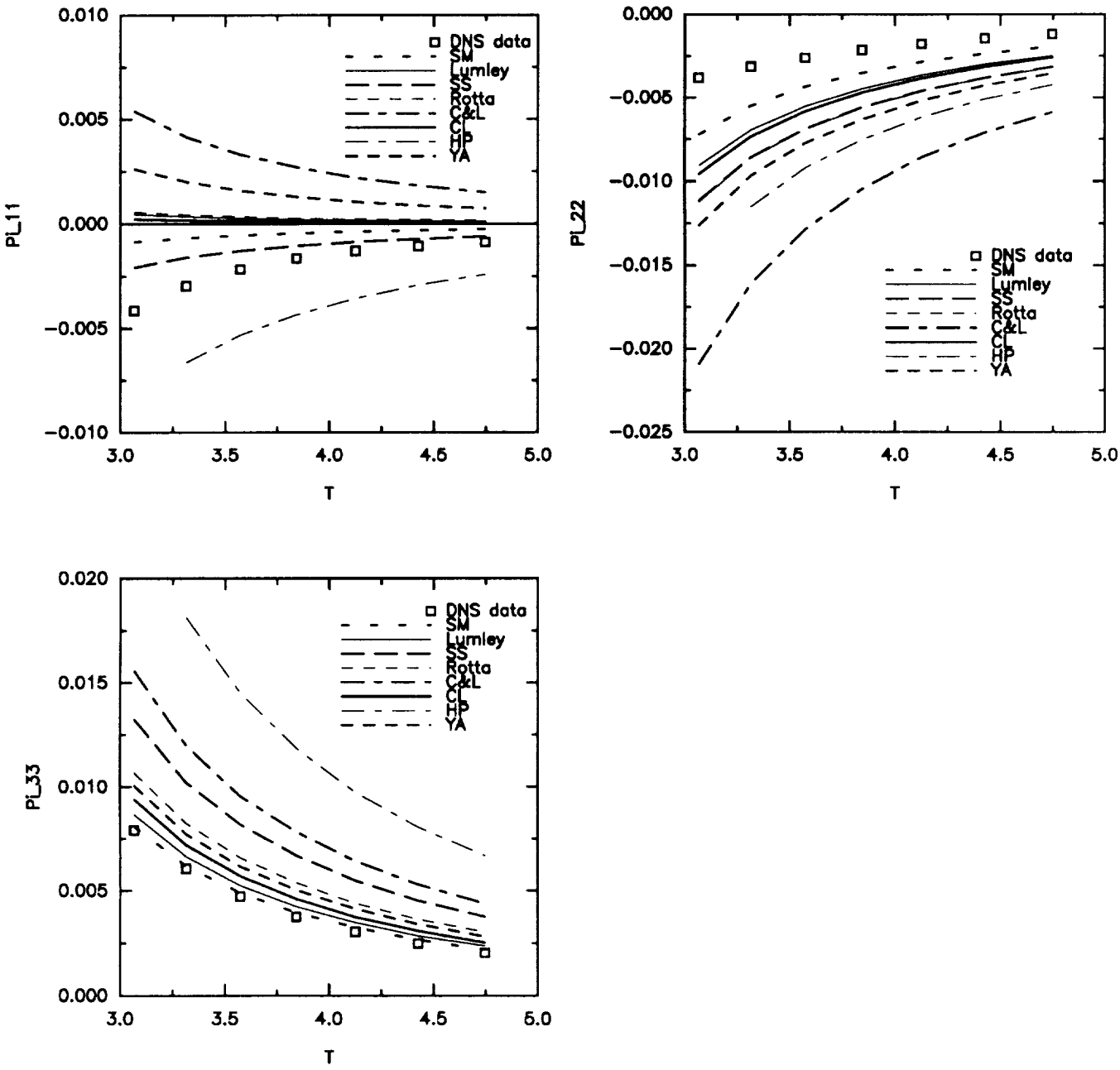

Figure 30. Direct comparison of the return-to-isotropy models with the DNS data of the relaxation from the plane strain A4R (Lee et al.[14]).

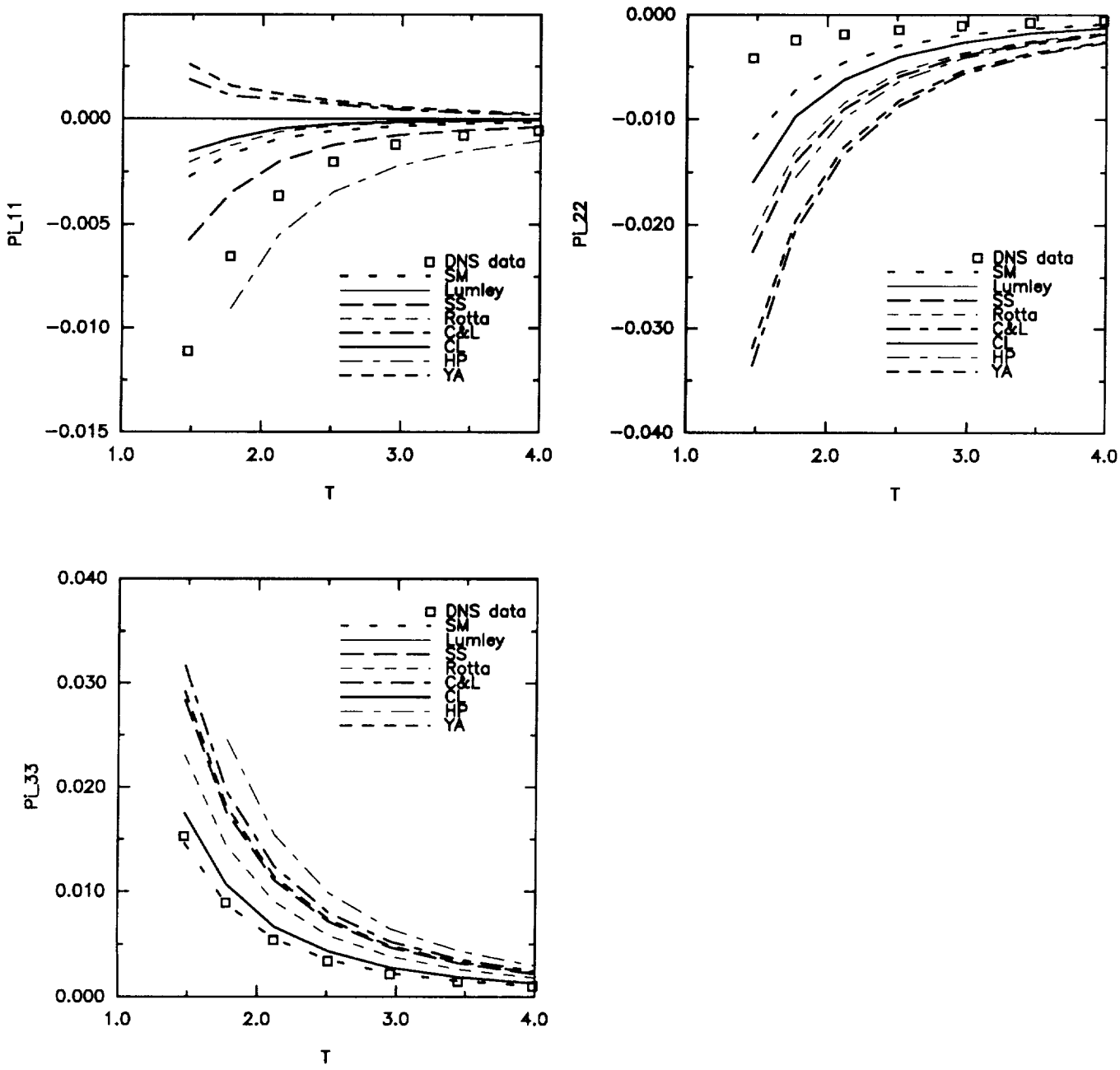

Figure 31. Direct comparison of the return-to-isotropy models with the DNS data of the relaxation from the plane strain B2R (Lee et al.[14]).

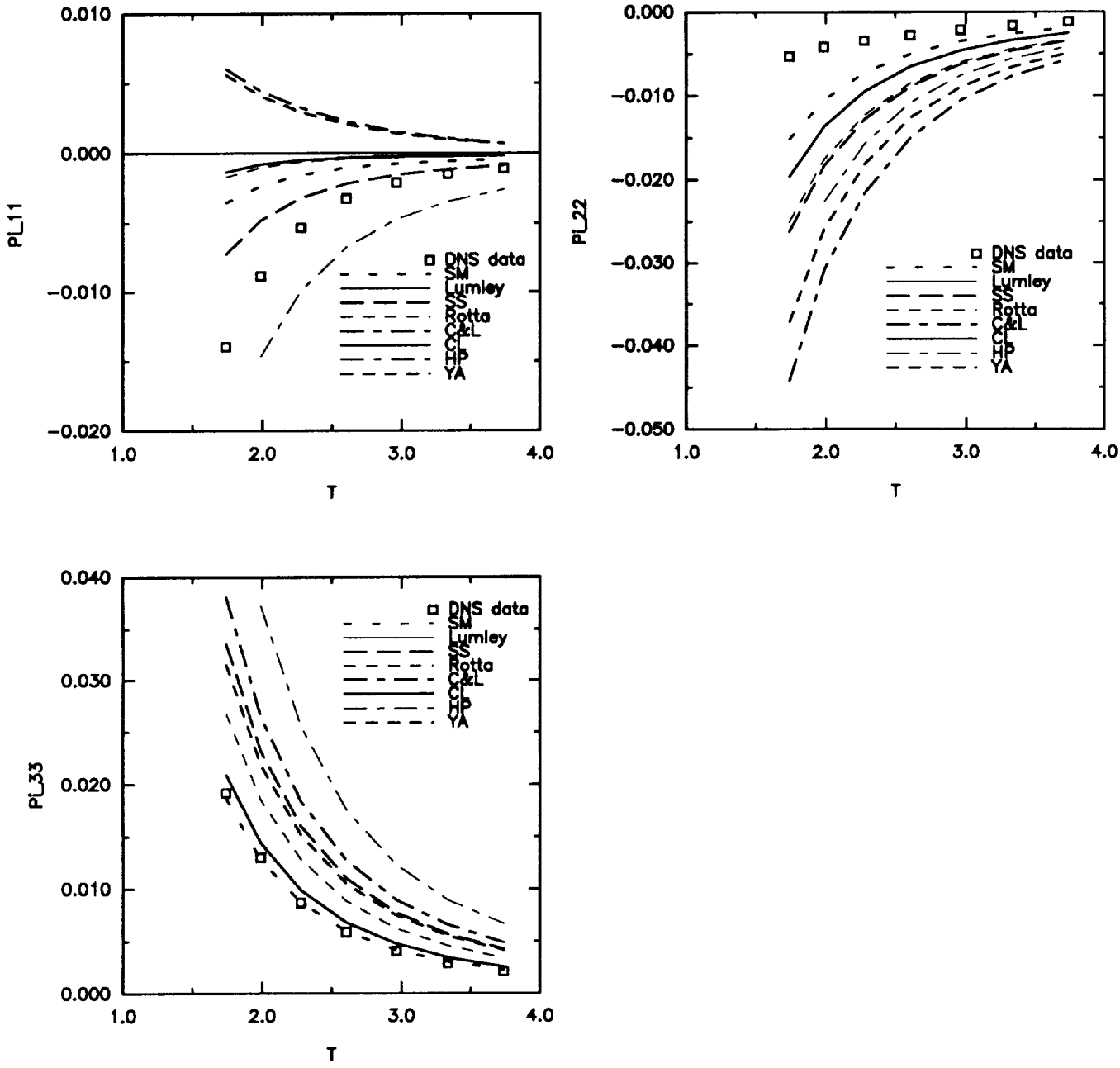

Figure 32. Direct comparison of the return-to-isotropy models with the DNS data of the relaxation from the plane strain B3R (Lee et al.[14]).

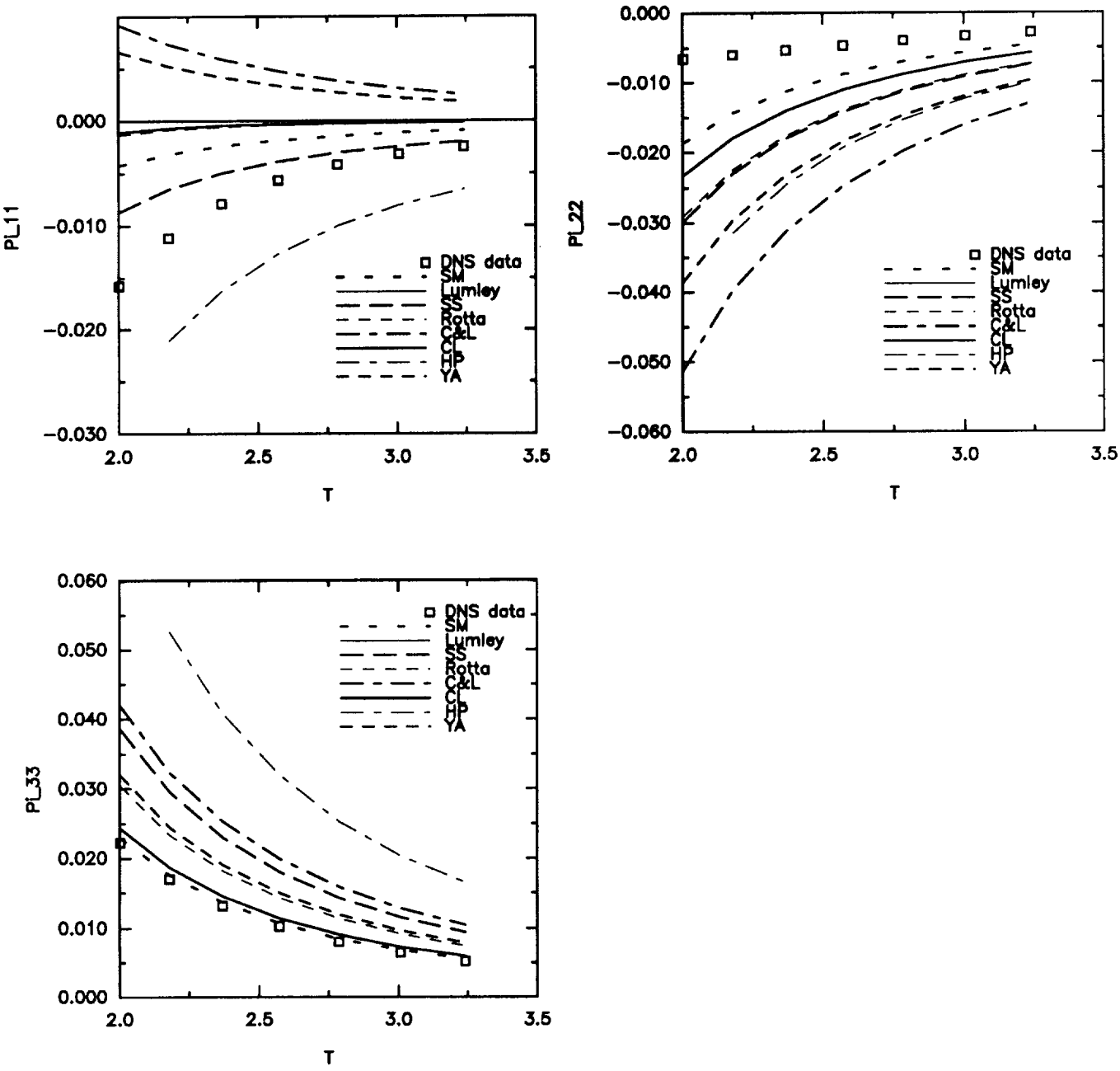

Figure 33. Direct comparison of the return-to-isotropy models with the DNS data of the relaxation from the plane strain B4R (Lee et al.[14]).

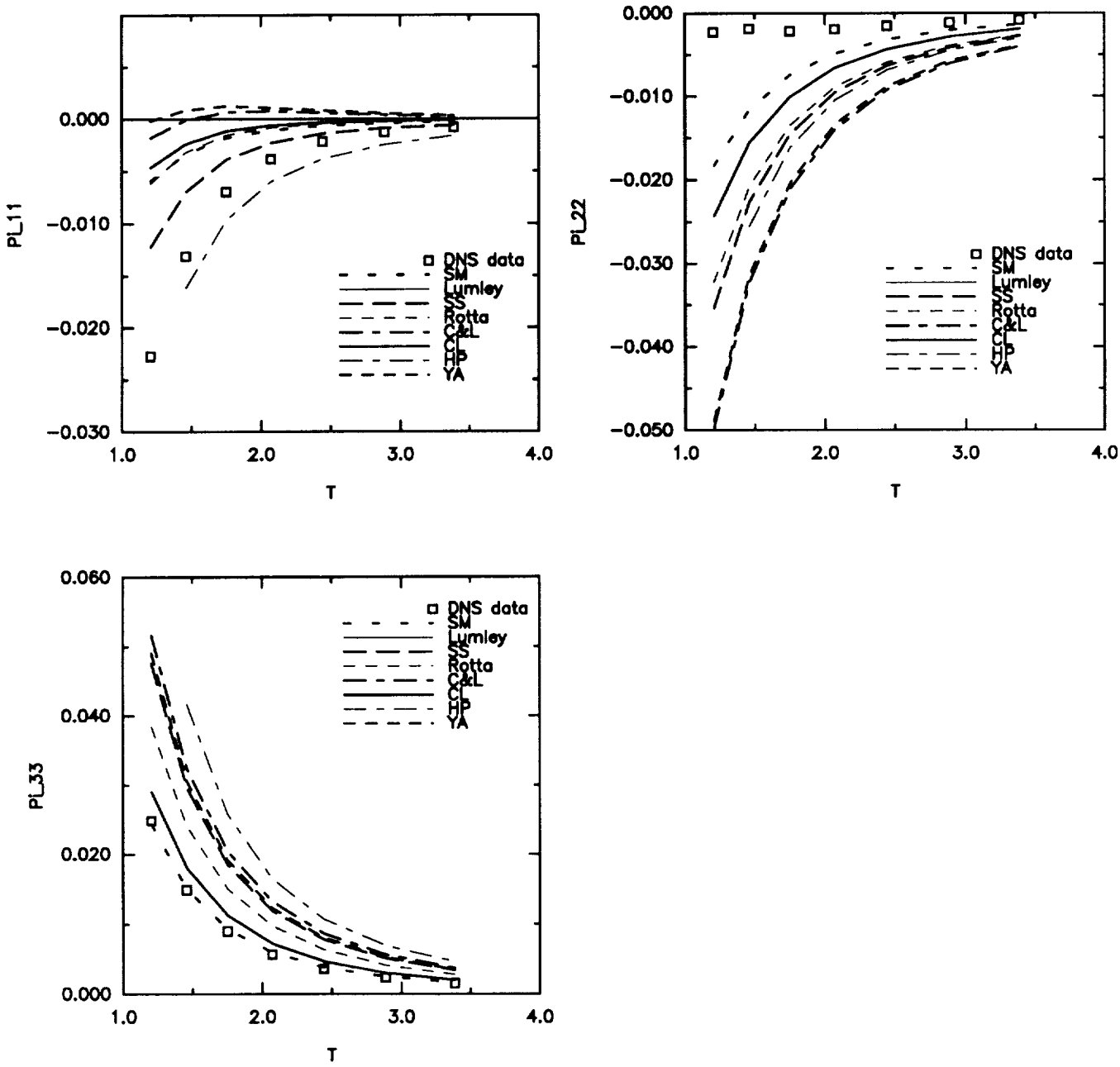

Figure 34. Direct comparison of the return-to-isotropy models with the DNS data of the relaxation from the plane strain C2R (Lee et al.[14]).

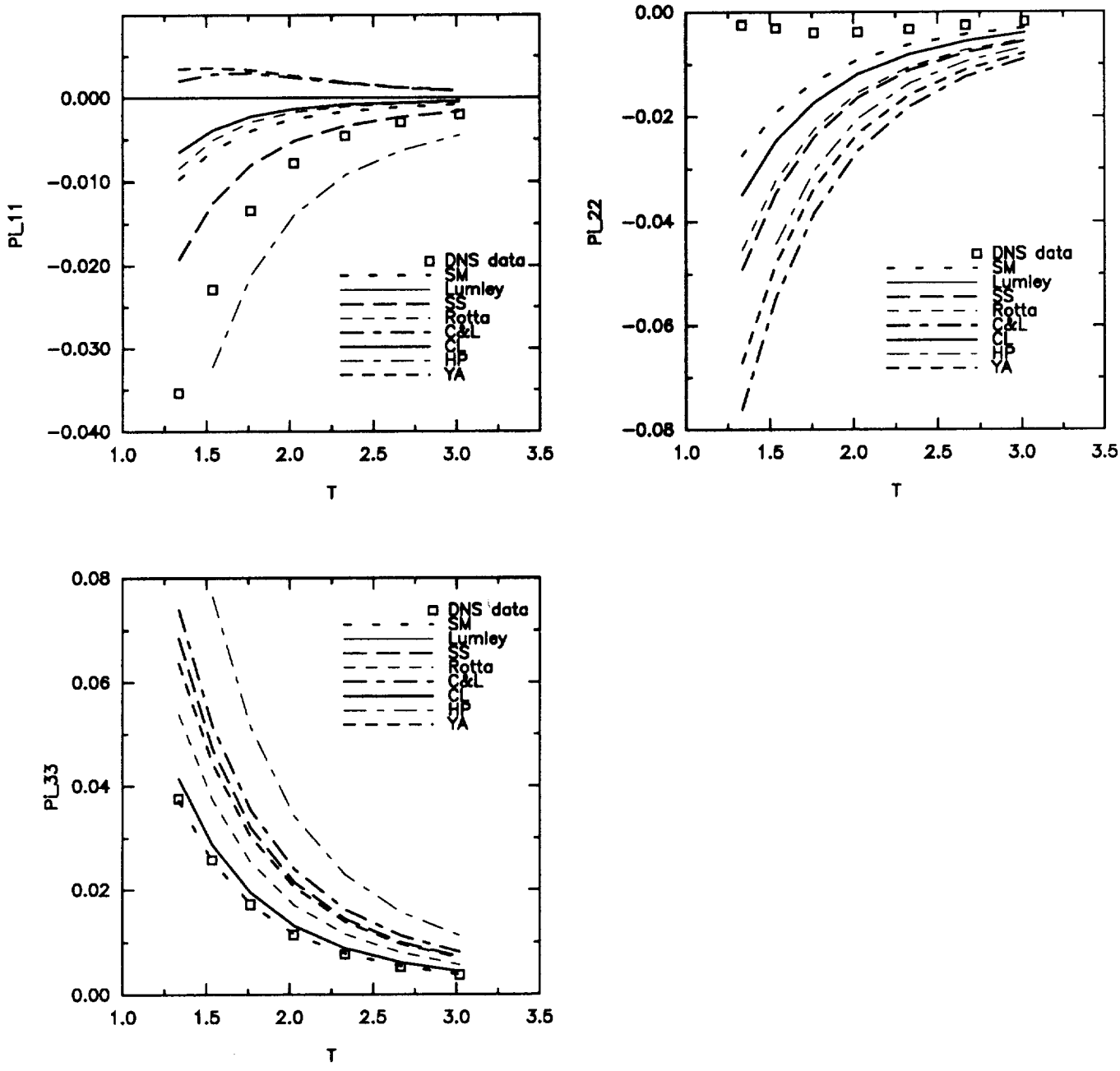

Figure 35. Direct comparison of the return-to-isotropy models with the DNS data of the relaxation from the plane strain C3R (Lee et al.[14]).

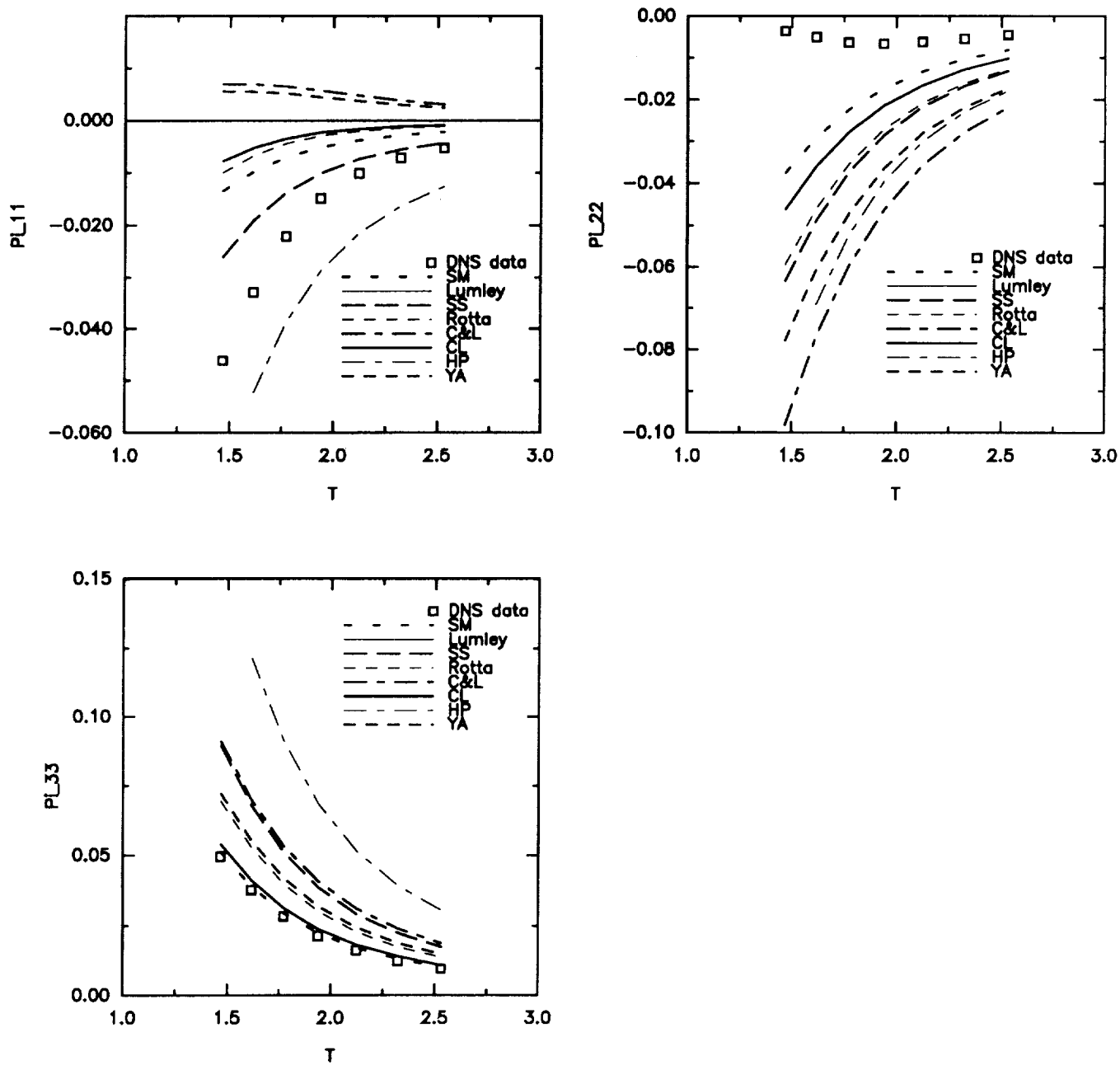

Figure 36. Direct comparison of the return-to-isotropy models with the DNS data of the relaxation from the plane strain C4R (Lee et al.[14]).

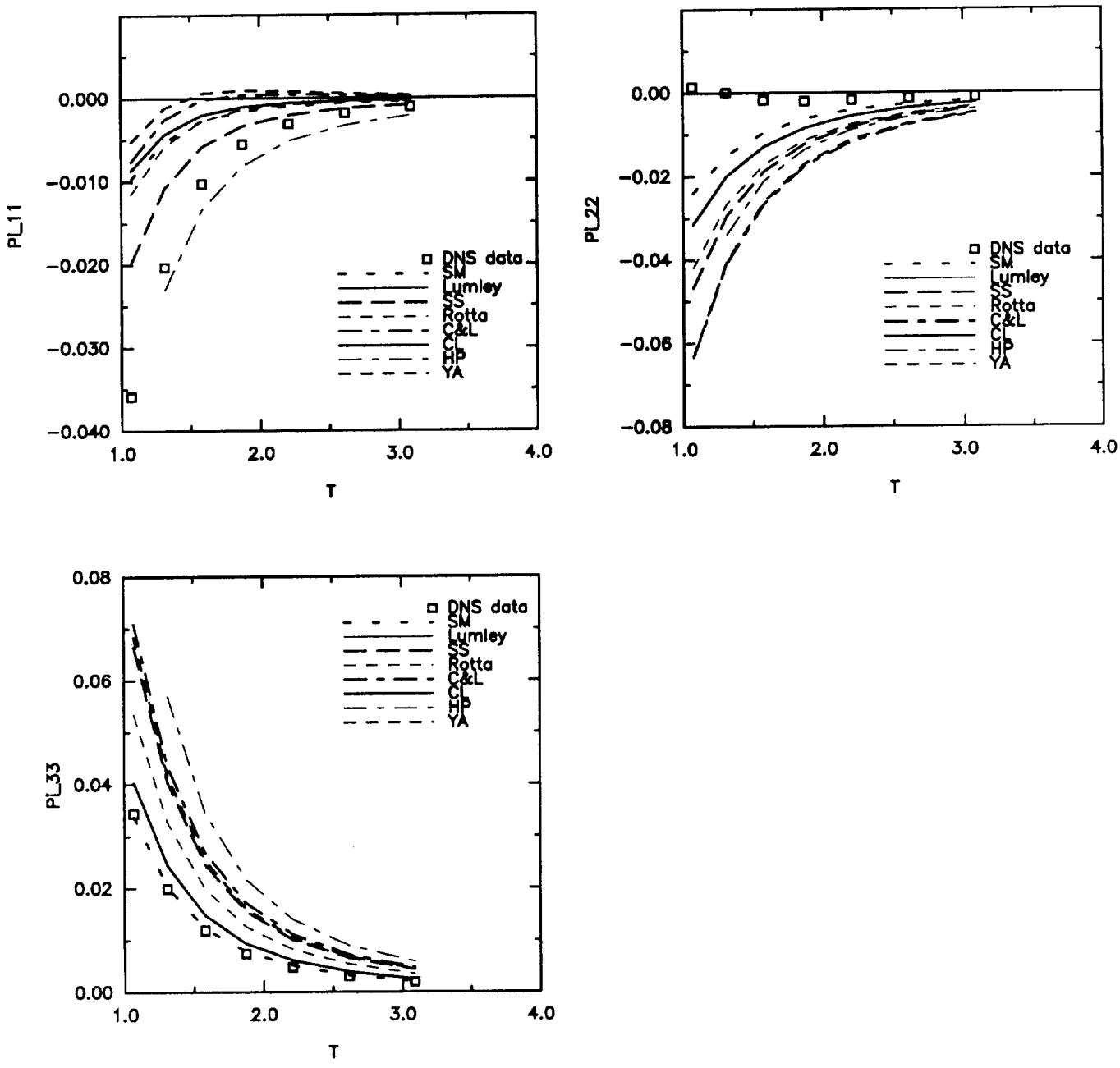

Figure 37. Direct comparison of the return-to-isotropy models with the DNS data of the relaxation from the plane strain D2R (Lee et al.[14]).

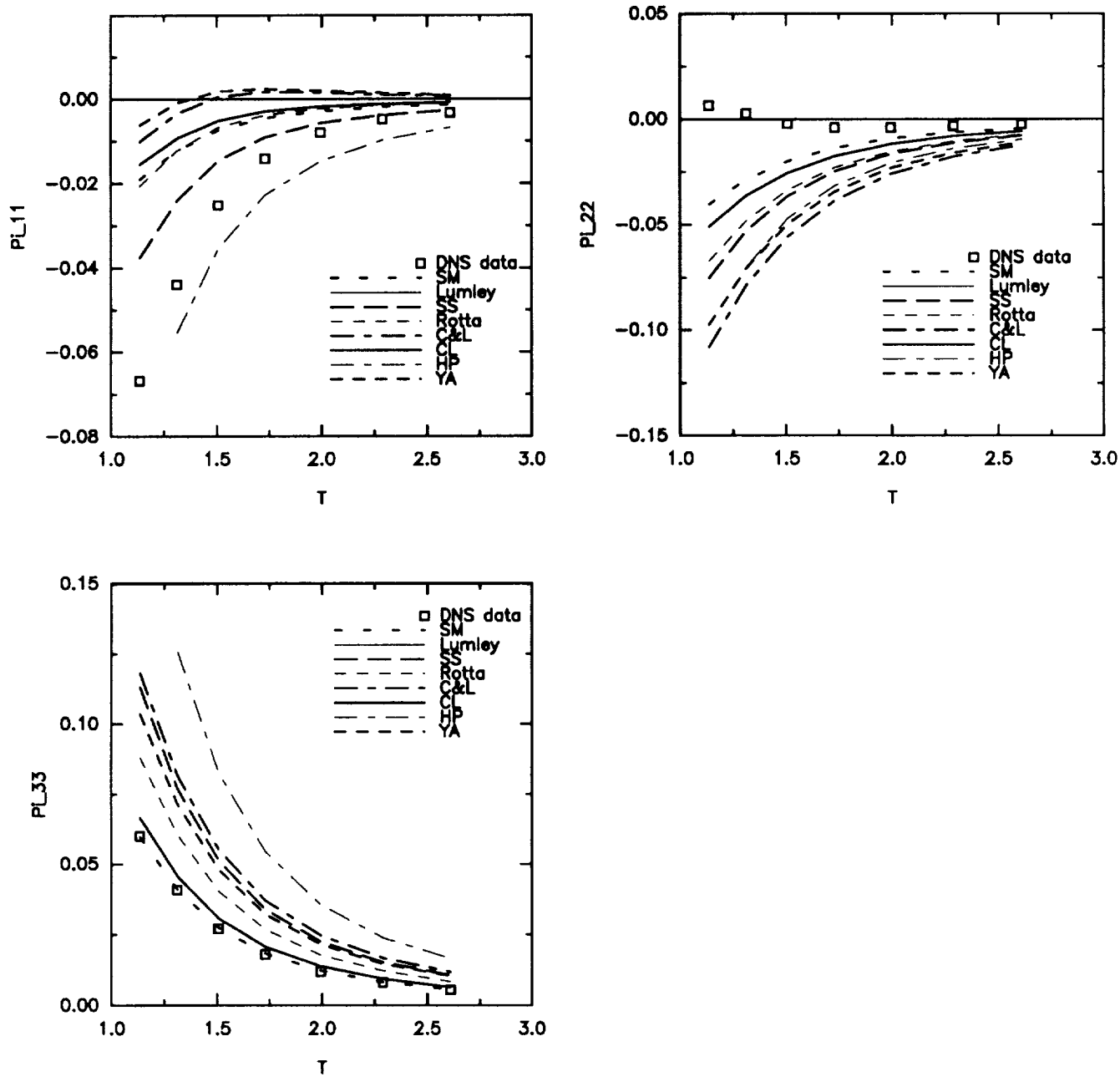

Figure 38. Direct comparison of the return-to-isotropy models with the DNS data of the relaxation from the plane strain D3R (Lee et al.[14]).

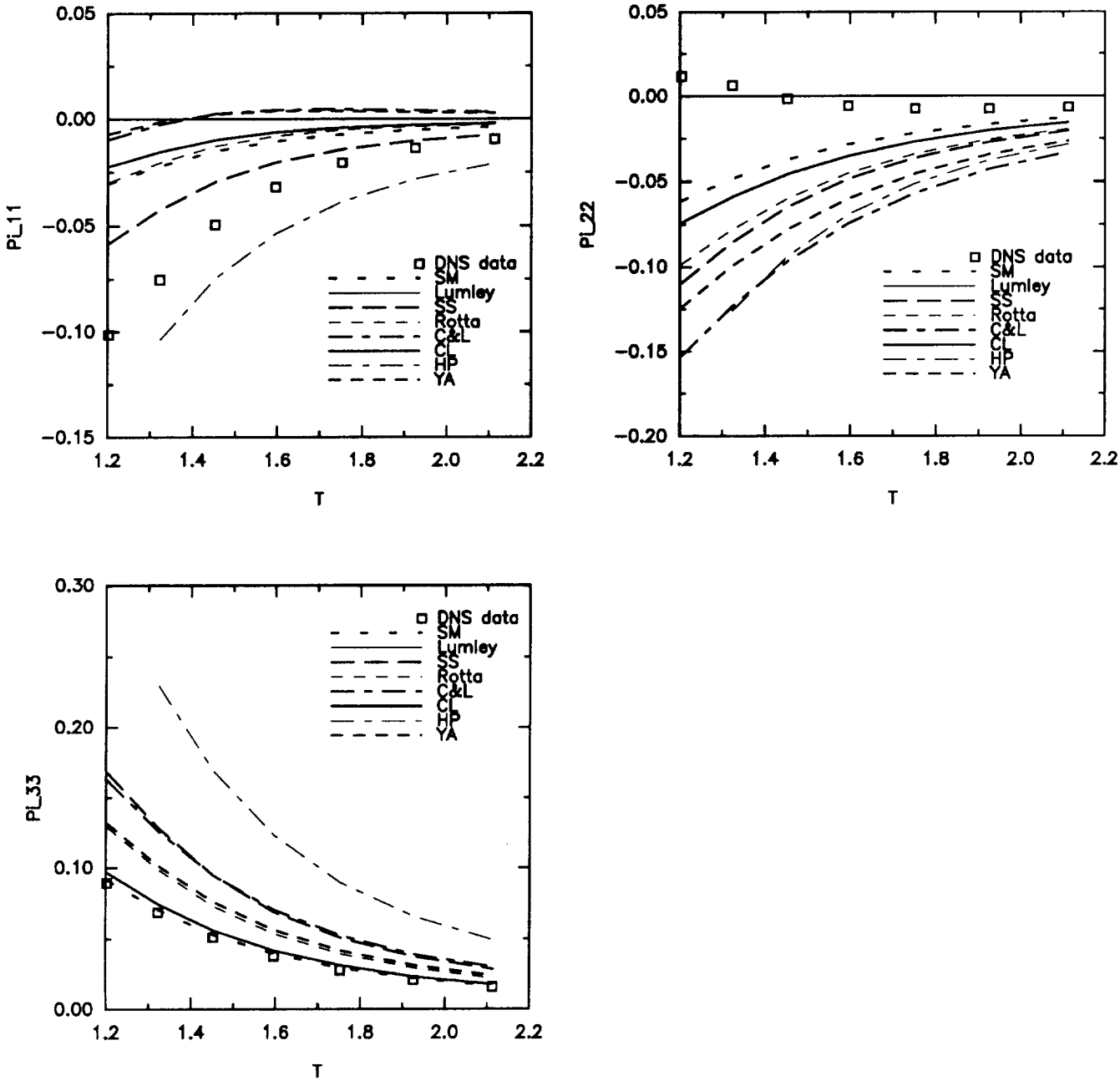

Figure 39. Direct comparison of the return-to-isotropy models with the DNS data of the relaxation from the plane strain D4R (Lee et al.[14]).

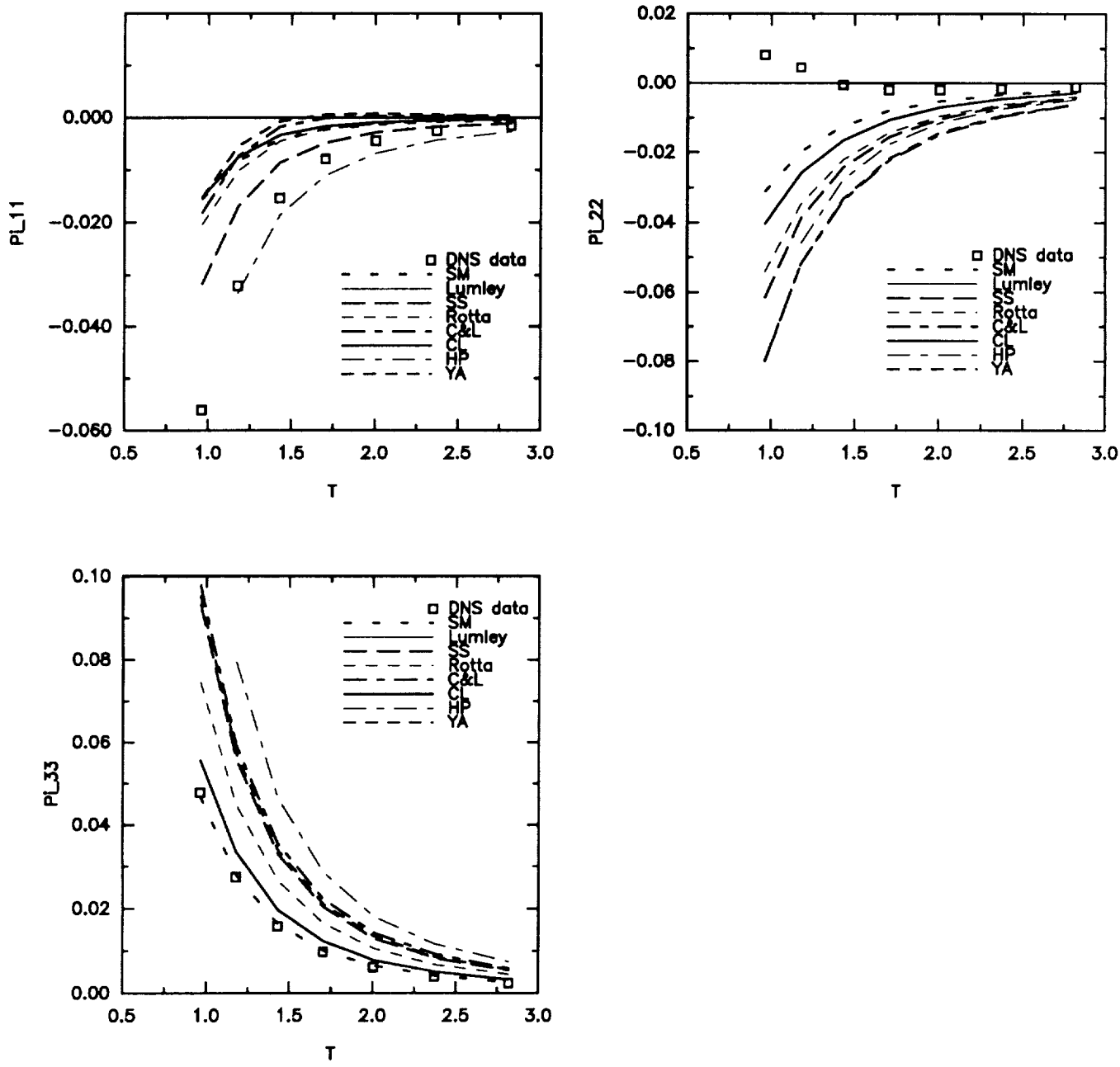

Figure 40. Direct comparison of the return-to-isotropy models with the DNS data of the relaxation from the plane strain E2R (Lee et al.[14]).

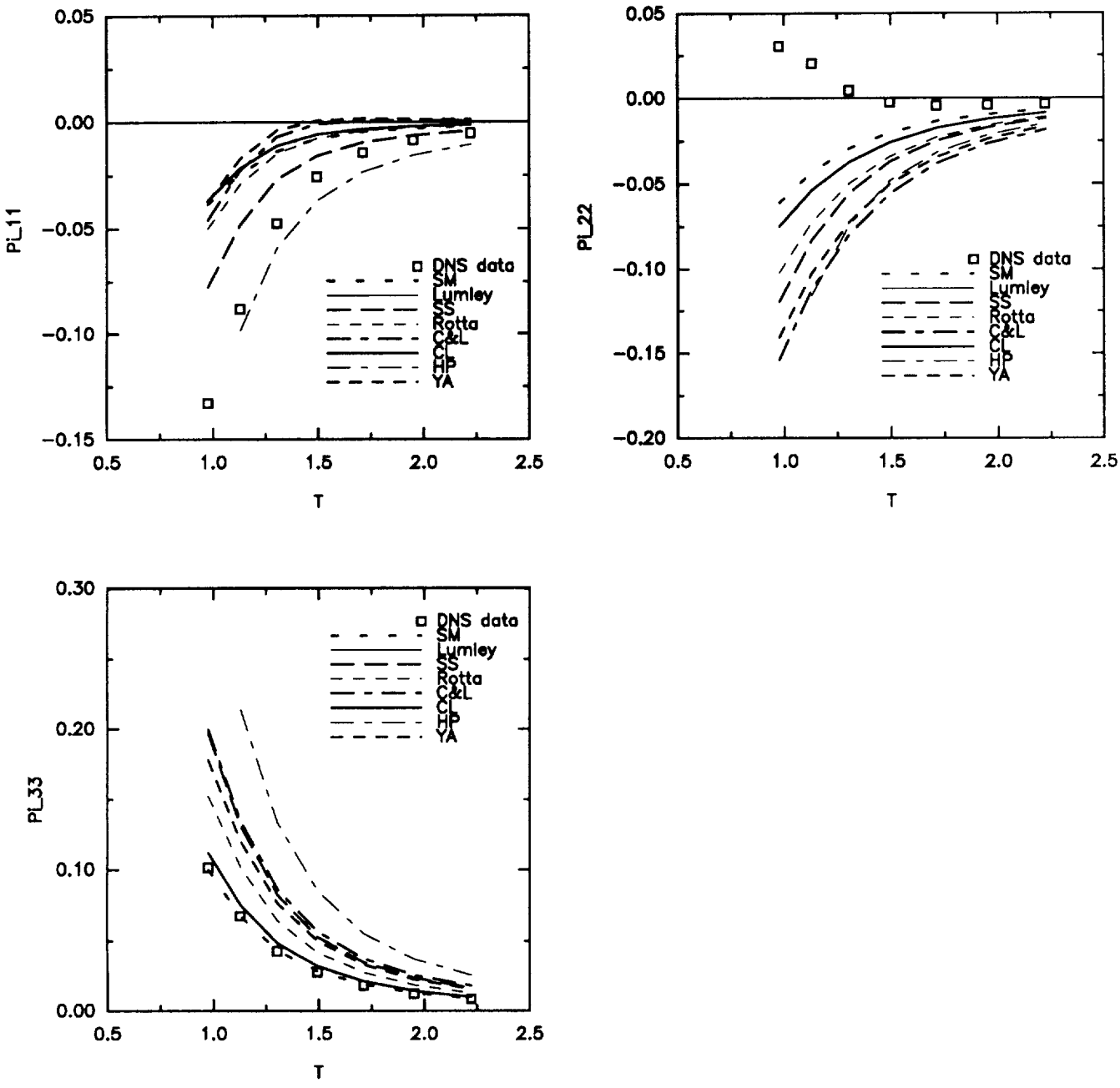

Figure 41. Direct comparison of the return-to-isotropy models with the DNS data of the relaxation from the plane strain E3R (Lee et al.[14]).

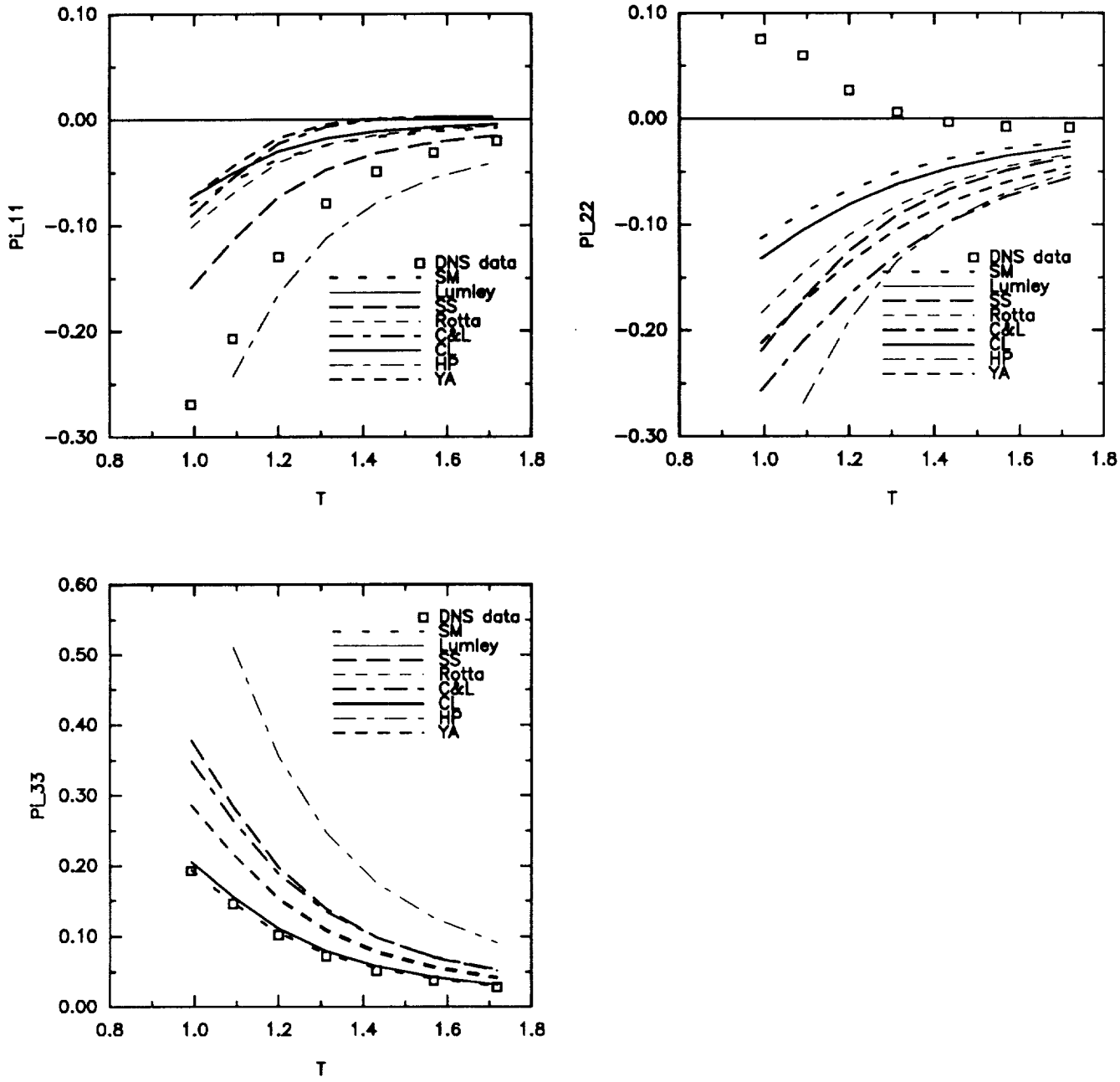

Figure 42. Direct comparison of the return-to-isotropy models with the DNS data of the relaxation from the plane strain E4R (Lee et al.[14]).

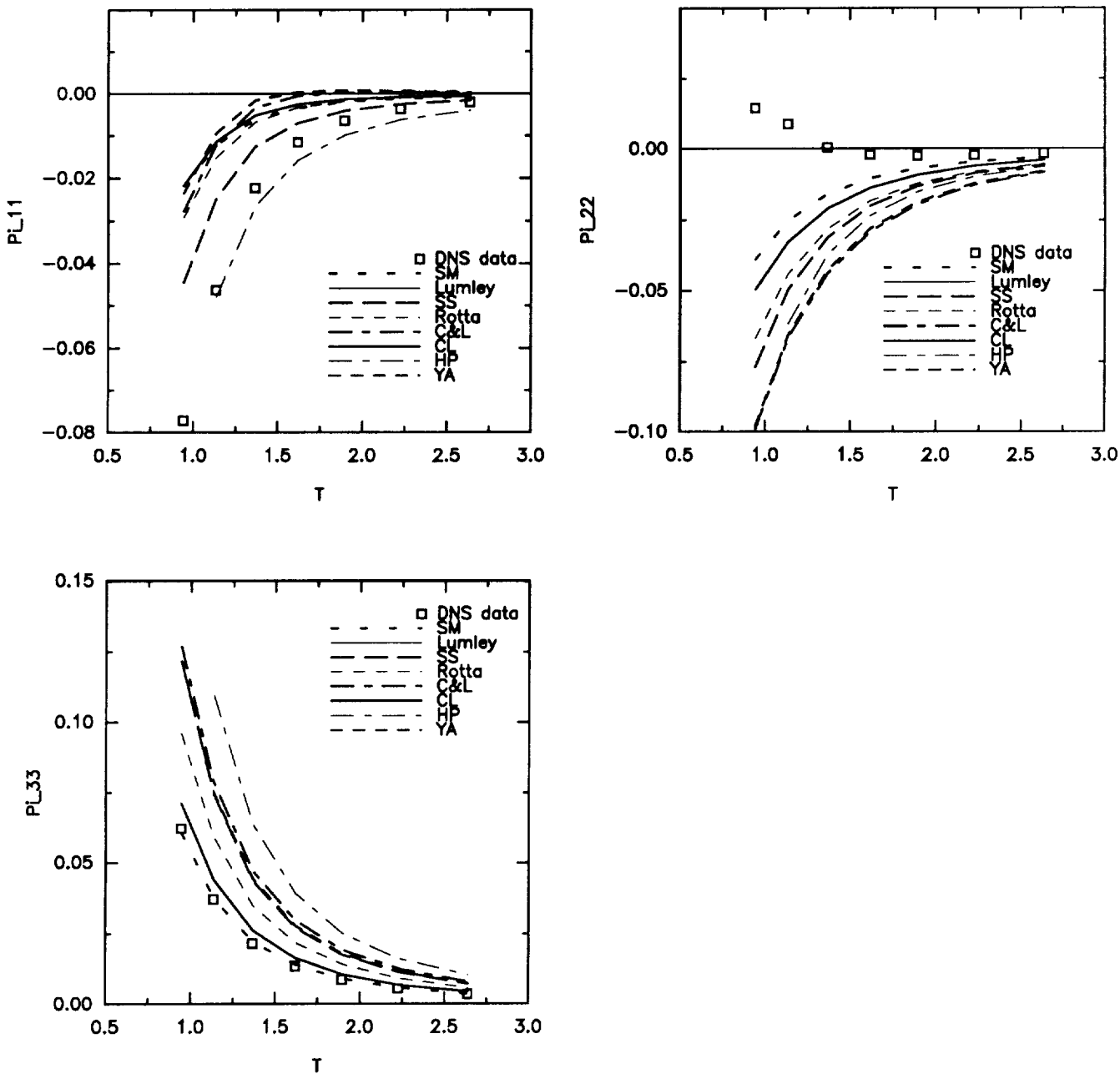

Figure 43. Direct comparison of the return-to-isotropy models with the DNS data of the relaxation from the plane strain F2R (Lee et al.[14]).

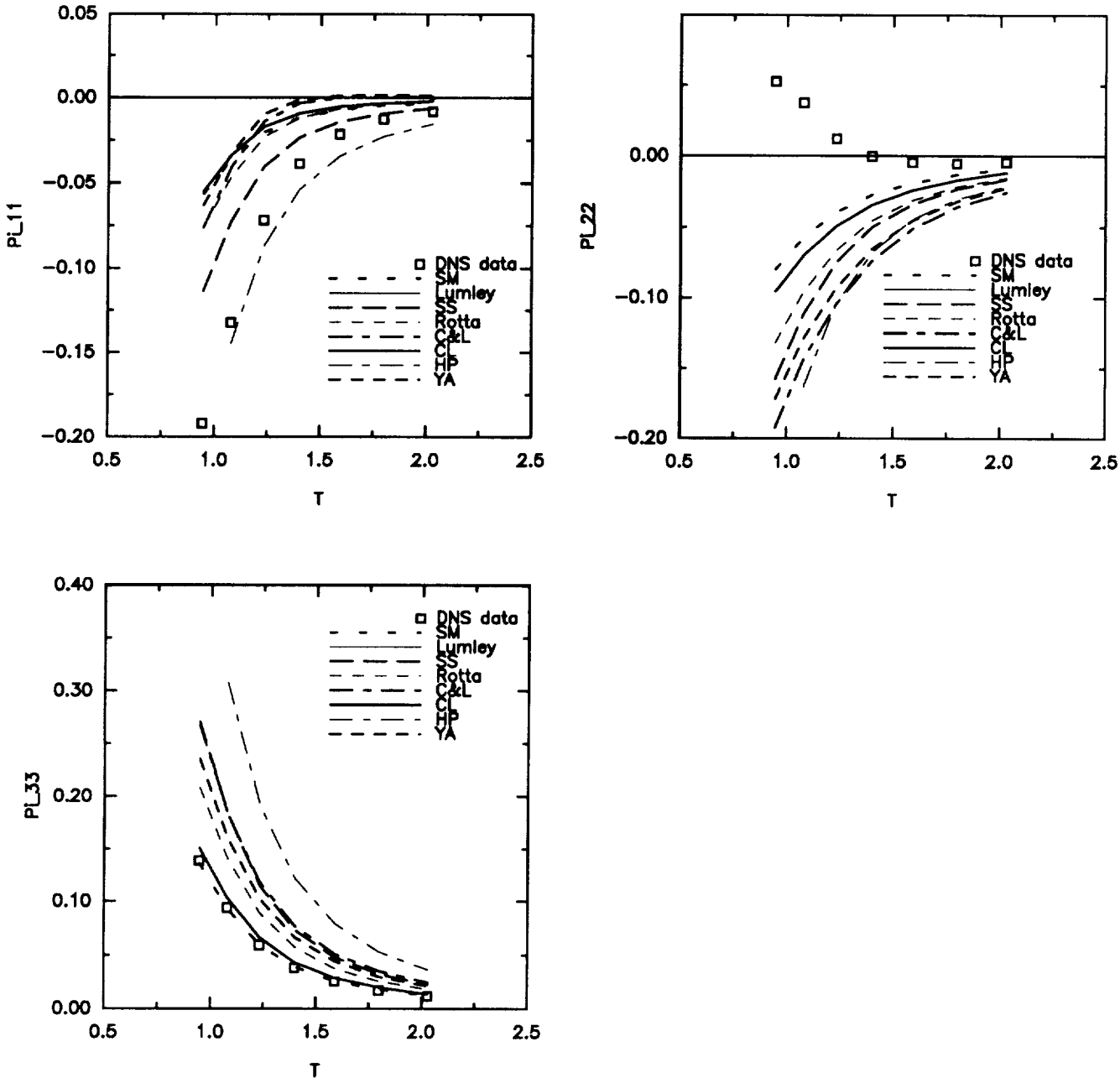

Figure 44. Direct comparison of the return-to-isotropy models with the DNS data of the relaxation from the plane strain F3R (Lee et al.[14]).

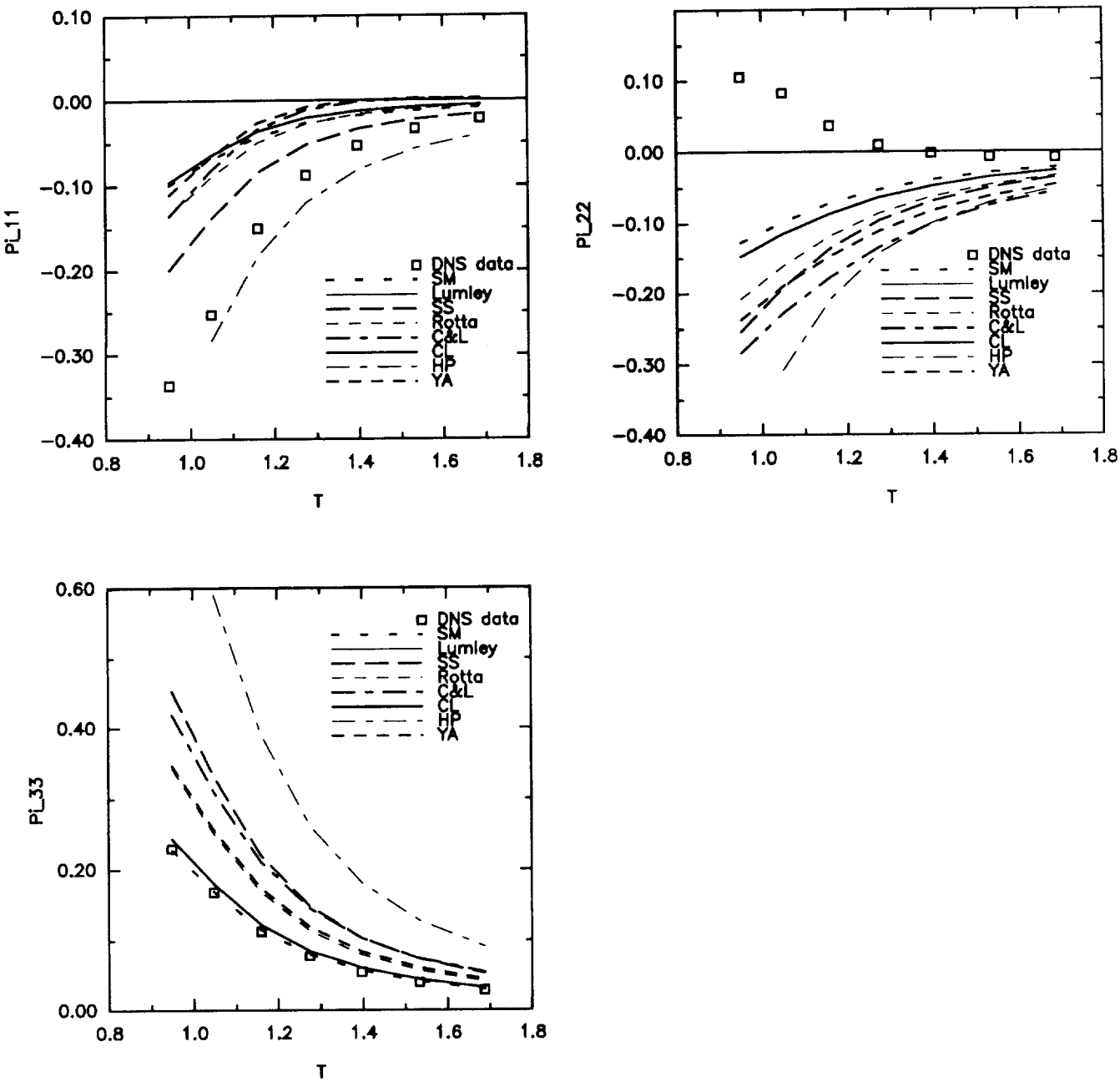

Figure 45. Direct comparison of the return-to-isotropy models with the DNS data of the relaxation from the plane strain F4R (Lee et al.[14]).

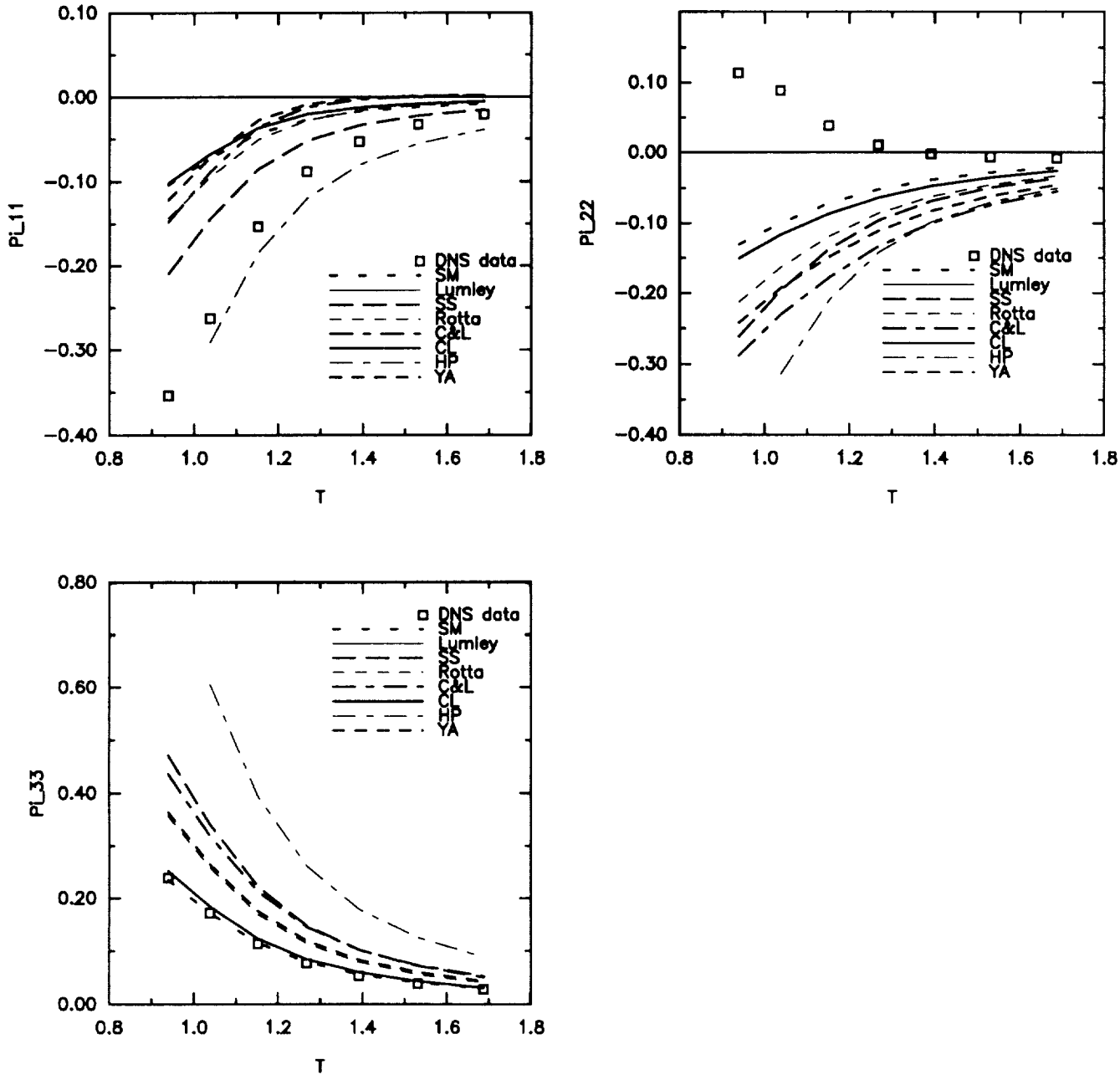

Figure 46. Direct comparison of the return-to-isotropy models with the DNS data of the relaxation from the plane strain G1R (Lee et al.[14]).

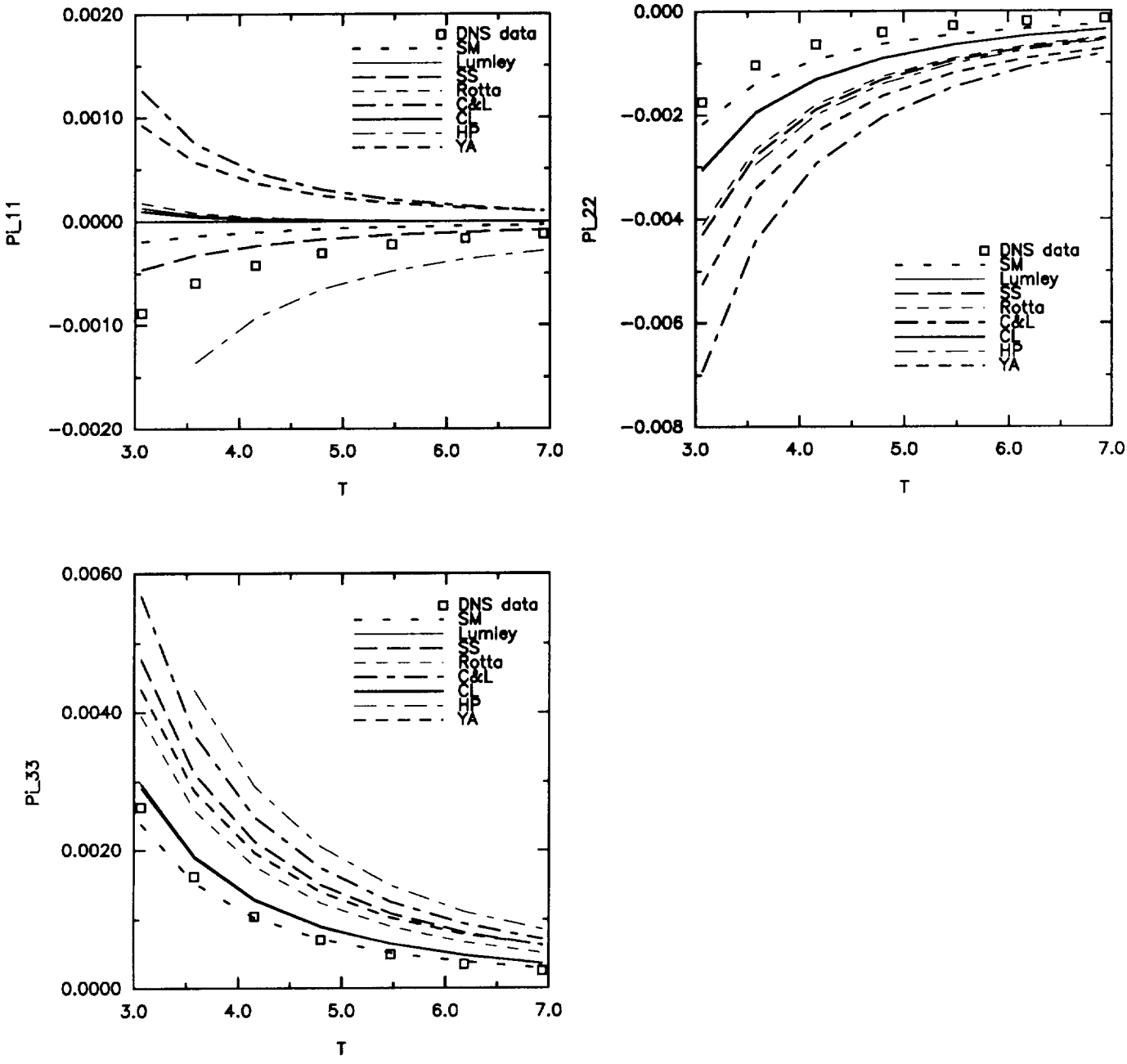

Figure 47. Direct comparison of the return-to-isotropy models with the DNS data of the relaxation from the plane strain H2R (Lee et al.[14]).

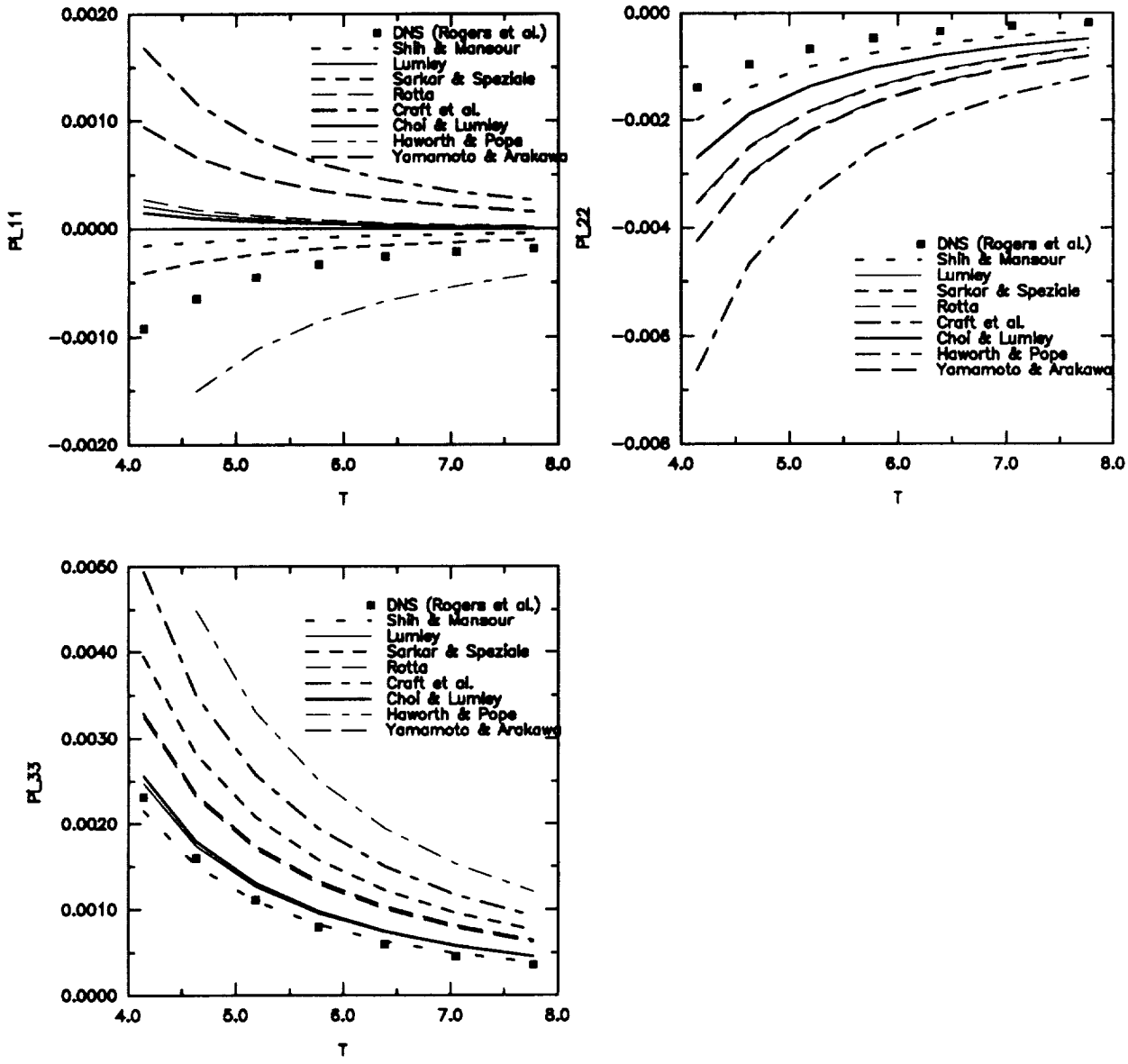

Figure 48. Direct comparison of the return-to-isotropy models with the DNS data of the relaxation from the plane strain H3R (Lee et al.[14]).

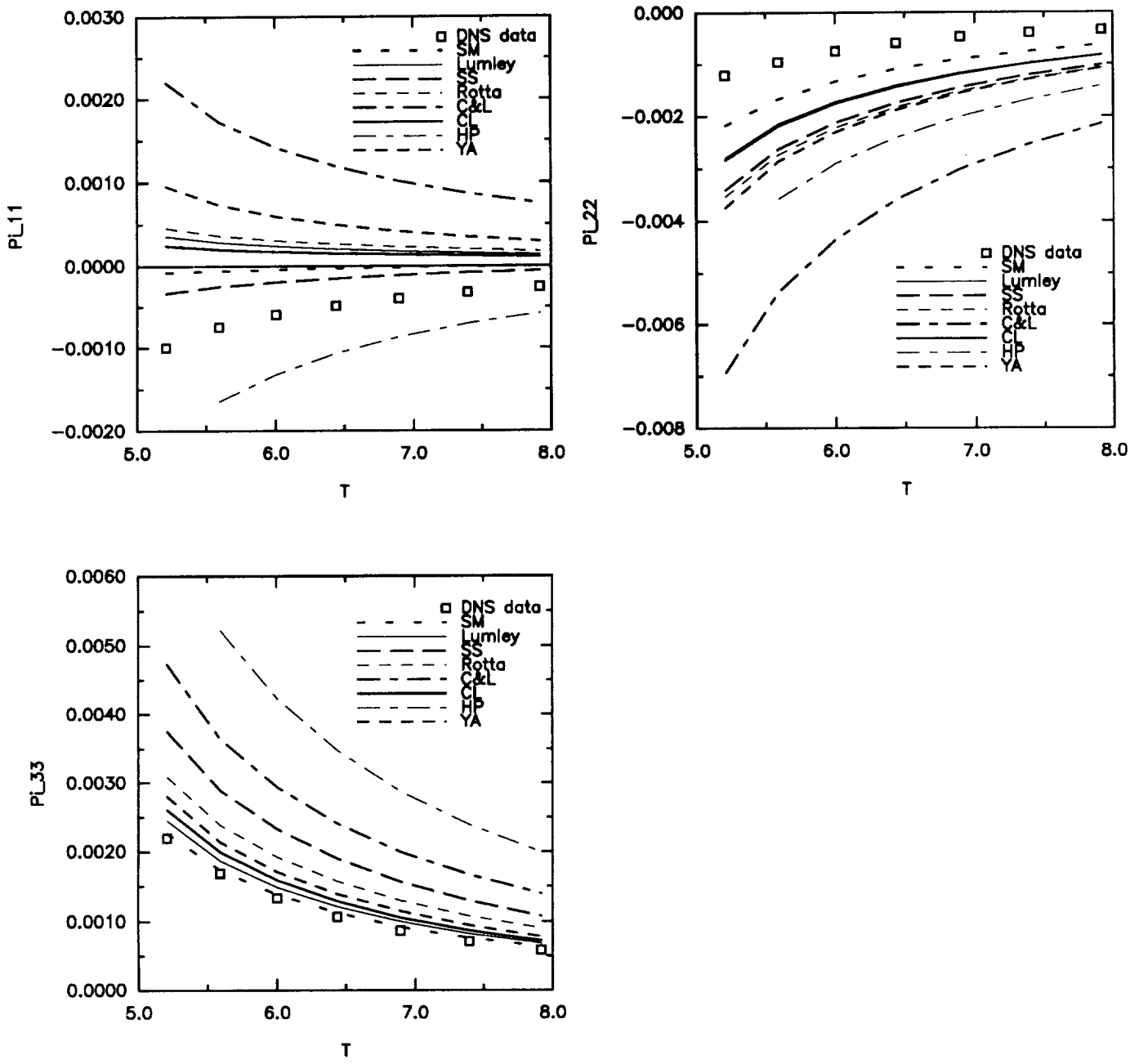

Figure 49. Direct comparison of the return-to-isotropy models with the DNS data of the relaxation from the plane strain H4R (Lee et al.[14]).

REPORT DOCUMENTATION PAGE

Form Approved
OMB No. 0704-0188

1. AGENCY USE ONLY (*Leave blank*)	2. REPORT DATE	3. REPORT TYPE AND DATES COVERED
	November 1991	Technical Memorandum

4. TITLE AND SUBTITLE

A Critical Comparison of Second Order Closures With Direct Numerical Simulation of Homogeneous Turbulence

5. FUNDING NUMBERS

WU-505-62-21

6. AUTHOR(S)

Tsan-Hsing Shih and John L. Lumley

7. PERFORMING ORGANIZATION NAME(S) AND ADDRESS(ES)

National Aeronautics and Space Administration
Lewis Research Center
Cleveland, Ohio 44135-3191

8. PERFORMING ORGANIZATION REPORT NUMBER

E-6725

9. SPONSORING/MONITORING AGENCY NAMES(S) AND ADDRESS(ES)

National Aeronautics and Space Administration
Washington, D.C. 20546-0001

10. SPONSORING/MONITORING AGENCY REPORT NUMBER

NASA TM-105351
ICOMP-91-25;
CMOTT-91-10

11. SUPPLEMENTARY NOTES

Tsan-Hsing Shih, Institute for Computational Mechanics in Propulsion and Center for Modeling of Turbulence and Transition, Lewis Research Center (work funded under Space Act Agreement C-99066-G). John L. Lumley, Cornell University, Ithaca, New York 14853. Space Act Monitor, Louis A. Povinelli, (216) 433-5818.

12a. DISTRIBUTION/AVAILABILITY STATEMENT

Unclassified - Unlimited
Subject Category 34

12b. DISTRIBUTION CODE

13. ABSTRACT (*Maximum 200 words*)

Recently several second order closure models have been proposed for closing the second moment equations, in which the velocity-pressure gradient (and scalar-pressure gradient) tensor and the dissipation rate tensor are the two of the most important terms. In the literature, these correlation tensors are usually decomposed into a so called rapid term and a return-to-isotropy term. Models of these terms have been used in global flow calculations together with other modeled terms. However, their individual behavior in different flows have not been fully examined because they are un-measurable in the laboratory. Recently, the development of direct numerical simulation (DNS) of turbulence has given us the opportunity to do this kind of study. With the direct numerical simulation, we may use the solution to exactly calculate the values of these correlation terms and then directly compare them with the values from their modeled formulations (models). In this paper, we make direct comparisons of five representative rapid models and eight return-to-isotropy models using the DNS data of forty five homogeneous flows which were done by Rogers et al. (1986) and Lee et al. (1985). The purpose of these direct comparisons is to explore the performance of these models in different flows and identify the ones which give the best performance. The paper also describes the modeling procedure, model constraints, and the various evaluated models. The detailed results of the direct comparisons are discussed, and a few concluding remarks on turbulence models are given.

14. SUBJECT TERMS	15. NUMBER OF PAGES
Turbulence modeling	62
	16. PRICE CODE: A04

17. SECURITY CLASSIFICATION OF REPORT	18. SECURITY CLASSIFICATION OF THIS PAGE	19. SECURITY CLASSIFICATION OF ABSTRACT	20. LIMITATION OF ABSTRACT
Unclassified	Unclassified	Unclassified	